



# A variational theory of hyperbolic Lagrangian Coherent Structures

George Haller\*

Department of Mechanical Engineering, McGill University, 817 Sherbrooke Ave. West, Montreal, Quebec H3A 2K6, Canada  
 Department of Mathematics and Statistics, McGill University, 817 Sherbrooke Ave. West, Montreal, Quebec H3A 2K6, Canada

## ARTICLE INFO

### Article history:

Received 6 July 2010  
 Received in revised form  
 12 November 2010  
 Accepted 17 November 2010  
 Available online 10 December 2010  
 Communicated by V. Rom-Kedar

### Keywords:

Lagrangian Coherent Structures  
 Invariant manifolds  
 Mixing

## ABSTRACT

We develop a mathematical theory that clarifies the relationship between observable Lagrangian Coherent Structures (LCSs) and invariants of the Cauchy–Green strain tensor field. Motivated by physical observations of trajectory patterns, we define hyperbolic LCSs as material surfaces (i.e., codimension-one invariant manifolds in the extended phase space) that extremize an appropriate finite-time normal repulsion or attraction measure over all nearby material surfaces. We also define weak LCSs (WLCSs) as stationary solutions of the above variational problem. Solving these variational problems, we obtain computable sufficient and necessary criteria for WLCSs and LCSs that link them rigorously to the Cauchy–Green strain tensor field. We also prove a condition for the robustness of an LCS under perturbations such as numerical errors or data imperfection. On several examples, we show how these results resolve earlier inconsistencies in the theory of LCS. Finally, we introduce the notion of a Constrained LCS (CLCS) that extremizes normal repulsion or attraction under constraints. This construct allows for the extraction of a unique observed LCS from linear systems, and for the identification of the most influential weak unstable manifold of an unstable node.

© 2010 Elsevier B.V. All rights reserved.

## 1. Introduction

### 1.1. Background

This paper is concerned with the development of a self-consistent theory of coherent trajectory patterns in dynamical systems defined over a finite time-interval. Following Haller and Yuan [1], we use the term *Lagrangian Coherent Structures* (or *LCSs*, for short) to describe the core surfaces around which such trajectory patterns form.

As an example, Fig. 1 shows the formation of passive tracer patterns in a quasi-geostrophic turbulence simulation described in [1]. We seek to locate the dynamically evolving LCSs that form the skeleton of these patterns. Beyond offering conceptual help in interpreting and forecasting complex time-dependent data sets, LCSs are natural targets through which to control ensembles of trajectories.

As proposed in [1], *repelling LCSs* are the core structures generating stretching, *attracting LCSs* act as centerpieces of folding, and *shear LCS* delineate swirling and jet-type tracer patterns. In order to act as organizing centers for Lagrangian patterns, LCSs are expected to have two key properties:

(1) *An LCS should be a material surface*, i.e., a codimension-one invariant surface in the extended phase space of a dynamical system. This is because (a) an LCS must have sufficiently high dimension to have visible impact and act as a transport barrier and (b) an LCS must move with the flow to act as an observable core of evolving Lagrangian patterns.

(2) *An LCS should exhibit locally the strongest attraction, repulsion or shearing in the flow*. This is essential to distinguish the LCS from all nearby material surfaces that will have the same stability type, as implied by the continuous dependence of the flow on initial conditions over finite times.

Based on (1)–(2), a purely physical definition of an observable LCS can be given as follows (cf. [1]):

**Definition 1** (*Physical Definition of Hyperbolic LCS*). A hyperbolic LCS over a finite time-interval  $\mathcal{I} = [\alpha, \beta]$  is a locally strongest repelling or attracting material surface over  $\mathcal{I}$  (cf. Fig. 2).

This definition does not favor any particular diagnostic quantity, such as finite-time or finite-size Lyapunov exponents, relative or absolute dispersion, vorticity, strain, measures of hyperbolicity, etc. Instead, it describes the main physical property of LCSs that enables us to observe them as cores of Lagrangian patterns. Ideally, a mathematical definition of an LCS should capture the essence of the above physical definition, and lead to computable mathematical criteria for the LCS. As we shall see below, however, such a mathematical definition and the corresponding criteria have been missing in the literature.

\* Corresponding address: Department of Mechanical Engineering, Macdonald Bldg. Rm. 270 B, McGill University, 817 Sherbrooke Ave. West, Montreal, QC H3A 2K6, Canada. Tel.: +1 (514) 398 6296.

E-mail address: [george.haller@mcgill.ca](mailto:george.haller@mcgill.ca).

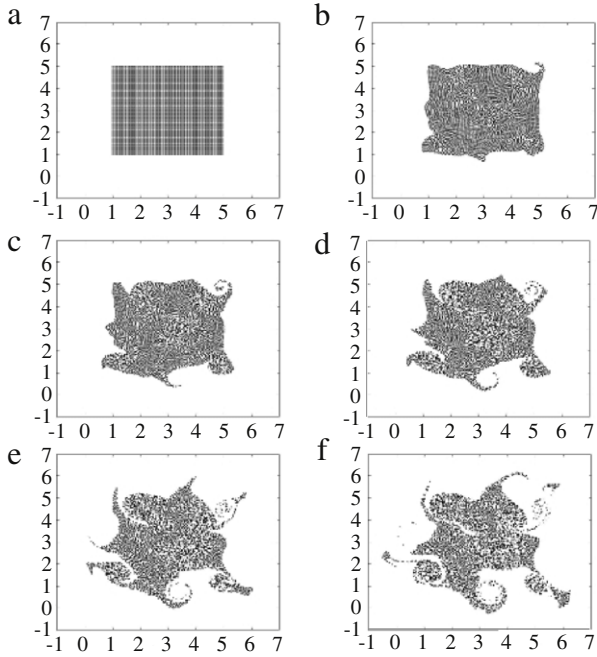


**Fig. 1.** An initially square set of fluid trajectories evolve into a complex material pattern in a two-dimensional turbulence simulation. The snapshots (a)–(f) are taken at different time instances. For more information, see [1].

In particular, while LCSs have *de facto* become identified with local maximizing curves (ridges) of the Finite-Time Lyapunov Exponent (FTLE) field (see, e.g., [2–5], and the recent review by Peacock and Dabiri [6]), simple counterexamples reveal conceptual problems with such an identification (see Section 2.3). Computational results on geophysical data sets also show that several FTLE ridges in real-life data sets do not repel or attract nearby trajectories (see, e.g., [7,8]).

The present paper addresses this theoretical gap by providing a mathematical version of the above physical LCS definition, and by deriving exact computable criteria for LCSs in  $n$ -dimensional dynamical systems defined over a finite time-interval. Our focus is hyperbolic (repelling or attracting) LCSs; a similar treatment of shear LCSs will appear elsewhere.

## 1.2. Summary of the main results

Our analysis is based on a new notion of finite-time hyperbolicity of material surfaces. This hyperbolicity concept is expressed through the normal repulsion rate and the normal repulsion ratio that are finite-time analogues of the Lyapunov-type numbers introduced by Fenichel [9] for normally hyperbolic invariant manifolds. Unlike Fenichel's numbers, however, the normal repulsion rate and ratio are smooth quantities that are computable for a given material surface and flow.

We employ a variational approach to locate LCSs as material surfaces that pointwise extremize the normal repulsion rate among all  $C^1$ -close material surfaces. We also introduce the notion of a *Weak LCS* (WLCS), which is a stationary surface – but not necessarily an extremum surface – for our variational problem. As we show, the use of WLCS resolves notable counterexamples to the identification of LCSs with FTLE ridges.

Solving the variational problem leads to a necessary and sufficient LCS criterion that involves invariants of the inverse Cauchy–Green strain tensor (Theorem 7). Specifically, WLCSs at time  $t_0$  must be hypersurfaces in the phase space satisfying the equation

$$\langle \nabla \lambda_n(\mathbf{x}_0), \xi_n(\mathbf{x}_0) \rangle = 0, \quad (1)$$

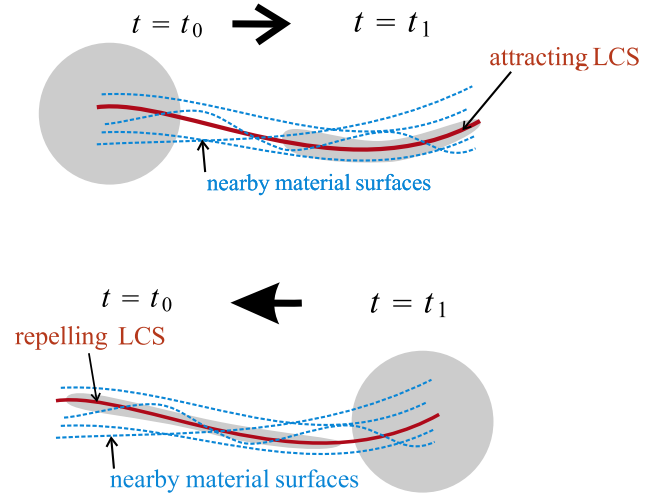


**Fig. 2.** The geometry of Definition 1: an attracting LCS is locally the strongest attracting material surface over the time interval  $[t_0, t_1]$  among all nearby (i.e., sufficiently  $C^1$ -close) material surfaces. A sphere of nearby initial conditions released at time  $t_0$  will then spread out in a fashion that the LCS will serve as its centerpiece at time  $t_1$ . A similar sketch is shown for a repelling LCS.

where  $\mathbf{x}_0 \in \mathbb{R}^n$  is the phase space variable,  $\lambda_n(\mathbf{x}_0)$  denotes the largest eigenvalue of  $\mathbf{C}(\mathbf{x}_0) = [\nabla \mathbf{F}_{t_0}^{t_0+T}(\mathbf{x}_0)]^* \nabla \mathbf{F}_{t_0}^{t_0+T}(\mathbf{x}_0)$ , the Cauchy–Green strain tensor computed from the flow map  $\mathbf{F}_{t_0}^{t_0+T}$  between time  $t_0$  and  $t_0+T$ ;  $\xi_n(\mathbf{x}_0)$  is the eigenvector corresponding to the largest eigenvalue of  $\mathbf{C}(\mathbf{x}_0)$ . Condition (1) turns out to be equivalent to

$$\nabla \mathbf{C}^{-1}(\mathbf{x}_0)[\xi_n(\mathbf{x}_0), \xi_n(\mathbf{x}_0), \xi_n(\mathbf{x}_0)] = 0, \quad (2)$$

where  $\nabla \mathbf{C}^{-1}(\mathbf{x}_0)$  is a three-tensor, the gradient of  $\mathbf{C}^{-1}$ , evaluated on the vector  $\xi_n$ .

Theorem 7 also states that a material surface satisfying (1) at time  $t_0$  must be orthogonal to the  $\xi_n(\mathbf{x}_0)$  vector field in order to be a repelling LCS. This condition is non-restrictive for a long-lived LCS because all repelling material surfaces turn out to align at a rate  $e^{-bT} \approx \sqrt{\lambda_{n-1}/\lambda_n}$  with directions normal to  $\xi_n(\mathbf{x}_0)$  (Theorem 4 and formula (30)). For small  $T$ , however, the orthogonality condition may not hold on any material surface, which underscores a fundamental limitation to identifying cores of Lagrangian patterns from short-term observations.

Finally, Theorem 7 requires a matrix  $\mathbf{L}(\mathbf{x}_0, t_0, T)$ , defined in (31), to be positive definite on the zero set (1) in order for the underlying WLCS to be an LCS. A necessary condition for the positive definiteness of  $\mathbf{L}$  is

$$\nabla^2 \mathbf{C}^{-1}(\mathbf{x}_0)[\xi_n(\mathbf{x}_0), \xi_n(\mathbf{x}_0), \xi_n(\mathbf{x}_0), \xi_n(\mathbf{x}_0)] > 0, \quad (3)$$

with the four-tensor  $\nabla^2 \mathbf{C}^{-1}(\mathbf{x}_0)$ , the second derivative of  $\mathbf{C}^{-1}$ , evaluated on the strongest strain eigenvector field  $\xi_n(\mathbf{x}_0)$  (Proposition 8).

The LCSs we identify are robust under perturbations as long as

$$\langle \xi_n, \nabla^2 \lambda_n \xi_n \rangle + \langle \nabla \lambda_n, \nabla \xi_n \xi_n \rangle \neq 0 \quad (4)$$

holds along them (Theorem 11). The admissible perturbations to the underlying dynamical system need not be pointwise small as long as they translate to small perturbations to the flow map. For example, large amplitude but short-lived localized perturbations to the vector field governing the dynamics are admissible.

These general results allow us to examine the relevance of FTLE for LCS detection in rigorous terms. FTLE ridges turn out to mark the presence of LCSs under four conditions. First, along FTLE ridges,  $\lambda_n$  must be larger than one and of multiplicity one. Second, FTLE ridges have to be normal to the  $\xi_n(\mathbf{x}_0)$  field. Third, along FTLE

ridges, the gradient of  $\xi_n(\mathbf{x}_0)$  in directions parallel to  $\xi_n(\mathbf{x}_0)$  must be small enough. Fourth, the FTLE ridge must be steep enough (cf. Proposition 14).

For LCSs marked by such FTLE ridges, the robustness criterion (4) takes the more specific form

$$\langle \xi_n, \nabla^2 \lambda_n \xi_n \rangle + \langle \nabla \lambda_n, \nabla \xi_n \xi_n \rangle < 0,$$

as we show in Proposition 15. This again implies that FTLE ridges that are steep (i.e.,  $\langle \xi_n, \nabla^2 \lambda_n \xi_n \rangle \ll 0$ ), nearly flat (i.e.,  $|\nabla \lambda_n| \approx 0$ ), and lie in regions of moderately nonlinear strain (i.e.,  $|\nabla \xi_n \xi_n| \leq 1$ ) are the most robust under perturbations.

The present approach also allows for the treatment of a *Constrained LCS* (or *CLCS*), which is a solution of the above maximum repulsion problem under constraints. In this paper, we explore two such constraints: (1) The constraint that the LCS be an invariant manifold in phase space, not just in extended phase space. (2) The constraint that the LCS be a level surface of a first integral.

The CLCS approach enables us to identify unique attracting and repelling LCSs in linear flows that have so far defied LCS extraction techniques. CLCSs also turn out to be useful in extracting unique weak unstable manifolds from finite-time data sets, even though such manifolds are nonunique in the classic theory of invariant manifolds.

We believe that these results establish the first rigorous link between a Lagrangian diagnostic tool, the Cauchy–Green stains tensor, and invariant coherent structures in a finite-time dynamical system. Notably, however, the recent work of Froyland et al. [10] provides a rigorous link between properties of the Perron–Frobenius operator and almost invariant coherent sets of non-autonomous dynamical systems defined over infinite times.

### 1.3. Organization of the paper

In Section 2, we fix our notation and review discrepancies between observable LCSs and their commonly assumed FTLE signature.

In Section 3, we develop the notion of finite-time hyperbolicity for material surfaces and show that normals of finite-time hyperbolic material surfaces align exponentially fast with the largest strain eigenvector of the Cauchy–Green strain tensor. In Section 4, we define Weak LCSs and LCSs as repelling material surfaces that are pointwise stationary surfaces and extrema, respectively, of a variational principle for the repulsion rate. We then solve this variational problem and obtain sufficient and necessary conditions for WLCSs and LCSs.

Section 5 discusses the robustness of LCSs obtained from our theory with respect to perturbations to the underlying dynamical system. Applying our general results, we examine the relevance of FTLE ridges in LCS detection in Section 6. In Section 7, we discuss implications for the numerical detection of LCSs.

In Section 8, we review the counterexamples of Section 2.3 and show how they are resolved by our main result, Theorem 7. Section 9 discusses constrained LCS problems with applications to linear flows and weak unstable manifolds. We present our conclusions and directions for future work in Section 10.

## 2. LCS and FTLE

### 2.1. Set-up and notation

Consider a dynamical system of the form

$$\dot{\mathbf{x}} = \mathbf{v}(\mathbf{x}, t), \quad \mathbf{x} \in U \subset \mathbb{R}^n, \quad t \in [\alpha, \beta], \quad (5)$$

with a smooth vector field  $\mathbf{v}(\mathbf{x}, t)$  defined on the  $n$ -dimensional bounded, open domain  $U$  over a time interval  $[\alpha, \beta]$ , and with

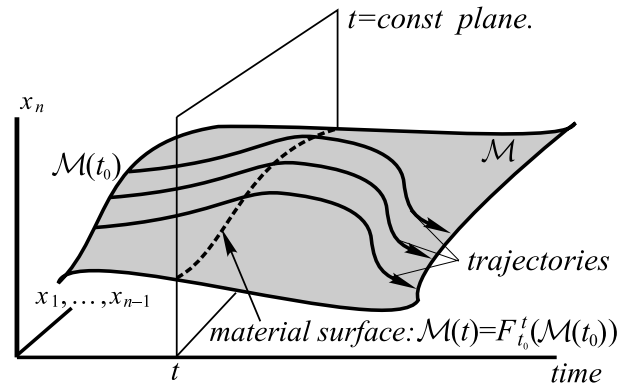


Fig. 3. Material surface  $\mathcal{M}(t)$  generated in the extended phase space by the flow map from a surface  $\mathcal{M}(t_0)$  of initial conditions.

the dot denoting differentiation with respect to the time variable  $t$ . This paper is primarily motivated by applications to fluid mechanics, in which case we have  $n = 2$  (planar flows) or  $n = 3$  (three-dimensional flows). The finite length of the time interval  $[\alpha, \beta]$  reflects temporal limitations to the available experimental or numerical flow data.

At time  $t$ , a trajectory of (5) system is denoted by  $\mathbf{x}(t, t_0, \mathbf{x}_0)$ , starting from the initial condition  $\mathbf{x}_0$  at time  $t_0$ . The flow map  $\mathbf{F}_{t_0}^t(\mathbf{x}_0)$  maps the initial position  $\mathbf{x}_0$  of the trajectory into its position at time  $t$ :

$$\begin{aligned} \mathbf{F}_{t_0}^t : U &\rightarrow U, \\ \mathbf{x}_0 &\mapsto \mathbf{x}(t, t_0, \mathbf{x}_0). \end{aligned}$$

Classic results from the theory of differential equations guarantee that the flow map is as many times differentiable in  $\mathbf{x}_0$  as is  $\mathbf{v}(\mathbf{x}, t)$  in  $\mathbf{x}$  (see [11]).

We recall that the *Lagrangian approach* to the analysis of the dynamical system (5) focuses on the trajectories of the system. By contrast, the *Eulerian approach* to analyzing (5) is concerned with the properties of the underlying vector field  $\mathbf{v}(\mathbf{x}, t)$ . Central to the Lagrangian view is the overall qualitative behavior of *ensembles of trajectories*  $\mathbf{x}(t, t_0, \mathbf{x}_0)$ . The most important such ensembles are codimension-one sets of trajectories, because they locally divide the extended phase space into two regions between which no transport is possible.

Specifically, a *material surface*  $\mathcal{M}(t)$  is the  $t = \text{const.}$  slice of an invariant manifold  $\mathcal{M}$  of system (5) in the extended phase space  $U \times [\alpha, \beta]$ , generated by the advection of an  $n - 1$ -dimensional surface of initial conditions  $\mathcal{M}(t_0)$  by the flow map  $\mathbf{F}_{t_0}^t$ :

$$\begin{aligned} \mathcal{M}(t) &= \mathbf{F}_{t_0}^t(\mathcal{M}(t_0)), \quad \dim \mathcal{M}(t_0) = n - 1, \\ \mathcal{M}(t_0) &\subset U, \quad \alpha \leq t_0 \leq t \leq \beta, \end{aligned} \quad (6)$$

with the corresponding geometry sketched in Fig. 3.

Since  $\mathbf{F}_{t_0}^t$  is a diffeomorphism, the material surface  $\mathcal{M}(t)$  is as smooth as the initial surface  $\mathcal{M}(t_0)$ , and has the same dimension.

### 2.2. Finite-Time Lyapunov Exponents (FTLE)

Since Definition 1 involves repulsion and attraction, it is plausible to explore how the maximal finite-time Lyapunov exponent, a local measure of the largest particle separation rate in system (5), could be used to characterize LCSs.

We recall that an infinitesimal perturbation  $\xi_0$  to the trajectory  $\mathbf{x}(t, t_0, \mathbf{x}_0)$  at time  $t_0$  evolves into the vector  $\nabla \mathbf{F}_{t_0}^t(\mathbf{x}_0) \xi_0$  at time  $t$  under the linearized flow. The largest singular value of the deformation gradient  $\nabla \mathbf{F}_{t_0}^t(\mathbf{x}_0)$ , therefore, gives the largest possible infinitesimal stretching along  $\mathbf{x}(t, t_0, \mathbf{x}_0)$  over the time interval  $[t_0, t]$ .

We introduce the *Cauchy–Green strain tensor*

$$\mathbf{C}_{t_0}^{t_0+T} = [\nabla \mathbf{F}_{t_0}^{t_0+T}]^* \nabla \mathbf{F}_{t_0}^{t_0+T}, \quad (7)$$

with the star denoting the transpose. We will use the notation  $\xi_1(\mathbf{x}_0, t_0, T), \dots, \xi_n(\mathbf{x}_0, t_0, T)$  for an orthonormal eigenbasis of  $\mathbf{C}_{t_0}^{t_0+T}(\mathbf{x}_0)$ , with the corresponding eigenvalues

$$0 < \lambda_1(\mathbf{x}_0, t_0, T) \leq \dots \leq \lambda_{n-1}(\mathbf{x}_0, t_0, T) \leq \lambda_n(\mathbf{x}_0, t_0, T) \quad (8)$$

that satisfy

$$\mathbf{C}_{t_0}^{t_0+T}(\mathbf{x}_0) \xi_i(\mathbf{x}_0, t_0, T) = \lambda_i(\mathbf{x}_0, t_0, T) \xi_i(\mathbf{x}_0, t_0, T), \quad i = 1, \dots, n.$$

The *Finite-Time Lyapunov Exponent* (FTLE) is defined as

$$\Lambda_{t_0}^{t_0+T}(\mathbf{x}_0) = \frac{1}{T} \log \left\| \nabla \mathbf{F}_{t_0}^{t_0+T}(\mathbf{x}_0) \right\| = \frac{1}{2T} \log \lambda_n(\mathbf{x}_0, t_0, T), \quad (9)$$

where  $\left\| \nabla \mathbf{F}_{t_0}^{t_0+T}(\mathbf{x}_0) \right\|$  denotes the operator norm of the deformation gradient  $\nabla \mathbf{F}_{t_0}^{t_0+T}$ . This norm is equal to the square root of  $\lambda_n(\mathbf{x}_0, t_0, T)$ , the maximum eigenvalue of the Cauchy–Green strain tensor. When  $T > 0$ , we will refer to  $\Lambda_{t_0}^{t_0+T}(\mathbf{x}_0)$  as the *forward FTLE*; for  $T < 0$ , we refer to the same quantity as *backward FTLE*.

Formula (9) shows that for finite  $T$ , the FTLE and  $\lambda_n$  are directly related. In what follows, we shall use  $\lambda_n$  in our analysis.

### 2.3. Relationship between FTLE and LCS: views and counterexamples

In [2,3], we suggested that at time  $t_0$ , a repelling LCS over  $[t_0, t]$  should appear as a local maximizing curve, or *ridge*, of the Finite-Time Lyapunov Exponent (FTLE) field computed over initial conditions at  $t_0$ . Similarly, an attracting LCS  $[t_0, t]$  should be a ridge of the backward-time FTLE field.

LCSs indeed appear to create ridges in the FTLE field in several applications (see [6] for a recent review). In [3], however, we presented an example where an FTLE ridge indicates maxima of shear, as opposed to a repelling LCS.

Shadden et al. [4] (see also Lekien et al. [5]) propose an alternative view by *defining* a repelling LCS at  $t_0$  as a ridge of the FTLE field computed over an interval  $[t_0, t]$ . As they note, under this definition, LCSs are no longer guaranteed to be Lagrangian. Indeed, when the vector field  $\mathbf{v}(\mathbf{x}, t)$  has general time dependence over a time interval  $[t_0, t_1]$ , ridges of the scalar field  $\Lambda_{t_0}^{t_0+T}$  will typically not evolve into ridges of  $\Lambda_{t_1}^{t_1+T}$  under the flow map  $\mathbf{F}_{t_0}^{t_1}$ . To quantify the degree of non-invariance of FTLE ridges, [4,5] present an elegant expression for the leading-order material flux through FTLE ridges.

Below we use four simple examples to demonstrate that observable LCSs need not be FTLE ridges, and FTLE ridges need not mark observable LCSs. We show that this mismatch also arises in area-preserving versions of our examples, and hence is relevant even for incompressible fluid flows. Finally, in Example 4, we highlight limitations to the validity of the above-mentioned ridge flux formula (cf. Example 11 and Appendix C).

#### 2.3.1. Example 1: LCSs in systems with no FTLE ridges

With the notation  $\mathbf{x} = (x, y)$ , consider the two-dimensional nonlinear saddle flow

$$\begin{aligned} \dot{x} &= x, \\ \dot{y} &= -y - y^3, \end{aligned} \quad (10)$$

for which the  $y$  axis is a readily observable repelling LCS, i.e., the stable manifold shown in Fig. 4. By contrast, as we show in

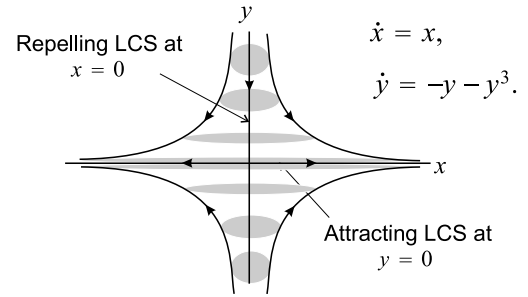


Fig. 4. A nonlinear strain flow with a repelling LCS that is *not* a ridge of the forward FTLE field.

Appendix B, the forward FTLE field is simply the constant field

$$\Lambda_{t_0}^{t_0+T}(\mathbf{x}_0) \equiv 1, \quad (11)$$

which has *no* ridges for any  $T > 0$ .

The even simpler linear, area-preserving strain flow

$$\begin{aligned} \dot{x} &= x, \\ \dot{y} &= -y, \end{aligned} \quad (12)$$

has a phase portrait topologically equivalent to Fig. 4, but neither its repelling LCS nor its attracting LCS can be detected as ridges of the forward or backward FTLE field. Specifically, both the forward FTLE and the backward FTLE fields are constant ( $\Lambda_{t_0}^{t_0\pm T}(\mathbf{x}_0) \equiv 1$ ) and hence admit no ridges.

An area-preserving version of (10) is given by the system

$$\begin{aligned} \dot{x} &= x(1 + 3y^2), \\ \dot{y} &= -y - y^3. \end{aligned} \quad (13)$$

Because of the coupling between the two equations, an analytic calculation of FTLE is more cumbersome. Still, a numerical computation of the forward FTLE field shows that system (13) admits no FTLE ridges, even though the  $x = 0$  axis is an observable repelling LCS.

#### 2.3.2. Example 2: LCS that is a trough of the FTLE field

Consider the saddle flow

$$\begin{aligned} \dot{x} &= x, \\ \dot{y} &= -y - y^3, \end{aligned} \quad (14)$$

studied in Example 1 above. From Fig. 4, it is apparent that the  $y = 0$  axis is an attracting Lagrangian structure. Yet, as we show in Appendix B, the  $y = 0$  axis is a trough of the backward-time FTLE field.

Again, an area-preserving version of the above example is given by (13). A numerical computation of the backward FTLE field reveals the same type of trough along the  $y = 0$  axis as the one found analytically in system (14) (see Fig. 5).

#### 2.3.3. Example 3: FTLE ridge that is not a repelling LCS

Consider the two-dimensional area-preserving dynamical system

$$\begin{aligned} \dot{x} &= 2 + \tanh y, \\ \dot{y} &= 0, \end{aligned} \quad (15)$$

whose phase portrait is just the parallel shear flow sketched in Fig. 6. As we show in more detail in Appendix B, the  $x$  axis of this example is a ridge of the forward, as well as the backward, FTLE field. As Fig. 6 shows, however, all trajectories preserve their distance from the  $x$  axis for all times, thus the  $x$  axis is neither a repelling nor an attracting LCS.

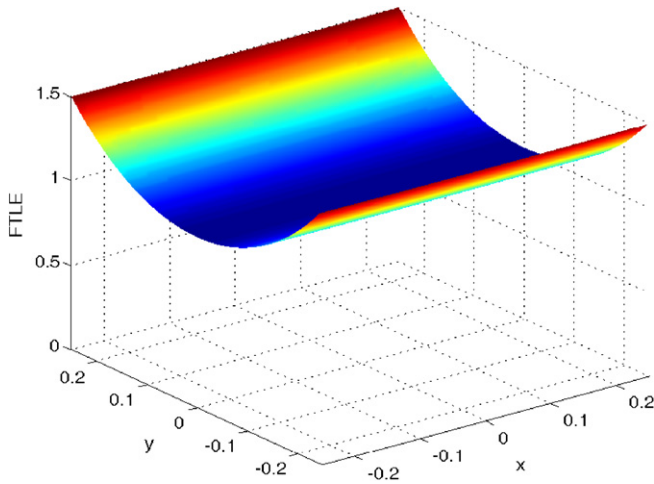


**Fig. 5.** The backward FTLE field admits a trough along the  $x$  axis, which is an observable attracting LCS of example (13). The integration time was selected as  $t - t_0 = -0.7450$ .

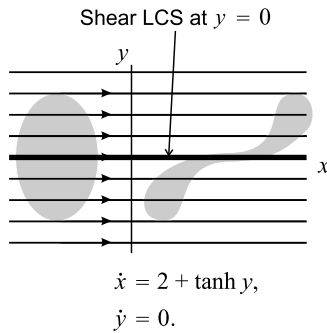


**Fig. 6.** A parallel shear flow with an FTLE ridge that is *not* a repelling LCS, but a shear LCS, as shown by the deformation of a set of initial conditions.

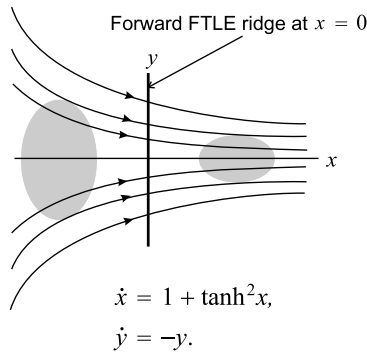


**Fig. 7.** A flow with a forward FTLE ridge that has no LCS in its proximity.

**2.3.4. Example 4: FTLE ridge that is far from any LCS**

Consider the dynamical system

$$\begin{aligned} \dot{x} &= 1 + \tanh^2 x, \\ \dot{y} &= -y, \end{aligned} \tag{16}$$

whose phase portrait is shown in Fig. 7, along with the deformation of a set of initial conditions under the flow. As we show in Appendix B, the FTLE field computed for this flow admits a ridge along the  $y$  axis for any choice of  $t_0$  and large enough  $t > t_0$ . Defining an LCS as a time-evolving surface which, at any time  $t$ , coincides with a ridge of the FTLE field  $\Lambda_t^{t+T}$ , would render the  $y$  axis a repelling LCS of the form

$$\hat{\mathcal{M}}(t) \equiv \left\{ \begin{pmatrix} 0 \\ y_0 \end{pmatrix} \in \mathbb{R}^2; y_0 \in \mathbb{R} \right\}. \tag{17}$$

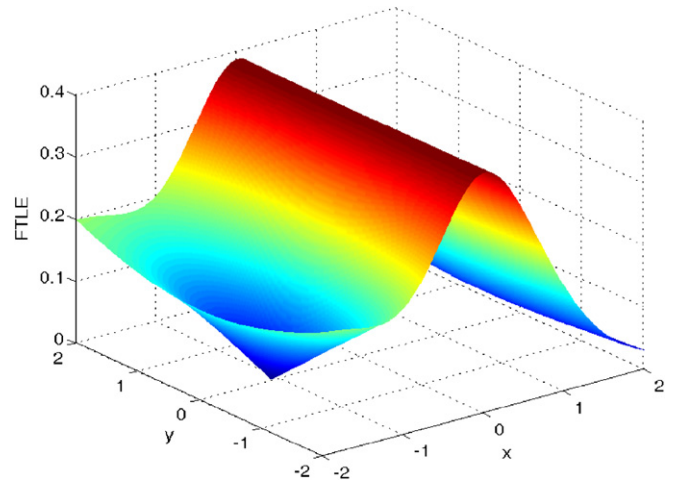


**Fig. 8.** FTLE ridge at  $x = 0$  for the area-preserving system (18) for  $t - t_0 = 1.78$ . This ridge remains at the same location for all  $t_0$ , but no such fixed LCS exists in the flow.

Note, however, that  $\hat{\mathcal{M}}(t)$  is far from being Lagrangian: the flow of (16) crosses it orthogonally with speed  $\dot{x} = 1$ . Thus the area flux per unit length through  $\hat{\mathcal{M}}(t)$  is equal to one. This is at odds with the flux formula proposed in [4], which predicts an order  $\mathcal{O}(1/|t - t_0|)$  flux through  $\hat{\mathcal{M}}(t)$  as  $t$  increases (cf. Appendix B).

An area-preserving version of Example 4 is given by

$$\begin{aligned} \dot{x} &= 1 + \tanh^2 x, \\ \dot{y} &= -\frac{2 \tanh x}{\cosh^2 x} y. \end{aligned} \tag{18}$$

A numerical computation of the FTLE field for (18) again reveals the development of a ridge along the  $y$  axis for large enough integration times and for any  $t_0$ , even though no fixed LCS of the form (17) exists (cf. Fig. 8). The unit flux through  $\hat{\mathcal{M}}(t)$  is again erroneously predicted by formula (107) as  $\mathcal{O}(1/|t - t_0|)$  for growing  $t$ , as opposed to the correct value  $\varphi((0, y_0), t) \equiv 1$ .

**2.4. Summary**

The above examples highlight the following points:

1. *Observable LCS are not necessarily ridges of the FTLE field.* Specifically, Fig. 9a, the usual motivating picture used in the literature for equating FTLE ridges with LCSs is not universally applicable, as illustrated by the examples in Fig. 9b and c.
2. *Ridges of the FTLE field are not necessarily observable LCSs.* Specifically, FTLE ridges may be indicators of large shear (see Example 3), or indicators of locally large stretching without any underlying coherent structure (see Example 11).
3. *Ridges of the FTLE field may in fact be far from any Lagrangian structure* (see Examples 4 and 11).
4. *The flux formula proposed in [4] for FTLE ridges is not generally applicable:* its higher-order neglected terms may be as large or larger than its explicit leading-order terms, even as  $T \rightarrow \infty$  (cf. Examples 4 and 11, and Appendix C).

In the following, we describe a mathematical theory that resolves these inconsistencies and gives a unified view on LCSs.

**3. Hyperbolicity of material surfaces**

In our setting, LCSs are only assumed to exist over a finite time-interval  $[\alpha, \beta]$ . To describe their attracting and repelling properties, therefore, we cannot rely on classic notions of hyperbolicity that are inherently asymptotic in time (see, e.g., [9]).

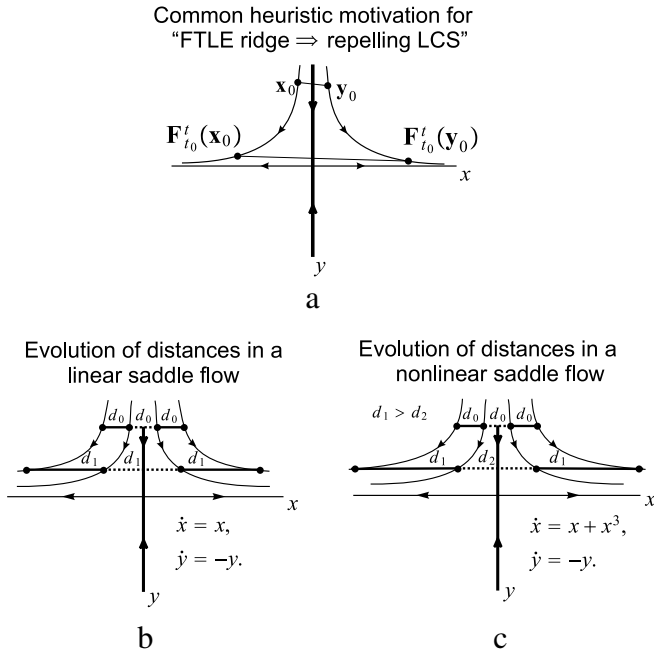


**Fig. 9.** (a) Heuristic motivation for the assertion that FTLE ridges mark repelling LCSs. It is at odds with the following two examples: (b) Linear saddle flow without an FTLE ridge that has an observable repelling LCS at  $x = 0$ . (c) Nonlinear saddle flow with an FTLE trough and an observable repelling LCS at  $x = 0$ .

The concept of *uniform finite-time hyperbolicity for individual trajectories* was apparently first introduced in [12], then elaborated on in [13,1,22,2,3,14]. Extensions of these results to higher-dimensional and non-volume-preserving systems are given by Duc and Siegmund [15], Berger et al. [16,17] and Berger [18].

Haller and Yuan [12] extended the concept of uniform finite-time hyperbolicity to material surfaces. They require the normal component of normal perturbations to a material surface to grow at a uniform rate over all subintervals of a finite time-interval  $[\alpha, \beta]$ . Numerical simulations in the same paper and experimental results in [19] show, however, that this notion of finite-time hyperbolicity captures only a small subset of observed Lagrangian coherent structures.

In our discussion below, we relax this requirement of uniform hyperbolicity to a weaker notion of finite-time hyperbolicity that ultimately enables us to locate LCSs more efficiently. This notion of finite-time hyperbolicity resembles that used by Lin and Young [20] in a different context.

### 3.1. Repulsion rate and repulsion ratio

Consider a compact material surface  $\mathcal{M}(t) \subset \mathbb{R}^n$ , as defined by formula (6). We want to express the physically observed repelling or attracting nature of this surface over a time interval  $[t_0, t]$  in mathematical terms.

To this end, at an arbitrary point  $\mathbf{x}_0 \in \mathcal{M}(t_0)$ , we consider the  $(n - 1)$ -dimensional tangent space  $T_{\mathbf{x}_0}\mathcal{M}(t_0)$  of  $\mathcal{M}(t_0)$ , as well as the one-dimensional normal space  $N_{\mathbf{x}_0}\mathcal{M}(t_0)$ , as shown in Fig. 10. The tangent space  $T_{\mathbf{x}_0}\mathcal{M}(t_0)$  is carried forward along the trajectory  $\mathbf{x}_t \stackrel{\text{def.}}{=} \mathbf{x}(t, t_0; \mathbf{x}_0) = \mathbf{F}_{t_0}^t(\mathbf{x}_0)$  by the linearized flow map  $\nabla \mathbf{F}_{t_0}^t(\mathbf{x}_0)$  into the tangent space

$$T_{\mathbf{x}_t}\mathcal{M}(t) = \nabla \mathbf{F}_{t_0}^t(\mathbf{x}_0)T_{\mathbf{x}_0}\mathcal{M}(t_0)$$

by the invariance of  $\mathcal{M}(t)$  under the flow map. In particular, a unit tangent vector  $\mathbf{e}_0 \in T_{\mathbf{x}_0}\mathcal{M}(t_0)$  is mapped by the linearized flow into  $\nabla \mathbf{F}_{t_0}^t(\mathbf{x}_0)\mathbf{e}_0$ , a tangent vector to  $\mathcal{M}(t)$  at the point  $\mathbf{x}_t$ . By contrast,  $\nabla \mathbf{F}_{t_0}^t(\mathbf{x}_0)N_{\mathbf{x}_0}\mathcal{M}(t_0)$  is generally not contained in the normal

space  $N_{\mathbf{x}_t}\mathcal{M}(t)$ , and hence a unit vector  $\mathbf{n}_0(\mathbf{x}_0, t_0) \in N_{\mathbf{x}_0}\mathcal{M}(t_0)$  will typically not be mapped into the normal space  $N_{\mathbf{x}_t}\mathcal{M}(t)$  by the linearized flow. Rather, its image,  $\nabla \mathbf{F}_{t_0}^t(\mathbf{x}_0)\mathbf{n}_0$ , will be a vector of general orientation, as shown in Fig. 10.

Let  $\mathbf{n}_t \in N_{\mathbf{x}_t}\mathcal{M}(t)$  denote a smoothly varying family of unit normal vectors along  $\mathbf{x}_t$ . To assess the growth of perturbations in the direction normal to  $\mathcal{M}(t)$ , we need to consider the projection of  $\nabla \mathbf{F}_{t_0}^t(\mathbf{x}_0)\mathbf{n}_0$  onto  $\mathbf{n}_t$ , given by the *repulsion rate*

$$\rho_{t_0}^t(\mathbf{x}_0, \mathbf{n}_0) = \langle \mathbf{n}_t, \nabla \mathbf{F}_{t_0}^t(\mathbf{x}_0)\mathbf{n}_0 \rangle. \quad (19)$$

If this projection is larger than one, the normal component of an infinitesimal normal perturbation to  $\mathcal{M}(t_0)$  grows by the end of the time interval  $[t_0, t]$ . Similarly,  $\rho_{t_0}^t(\mathbf{x}_0, \mathbf{n}_0) < 1$  indicates that the normal component of normal perturbations to  $\mathcal{M}(t_0)$  decreases by time  $t$ .

We also introduce the *repulsion ratio*, a measure of the ratio between normal and tangential growth rates along  $\mathcal{M}(t)$ :

$$v_{t_0}^t(\mathbf{x}_0, \mathbf{n}_0) = \min_{\substack{|\mathbf{e}_0|=1 \\ \mathbf{e}_0 \in T_{\mathbf{x}_0}\mathcal{M}(t_0)}} \frac{\langle \mathbf{n}_t, \nabla \mathbf{F}_{t_0}^t(\mathbf{x}_0)\mathbf{n}_0 \rangle}{|\nabla \mathbf{F}_{t_0}^t(\mathbf{x}_0)\mathbf{e}_0|}.$$

If  $v_{t_0}^t(\mathbf{x}_0, \mathbf{n}_0) > 1$  holds, then infinitesimal normal growth along  $\mathcal{M}(t)$  dominates the largest tangential growth along  $\mathcal{M}(t)$  over the time interval  $[t_0, t]$ . In this case, the material surface  $\mathcal{M}(t)$  is indeed observed as the locally dominant repelling structure.

The following proposition gives computable expressions for  $\rho_{t_0}^t(\mathbf{x}_0, \mathbf{n}_0)$  and  $v_{t_0}^t(\mathbf{x}_0, \mathbf{n}_0)$  in terms of the Cauchy–Green strain tensor.

**Proposition 2.** *The quantities  $\rho_{t_0}^t$  and  $v_{t_0}^t$  can be computed and estimated as follows:*

(i)

$$\rho_{t_0}^t(\mathbf{x}_0, \mathbf{n}_0) = \frac{1}{\sqrt{\langle \mathbf{n}_0, [\mathbf{C}_{t_0}^t(\mathbf{x}_0)]^{-1}\mathbf{n}_0 \rangle}},$$

$$v_{t_0}^t(\mathbf{x}_0, \mathbf{n}_0) = \min_{\substack{|\mathbf{e}_0|=1 \\ \mathbf{e}_0 \in T_{\mathbf{x}_0}\mathcal{M}(t_0)}} \frac{\rho_{t_0}^t(\mathbf{x}_0, \mathbf{n}_0)}{\sqrt{\langle \mathbf{e}_0, \mathbf{C}_{t_0}^t(\mathbf{x}_0)\mathbf{e}_0 \rangle}}.$$

(ii)

$$\sqrt{\lambda_1(\mathbf{x}_0, t_0, T)} \leq \rho_{t_0}^{t_0+T}(\mathbf{x}_0, \mathbf{n}_0) \leq \sqrt{\lambda_n(\mathbf{x}_0, t_0, T)},$$

$$\sqrt{\frac{\lambda_1(\mathbf{x}_0, t_0, T)}{\lambda_n(\mathbf{x}_0, t_0, T)}} \leq v_{t_0}^{t_0+T}(\mathbf{x}_0, \mathbf{n}_0) \leq \sqrt{\frac{\lambda_n(\mathbf{x}_0, t_0, T)}{\lambda_1(\mathbf{x}_0, t_0, T)}}.$$

**Proof.** Note that for any  $\mathbf{e}_0 \in T_{\mathbf{x}_0}\mathcal{M}(t_0)$ , we have  $\langle \mathbf{e}_0, \mathbf{n}_0 \rangle = 0$ , and hence

$$0 = \langle \mathbf{e}_0, \mathbf{n}_0 \rangle = \langle \mathbf{e}_0, (\nabla \mathbf{F}_{t_0}^t)^*(\nabla \mathbf{F}_t^{t_0})^*\mathbf{n}_0 \rangle$$

$$= \langle \nabla \mathbf{F}_{t_0}^t\mathbf{e}_0, (\nabla \mathbf{F}_t^{t_0})^*\mathbf{n}_0 \rangle, \quad (20)$$

where we have used the identity  $(\nabla \mathbf{F}_{t_0}^t)^*(\nabla \mathbf{F}_t^{t_0})^* = (\nabla \mathbf{F}_t^{t_0}\nabla \mathbf{F}_{t_0}^t)^* = \mathbf{I}$ . Formula (20) along with  $\nabla \mathbf{F}_{t_0}^t\mathbf{e}_0 \in T_{\mathbf{x}_t}\mathcal{M}(t)$  implies that  $\mathbf{n}_t = [(\nabla \mathbf{F}_t^{t_0})^*\mathbf{n}_0] / |(\nabla \mathbf{F}_t^{t_0})^*\mathbf{n}_0|$ . As a result, we have

$$\rho_{t_0}^t(\mathbf{x}_0, \mathbf{n}_0) = \langle \mathbf{n}_t, \nabla \mathbf{F}_{t_0}^t(\mathbf{x}_0)\mathbf{n}_0 \rangle = \left\langle \frac{(\nabla \mathbf{F}_t^{t_0})^*\mathbf{n}_0}{|(\nabla \mathbf{F}_t^{t_0})^*\mathbf{n}_0|}, \nabla \mathbf{F}_{t_0}^t(\mathbf{x}_0)\mathbf{n}_0 \right\rangle$$

$$= \frac{\langle \mathbf{n}_0, \nabla \mathbf{F}_t^{t_0}(\mathbf{x}_t)\nabla \mathbf{F}_{t_0}^t(\mathbf{x}_0)\mathbf{n}_0 \rangle}{\sqrt{\langle \mathbf{n}_0, (\nabla \mathbf{F}_t^{t_0})(\nabla \mathbf{F}_t^{t_0})^*\mathbf{n}_0 \rangle}}$$

$$= \frac{1}{\sqrt{\langle \mathbf{n}_0, [\mathbf{C}_{t_0}^t(\mathbf{x}_0)]^{-1}\mathbf{n}_0 \rangle}},$$

as claimed.

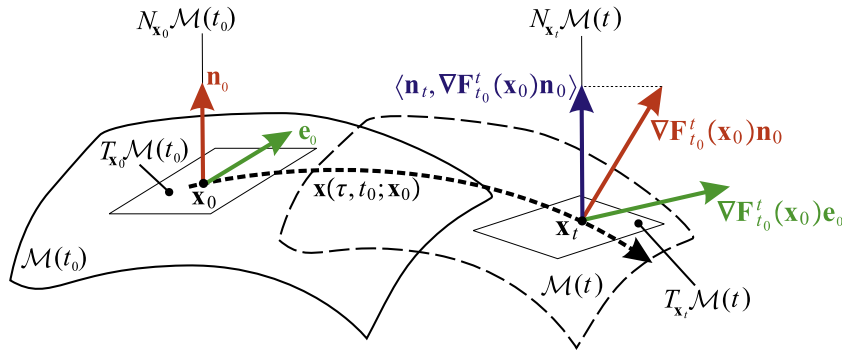


Fig. 10. Geometry of the linearized flow map along the material surface  $\mathcal{M}(t)$ .

We also have

$$\begin{aligned} \nu_{t_0}^t(\mathbf{x}_0, \mathbf{n}_0) &= \min_{\substack{|\mathbf{e}_0|=1 \\ \mathbf{e}_0 \in T_{\mathbf{x}_0} \mathcal{M}(t_0)}}} \frac{\langle \mathbf{n}_t, \nabla \mathbf{F}'_{t_0}(\mathbf{x}_0) \mathbf{n}_0 \rangle}{|\nabla \mathbf{F}'_{t_0}(\mathbf{x}_0) \mathbf{e}_0|} \\ &= \min_{\substack{|\mathbf{e}_0|=1 \\ \mathbf{e}_0 \in T_{\mathbf{x}_0} \mathcal{M}(t_0)}}} \frac{\rho_{t_0}^t(\mathbf{x}_0)}{\sqrt{\langle \mathbf{e}_0, \mathbf{C}_{t_0}^t(\mathbf{x}_0) \mathbf{e}_0 \rangle}}, \end{aligned}$$

completing the proof of statement (i) of the Proposition. The estimates in statement (ii) follow directly from the definition of  $\rho_{t_0}^t(\mathbf{x}_0, \mathbf{n}_0)$  and  $\nu_{t_0}^t(\mathbf{x}_0, \mathbf{n}_0)$ .  $\square$

### 3.2. Finite-time hyperbolic material surfaces and their alignment property

We are now in a position to define normal attraction and repulsion for a material surface over a finite time-interval.

**Definition 3** (Finite-Time Hyperbolic Material Surface). A material surface  $\mathcal{M}(t) \subset U$  is normally repelling over  $[t_0, t_0 + T] \subset \mathcal{I}$ , if there exist constants  $a, b > 0$  such that for all points  $\mathbf{x}_0 \in \mathcal{M}(t_0)$  and unit normals  $\mathbf{n}_0 \in N_{\mathbf{x}_0} \mathcal{M}(t_0)$ , we have

$$\begin{aligned} \rho_{t_0}^{t_0+T}(\mathbf{x}_0, \mathbf{n}_0) &\geq e^{aT}, \\ \nu_{t_0}^{t_0+T}(\mathbf{x}_0, \mathbf{n}_0) &\geq e^{bT}. \end{aligned} \tag{21}$$

Similarly, we call  $\mathcal{M}(t)$  normally attracting over  $[t_0, t_0 + T] \subset \mathcal{I}$  if it is normally repelling over  $[t_0, t_0 + T]$  in backward time. Finally, we call  $\mathcal{M}(t)$  hyperbolic over  $[t_0, t_0 + T]$  if it is normally repelling or normally attracting over  $[t_0, t_0 + T]$ .

The first condition in (21) requires all small normal perturbations to  $\mathcal{M}(t_0)$  to have strictly grown by time  $t = t_0 + T$ ; the second condition requires that by time  $t = t_0 + T$ , any growth along  $\mathcal{M}(t)$  is strictly smaller than growth normal to  $\mathcal{M}(t)$ . Since Definition 3 is only concerned with growth between the times  $t_0$  and  $t_0 + T$ , the exponential lower bounds in (21) will always exist as long as  $\rho_{t_0}^{t_0+T}$  and  $\nu_{t_0}^{t_0+T}$  are uniformly bounded from below by a constant larger than one.

We now derive a local geometric relationship between a normally repelling LCS and the largest eigenvector of the Cauchy-Green strain tensor. To state our result, for two codimension-one planes  $E, F \subset \mathbb{R}^n$  with respective unit normals  $\mathbf{n}_E$  and  $\mathbf{n}_F$ , we introduce the distance

$$\text{dist}[E, F] = \sqrt{1 - \langle \mathbf{n}_E, \mathbf{n}_F \rangle^2},$$

which is equal to  $|\sin \alpha(\mathbf{n}_E, \mathbf{n}_F)|$ , with  $\alpha(\mathbf{n}_E, \mathbf{n}_F)$  denoting the angle between  $\mathbf{n}_E$  and  $\mathbf{n}_F$ .

**Theorem 4** (Alignment Property of Hyperbolic Material Surfaces). Assume that for all  $T \in [T_-, T_+]$ , we have a normally repelling material surface  $\mathcal{M}(t)$  over  $[t_0, t_0 + T] \subset \mathcal{I}$  in the sense of Definition 3, with the constants  $a, b > 0$  selected uniformly in  $T$ .

Then the eigenspace spanned by the first  $n - 1$  eigenvalues of the Cauchy-Green strain tensor  $\mathbf{C}_{t_0}^{t_0+T}(\mathbf{x}_0)$  converges exponentially fast in  $T$  to the tangent space of  $\mathcal{M}(t_0)$  at the point  $\mathbf{x}_0$ . Specifically, we have

$$\begin{aligned} \text{dist}[T_{\mathbf{x}_0} \mathcal{M}(t_0), \text{span}\{\boldsymbol{\xi}_1(\mathbf{x}_0, t_0, T), \dots, \boldsymbol{\xi}_{n-1}(\mathbf{x}_0, t_0, T)\}] \\ \leq \sqrt{n-1} e^{-bT}, \\ |\sin \alpha(\mathbf{n}_0(\mathbf{x}_0, t_0, T), \boldsymbol{\xi}_n(\mathbf{x}_0, t_0, T))| \leq \sqrt{n-1} e^{-bT}, \end{aligned}$$

for all  $T \in [T_-, T_+]$ . A similar statement holds for normally attracting material surfaces in backward time.

**Proof.** Consider a point  $\mathbf{x}_0 \in \mathcal{M}(t_0)$  and let  $\mathbf{e}_1(\mathbf{x}_0, t_0, T), \dots, \mathbf{e}_{n-1}(\mathbf{x}_0, t_0, T)$  be an orthonormal basis in the tangent space  $T_{\mathbf{x}_0} \mathcal{M}(t_0)$ . For any basis vector  $\mathbf{e}_i(\mathbf{x}_0, t_0, T)$  and for the unit normal vector  $\mathbf{n}_0 \in N_{\mathbf{x}_0} \mathcal{M}(t_0)$ , we have the representation

$$\mathbf{e}_i(\mathbf{x}_0, t_0, T) = \sum_{j=1}^n a_{ij}(\mathbf{x}_0, t_0, T) \boldsymbol{\xi}_j(\mathbf{x}_0, t_0, T), \tag{22}$$

$$\mathbf{n}_0 = \sum_{j=1}^n b_j(\mathbf{x}_0, t_0, T) \boldsymbol{\xi}_j(\mathbf{x}_0, t_0, T).$$

Note that  $\boldsymbol{\xi}_j, \mathbf{e}_i$  and  $\mathbf{n}_0$  are all unit vectors, therefore we have

$$\left| \sum_{j=1}^n a_{ij}^2 \right| = 1, \quad \left| \sum_{j=1}^n b_j^2 \right| = 1. \tag{23}$$

The repelling property of  $\mathcal{M}(t)$  over  $[t_0, t_0 + T]$  (as assumed in the statement of the Theorem uniformly for  $T \in [T_-, T_+]$ ) implies

$$\begin{aligned} \frac{1}{[\rho_{t_0}^{t_0+T}(\mathbf{x}_0)]^2} &= \left\langle \mathbf{n}_0, [\mathbf{C}_{t_0}^{t_0+T}(\mathbf{x}_0)]^{-1} \mathbf{n}_0 \right\rangle \leq e^{-2aT}, \\ \frac{1}{[\nu_{t_0}^{t_0+T}(\mathbf{x}_0)]^2} &= \left\langle \mathbf{n}_0, [\mathbf{C}_{t_0}^{t_0+T}(\mathbf{x}_0)]^{-1} \mathbf{n}_0 \right\rangle \\ &\times \max_{\substack{|\mathbf{e}_0|=1 \\ \mathbf{e}_0 \in T_{\mathbf{x}_0} \mathcal{M}(t_0)}}} \left\langle \mathbf{e}_0, \mathbf{C}_{t_0}^{t_0+T}(\mathbf{x}_0) \mathbf{e}_0 \right\rangle \leq e^{-2bT}. \end{aligned} \tag{24}$$

Note that

$$\begin{aligned} \left\langle \mathbf{n}_0, [\mathbf{C}_{t_0}^{t_0+T}(\mathbf{x}_0)]^{-1} \mathbf{n}_0 \right\rangle &= \sum_{j=1}^n \frac{b_j^2}{\lambda_j}, \\ \left\langle \mathbf{e}_i, \mathbf{C}_{t_0}^{t_0+T}(\mathbf{x}_0) \mathbf{e}_i \right\rangle &= \sum_{j=1}^n \lambda_j a_{ij}^2, \end{aligned} \tag{25}$$

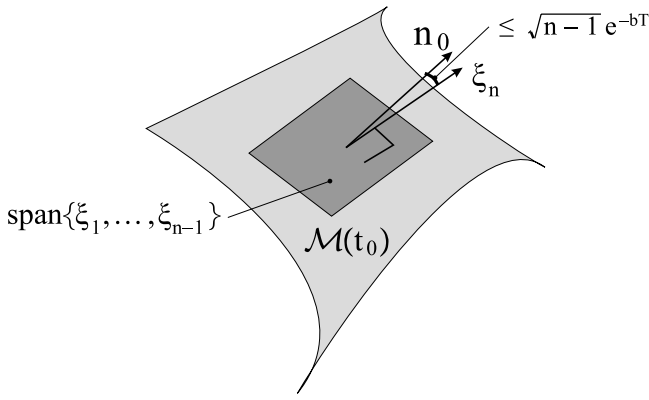


Fig. 11. Geometry of the linearized flow map along the material surface  $\mathcal{M}(t)$ .

therefore the first inequality in (24) yields, for any  $T \in [T_-, T_+]$ , the relation

$$\sum_{j=1}^n \frac{b_j^2}{\lambda_j} \leq e^{-2aT}, \quad (26)$$

which in turn, by (8) and (23), implies

$$e^{-2aT} \geq \sum_{j=1}^n \frac{b_j^2}{\lambda_j} \geq \sum_{j=1}^n \frac{b_j^2}{\lambda_n} = \frac{1}{\lambda_n},$$

or, equivalently,

$$\lambda_n \geq e^{2aT}, \quad T \in [T_-, T_+]. \quad (27)$$

Next, the second inequality in (24) can be re-written as

$$\left[ \sum_{j=1}^n \frac{b_j^2}{\lambda_j} \right] \left[ \sum_{k=1}^{n-1} a_{ik}^2 \lambda_k + a_{in}^2 \lambda_n \right] \leq e^{-2bT}, \quad i = 1, \dots, n-1, \quad T \in [T_-, T_+],$$

which implies

$$a_{in}^2 = a_m^2 \sum_{j=1}^n b_j^2 \leq a_m^2 \sum_{j=1}^n \frac{b_j^2 \lambda_n}{\lambda_j} \leq e^{-2bT},$$

or, equivalently,

$$a_{in} \leq e^{-bT}, \quad i = 1, \dots, n-1, \quad T \in [T_-, T_+].$$

Consequently, for any tangent vector  $\mathbf{e}_i \in T_{\mathbf{x}_0} \mathcal{M}(t_0)$ , we have

$$|\langle \mathbf{e}_i, \boldsymbol{\xi}_n \rangle| \leq e^{-bT}, \quad T \in [T_-, T_+], \quad (28)$$

and hence

$$\begin{aligned} \text{dist}[T_{\mathbf{x}_0} \mathcal{M}(t_0), \text{span}\{\boldsymbol{\xi}_1, \dots, \boldsymbol{\xi}_{n-1}\}] \\ = \sqrt{1 - \langle \mathbf{n}_0, \boldsymbol{\xi}_n \rangle^2} = \sqrt{\sum_{i=1}^{n-1} \langle \mathbf{e}_i, \boldsymbol{\xi}_n \rangle^2} \leq \sqrt{n-1} e^{-bT}, \end{aligned}$$

as claimed. Also, we have

$$\begin{aligned} |\sin \alpha(\mathbf{n}_0, \boldsymbol{\xi}_n)| &= \sqrt{1 - \cos^2 \alpha(\mathbf{n}_0, \boldsymbol{\xi}_n)} \\ &= \sqrt{1 - \langle \mathbf{n}_0, \boldsymbol{\xi}_n \rangle^2} \\ &\leq \sqrt{n-1} e^{-bT}, \end{aligned}$$

which concludes the proof of the Theorem.  $\square$

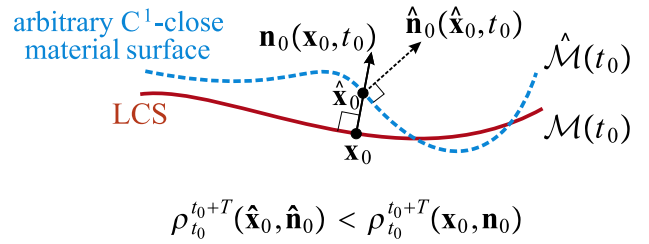


Fig. 12. The geometry of defining an LCS as an extremum surface for the normal repulsion rate.

The geometry of Theorem 4 is shown in Fig. 11. An inspection of the proof also reveals that along a material line satisfying the assumptions of Theorem 4, we can select

$$a < \frac{1}{2T} \log \lambda_n, \quad b < \frac{1}{2T} \log \frac{\lambda_n}{\lambda_{n-1}}, \quad (29)$$

in which case the rate of alignment can be approximated as

$$e^{-bT} \approx \sqrt{\frac{\lambda_{n-1}}{\lambda_n}}. \quad (30)$$

Therefore, the larger the spectral gap between  $\lambda_n$  and  $\lambda_{n-1}$ , the faster the normal of a repelling material surface aligns with  $\boldsymbol{\xi}_n$ .

As we shall see later, on the most influential repelling material surfaces (i.e., on LCSs), the vector field  $\boldsymbol{\xi}_n(\mathbf{x}_0, t_0, T)$  aligns exactly with the surface normals.

#### 4. Existence of hyperbolic Lagrangian coherent structures

##### 4.1. Weak LCS and LCS

Consider now material surfaces that are small and smooth deformations of a normally repelling material surface  $\mathcal{M}(t)$ . All such deformed material surfaces will be normally repelling by the continuity of the inequalities (21) in their arguments.

For a repelling material surface  $\mathcal{M}(t)$  to be a repelling LCS, we will require  $\mathcal{M}(t)$  to be pointwise more repelling over  $[t_0, t_0 + T]$  than any other nearby material surface. Specifically, at any point  $\mathbf{x}_0 \in \mathcal{M}(t_0)$ , perturbations to  $\mathcal{M}(t_0)$  along its normal  $\mathbf{n}_0 \in N_{\mathbf{x}_0} \mathcal{M}(t_0)$  will be required to yield  $\rho_{t_0}^{t_0+T}(\hat{\mathbf{x}}_0, \hat{\mathbf{n}}_0)$  values that are strictly smaller than  $\rho_{t_0}^{t_0+T}(\mathbf{x}_0, \mathbf{n}_0)$  (see Fig. 12).

We start by defining a weaker notion of an LCS, a repelling Weak Lagrangian Coherent Structure:

**Definition 5 (Hyperbolic Weak LCS).** Assume that  $\mathcal{M}(t) \subset U$  is a normally repelling material surface over  $[t_0, t_0 + T]$ . We call  $\mathcal{M}(t)$  a *repelling Weak LCS (WLCS)* over  $[t_0, t_0 + T]$  if its normal repulsion rate admits stationary values along  $\mathcal{M}(t_0)$  among all locally  $C^1$ -close material surfaces. We call  $\mathcal{M}(t)$  an *attracting WLCS* over  $[t_0, t_0 + T]$  if it is a repelling WLCS over  $[t_0, t_0 + T]$  in backward time. Finally, we call  $\mathcal{M}(t)$  a *hyperbolic WLCS* over  $[t_0, t_0 + T]$  if it is a repelling or attracting WLCS over  $[t_0, t_0 + T]$ .

Specifically, at each point  $\mathbf{x}_0$  of a WLCS, the repulsion rate field  $\rho_{t_0}^{t_0+T}(\hat{\mathbf{x}}_0, \hat{\mathbf{n}}_0)$  has a zero derivative in the direction of  $\mathbf{n}_0(\mathbf{x}_0, t_0)$ . A WLCS may not be a locally unique core of trajectory patterns. For instance, nearby attracting WLCSs obtained by normal translations may all converge to each other at the same rate, and hence may all be viewed as cores of an emerging trajectory pattern (see, e.g., Example 5).

The following stronger definition of an LCS guarantees that it is observed as a unique core of a coherent trajectory pattern.

**Definition 6** (Hyperbolic LCS). Assume that  $\mathcal{M}(t) \subset U$  is a normally repelling material surface over  $[t_0, t_0 + T]$ . We call  $\mathcal{M}(t)$  a repelling LCS over  $[t_0, t_0 + T]$  if its normal repulsion rate admits a pointwise nondegenerate maximum along  $\mathcal{M}(t_0)$  among all locally  $C^1$ -close material surfaces. We call  $\mathcal{M}(t)$  an attracting LCS over  $[t_0, t_0 + T]$  if it is a repelling LCS over  $[t_0, t_0 + T]$  in backward time. Finally, we call  $\mathcal{M}(t)$  a hyperbolic LCS over  $[t_0, t_0 + T]$  if it is a repelling or attracting LCS over  $[t_0, t_0 + T]$ .

By a nondegenerate maximum, we mean a local maximum for  $\rho_{t_0}^{t_0+T}(\mathbf{x}_0, \mathbf{n}_0)$  with a nondegenerate second derivative with respect to changes normal to  $\mathcal{M}(t_0)$ , as shown in Fig. 12.

4.2. Sufficient and necessary criteria for hyperbolic WLCS and LCS

The following result provides computable sufficient and necessary conditions for both weak LCS and LCS. In stating our main result, we will use the matrix (Eq. (31)) given in Box I whose first diagonal term, the second derivative of the inverse Cauchy–Green tensor, will be seen to equal

$$\nabla^2 \mathbf{C}^{-1}[\xi_n, \xi_n, \xi_n, \xi_n] = -\frac{1}{\lambda_n^2} \langle \xi_n, \nabla^2 \lambda_n \xi_n \rangle + 2 \sum_{q=1}^{n-1} \frac{\lambda_n - \lambda_q}{\lambda_q \lambda_n} \langle \xi_q, \nabla \xi_n \xi_n \rangle^2. \tag{32}$$

**Theorem 7** (Sufficient and Necessary Conditions for Hyperbolic WLCS and LCS). Consider a compact material surface  $\mathcal{M}(t) \subset U$  over the interval  $[t_0, t_0 + T]$ . Then

- (i)  $\mathcal{M}(t)$  is a repelling WLCS over  $[t_0, t_0 + T]$  if and only if all the following hold for all  $\mathbf{x}_0 \in \mathcal{M}(t_0)$ :
  1.  $\lambda_{n-1}(\mathbf{x}_0, t_0, T) \neq \lambda_n(\mathbf{x}_0, t_0, T) > 1$ ,
  2.  $\xi_n(\mathbf{x}_0, t_0, T) \perp T_{\mathbf{x}_0} \mathcal{M}(t_0)$ ,
  3.  $\langle \nabla \lambda_n(\mathbf{x}_0, t_0, T), \xi_n(\mathbf{x}_0, t_0, T) \rangle = 0$ .
- (ii)  $\mathcal{M}(t)$  is a repelling LCS over  $[t_0, t_0 + T]$  if and only if
  1.  $\mathcal{M}(t)$  is a repelling WLCS over  $[t_0, t_0 + T]$ ,
  2. The matrix  $\mathbf{L}(\mathbf{x}_0, t_0, T)$  is positive definite for all  $\mathbf{x}_0 \in \mathcal{M}(t_0)$ .

**Proof.** We first show that the conditions of the theorem are necessary, then argue that they are also sufficient.

A. Conditions (i)–(ii) are necessary

We start by formulating the extremum property of the repulsion rate  $\rho_{t_0}^{t_0+T}$  along  $\mathcal{M}(t)$  in precise terms. For a small number  $\varepsilon > 0$ , we consider nearby material surfaces  $\mathcal{M}_\varepsilon(t)$  such that  $\mathcal{M}_\varepsilon(t_0)$  is  $\mathcal{O}(\varepsilon)$   $C^1$ -close to  $\mathcal{M}(t_0)$ . On the compact time interval  $[t_0, t_0 + T]$ ,  $\mathcal{M}_\varepsilon(t)$  will then remain  $\mathcal{O}(\varepsilon)$   $C^1$ -close to  $\mathcal{M}(t)$  by the smoothness of the flow map  $\mathbf{F}_0^{t_0+T}$ . If  $\mathcal{M}(t)$  turns out to be a repelling surface over  $[t_0, t_0 + T]$ , then  $\mathcal{M}_\varepsilon(t)$  will be a repelling material surface over  $[t_0, t_0 + T]$ , for  $\varepsilon > 0$  small, by the continuity of the inequalities (21) in their arguments.

In order to compute  $\rho_{t_0}^{t_0+T}$  at points of  $\mathcal{M}_\varepsilon(t_0)$ , we need to derive a local representation of points and unit normals of  $\mathcal{M}_\varepsilon(t_0)$  in the vicinity of  $\mathbf{x}_0$ . For this, we consider a local parametrization of the  $(n - 1)$ -dimensional manifold  $\mathcal{M}(t_0)$  by a parameter vector  $\mathbf{s} = (s_1, \dots, s_{n-1}) \in V \subset \mathbb{R}^{n-1}$ , so that for some orthonormal basis  $\mathbf{e}_1, \dots, \mathbf{e}_{n-1}$  in the tangent space  $T_{\mathbf{x}_0} \mathcal{M}(t_0)$ , we have

$$\frac{\partial \mathbf{x}_0(\mathbf{s})}{\partial s_i} = \mathbf{e}_i, \quad i = 1, \dots, n - 1. \tag{33}$$

By the  $\mathcal{O}(\varepsilon)$   $C^1$ -closeness of  $\mathcal{M}_\varepsilon(t_0)$  to  $\mathcal{M}(t_0)$ , a point  $\mathbf{x}_\varepsilon \in \mathcal{M}_\varepsilon(t_0)$  can be uniquely represented as

$$\mathbf{x}_\varepsilon(\mathbf{s}, t_0) = \mathbf{x}_0(\mathbf{s}) + \varepsilon \alpha(\mathbf{s}, t_0) \mathbf{n}_0(\mathbf{x}_0(\mathbf{s}), t_0) \tag{34}$$

for an appropriate choice of  $\mathbf{x}_0(\mathbf{s})$ , and for some smooth function  $\alpha(\mathbf{s}, t_0): V \times \mathbb{R} \rightarrow \mathbb{R}$ .

To derive an expression for the unit normal  $\mathbf{n}_\varepsilon \in N_{\mathbf{x}_\varepsilon} \mathcal{M}_\varepsilon(t_0)$ , we differentiate (34) with respect to  $s_i$  and substitute (33) into the result to obtain

$$\frac{\partial \mathbf{x}_\varepsilon}{\partial s_i} = \mathbf{e}_i + \varepsilon \frac{\partial \alpha}{\partial s_i} \mathbf{n}_0 + \varepsilon \alpha \frac{\partial \mathbf{n}_0}{\partial s_i} \in T_{\mathbf{x}_\varepsilon} \mathcal{M}_\varepsilon(t_0), \tag{35}$$

$$i = 1, \dots, n - 1.$$

Seeking the unit normal  $\mathbf{n}_\varepsilon \in N_{\mathbf{x}_\varepsilon} \mathcal{M}_\varepsilon(t)$  in the form

$$\mathbf{n}_\varepsilon(\mathbf{s}, t_0) = \mathbf{n}_0(\mathbf{x}_0, t_0) + \varepsilon \boldsymbol{\beta}(\mathbf{s}, t_0) + \varepsilon^2 \boldsymbol{\gamma}(\mathbf{s}, t_0) + \mathcal{O}(\varepsilon^3), \tag{36}$$

we substitute the expressions (35) and (36) into the two constraints

$$\langle \mathbf{n}_\varepsilon, \mathbf{n}_\varepsilon \rangle = 1, \quad \left\langle \frac{\partial \mathbf{x}_\varepsilon}{\partial s_i}, \mathbf{n}_\varepsilon \right\rangle = 0, \quad i = 1, \dots, n - 1,$$

and compare equal powers of  $\varepsilon$  to deduce

$$\boldsymbol{\beta} = - \sum_{i=1}^{n-1} \frac{\partial \alpha}{\partial s_i} \mathbf{e}_i, \tag{37}$$

$$\boldsymbol{\gamma} = - \frac{1}{2} \sum_{i=1}^{n-1} \left( \frac{\partial \alpha}{\partial s_i} \right)^2 \mathbf{n}_0 - \alpha \sum_{i=1}^{n-1} \left\langle \frac{\partial \mathbf{n}_0}{\partial s_i}, \boldsymbol{\beta} \right\rangle \mathbf{e}_i,$$

where we have used  $\left\langle \frac{\partial \mathbf{n}_0}{\partial s_i}, \mathbf{n}_0 \right\rangle = 0$ . Eqs. (36) and (37) provide an expression for the unit normal to  $\mathcal{M}_\varepsilon(t)$  at the point  $\mathbf{x}_\varepsilon$ .

We now derive a necessary condition for the normal repulsion measure  $\rho_{t_0}^{t_0+T}(\mathbf{x}_0, \mathbf{n}_0)$  to attain a pointwise extremum along  $\mathcal{M}(t_0)$  relative to all other material surfaces  $\mathcal{M}_\varepsilon(t_0)$  that are locally  $\mathcal{O}(\varepsilon)$   $C^1$ -close to  $\mathcal{M}(t_0)$ . First note that Definition 5 is equivalent to the requirement

$$\frac{\partial}{\partial \varepsilon} \rho_{t_0}^{t_0+T}(\mathbf{x}_\varepsilon(\mathbf{s}, t_0), \mathbf{n}_\varepsilon(\mathbf{s}, t_0))|_{\varepsilon=0} = 0, \tag{38}$$

which is to be satisfied for all  $\mathbf{x}_\varepsilon \in \mathcal{M}_\varepsilon(t_0)$ , and for any choice of the smooth function  $\alpha(\mathbf{s}, t_0)$  in (34).

We compute (38) using tensor notation with summation implied over repeated indices. We use the notation

$$\begin{aligned} \mathbf{x}_\varepsilon(\mathbf{s}) &= (x_\varepsilon^1, \dots, x_\varepsilon^n), & \mathbf{n}_\varepsilon(\mathbf{s}) &= (n_\varepsilon^1, \dots, n_\varepsilon^n), \\ \mathbf{n}_0(\mathbf{s}) &= (n_0^1, \dots, n_0^n), & \mathbf{e}_p(\mathbf{s}) &= (e_p^1, \dots, e_p^n), \\ & & p &= 1, \dots, n - 1, \end{aligned}$$

$$\rho_{t_0}^{t_0+T}(\mathbf{x}_\varepsilon(\mathbf{s}), \mathbf{n}_\varepsilon(\mathbf{s})) = \frac{1}{\sqrt{C_{ij}^{-1}(\mathbf{x}_\varepsilon(\mathbf{s})) n_\varepsilon^i(\mathbf{s}) n_\varepsilon^j(\mathbf{s})}}, \tag{39}$$

with indices  $i, j, k, l$  varying over the integers  $1, \dots, n$ , and with the indices  $p, q$  varying over  $1, \dots, n - 1$ . We denote differentiation with respect to  $\varepsilon$  by prime. There will be no summation implied over repeated occurrences of the index  $n$ .

In this notation, condition (38) can be written as

$$\begin{aligned} \rho'|_{\varepsilon=0} &= -\frac{1}{2} [\rho^3 (C_{ij,k}^{-1} n_\varepsilon^i n_\varepsilon^j (x_\varepsilon^k)') + 2C_{ij}^{-1} (n_\varepsilon^i)' n_\varepsilon^j]_{\varepsilon=0} \\ &= -\frac{1}{2} \rho^3(\mathbf{x}_0, \mathbf{n}_0) [\alpha C_{ij,k}^{-1}(\mathbf{x}_0) n_0^i n_0^j n_0^k - 2\alpha_{,p} C_{ij}^{-1}(\mathbf{x}_0) e_p^i n_0^j], \end{aligned} \tag{40}$$

where we have used (36) and (37). From this equation we conclude that  $\rho'|_{\varepsilon=0} = 0$  can only hold for all choices of the smooth function  $\alpha$ , if we require

$$C_{ij,k}^{-1}(\mathbf{x}_0) n_0^i n_0^j n_0^k = 0, \tag{41}$$

$$C_{ij}^{-1}(\mathbf{x}_0) e_p^i n_0^j = 0, \quad p = 1, \dots, n - 1. \tag{42}$$

$$\mathbf{L} = \begin{pmatrix} \nabla^2 \mathbf{C}^{-1} [\boldsymbol{\xi}_n, \boldsymbol{\xi}_n, \boldsymbol{\xi}_n, \boldsymbol{\xi}_n] & 2 \frac{\lambda_n - \lambda_1}{\lambda_1 \lambda_n} \langle \boldsymbol{\xi}_1, \nabla \boldsymbol{\xi}_n \boldsymbol{\xi}_n \rangle & \cdots & 2 \frac{\lambda_n - \lambda_{n-1}}{\lambda_{n-1} \lambda_n} \langle \boldsymbol{\xi}_{n-1}, \nabla \boldsymbol{\xi}_n \boldsymbol{\xi}_n \rangle \\ 2 \frac{\lambda_n - \lambda_1}{\lambda_1 \lambda_n} \langle \boldsymbol{\xi}_1, \nabla \boldsymbol{\xi}_n \boldsymbol{\xi}_n \rangle & \frac{2\lambda_n - \lambda_1}{\lambda_1 \lambda_n} & \cdots & 0 \\ \vdots & \vdots & \ddots & \vdots \\ 2 \frac{\lambda_n - \lambda_{n-1}}{\lambda_{n-1} \lambda_n} \langle \boldsymbol{\xi}_{n-1}, \nabla \boldsymbol{\xi}_n \boldsymbol{\xi}_n \rangle & 0 & \cdots & \frac{2\lambda_n - \lambda_{n-1}}{\lambda_{n-1} \lambda_n} \end{pmatrix} \quad (31)$$

**Box I.**

Note that (42) implies  $\mathbf{C}^{-1} \mathbf{n}_0 \perp T_{\mathbf{x}_0} \mathcal{M}(t_0)$ , or, equivalently,  $\mathbf{C}^{-1} \mathbf{n}_0 \parallel \mathbf{n}_0$ ; in other words,  $\mathbf{n}_0$  must be an eigenvector of  $\mathbf{C}^{-1}$ . For  $\mathcal{M}(t_0)$  to be normally repelling (cf. Definition 3),  $\mathbf{n}_0$  must in fact coincide with  $\boldsymbol{\xi}_n(\mathbf{x}_0, t_0, T)$  and the corresponding eigenvalue  $\lambda_n(\mathbf{x}_0, t_0, T)$  must be multiplicity one, otherwise growth normal to  $\mathcal{M}(t)$  would not strictly dominate growth tangent to  $\mathcal{M}(t)$  over  $[t_0, t_0 + T]$ , and hence  $\mathcal{M}(t)$  would not be normally repelling by Definition 3. We conclude that for condition (42) to hold, we must necessarily have

$$\mathbf{n}_0 = \boldsymbol{\xi}_n, \quad \lambda_{n-1} \neq \lambda_n > 1. \quad (43)$$

This in turn implies that condition (41) is equivalent to

$$C_{ij,k}^{-1}(\mathbf{x}_0) \xi_n^i(\mathbf{x}_0, t_0, T) \xi_n^j(\mathbf{x}_0, t_0, T) \xi_n^k(\mathbf{x}_0, t_0, T) = 0. \quad (44)$$

To analyze the expression (44) further, we consider the eigenvalue problem

$$C_{ij}^{-1} \xi_n^j = \frac{1}{\lambda_n} \xi_n^i,$$

and differentiate it with respect to  $x^k$  to obtain

$$C_{ij,k}^{-1} \xi_n^j + C_{ij}^{-1} \xi_{n,k}^j = -\frac{\lambda_{n,k}}{\lambda_n^2} \xi_n^i + \frac{1}{\lambda_n} \xi_{n,k}^i.$$

Multiplying both sides by  $\xi_n^i$  and using the identity

$$\xi_{n,k}^j \xi_n^k = 0, \quad (45)$$

(which follows from  $\xi_n^j \xi_n^j = 1$ ), we obtain

$$C_{ij,k}^{-1} \xi_n^i \xi_n^j = -\frac{\lambda_{n,k}}{\lambda_n^2}, \quad (46)$$

which implies

$$\langle \nabla \lambda_n, \boldsymbol{\xi}_n \rangle = \lambda_{n,k} \xi_n^k = -\lambda_n^2 C_{ij,k}^{-1} \xi_n^i \xi_n^j. \quad (47)$$

Therefore, by (47), the necessary condition (44) is equivalent to

$$\langle \nabla \lambda_n, \boldsymbol{\xi}_n \rangle = 0. \quad (48)$$

Note that (43) and (48) together complete the proof of necessity for the conditions in statement (i) of the theorem. Also note that by (43), the orthonormal basis  $\{\mathbf{e}_i\}_{i=1}^{n-1}$  can be chosen as

$$\mathbf{e}_p(\mathbf{s}) = \boldsymbol{\xi}_p(\mathbf{x}_0(\mathbf{s}), t_0, T), \quad p = 1, \dots, n-1. \quad (49)$$

To prove the necessity of conditions (ii)/1 and (ii)/2 for the existence of an LCS, first observe that (ii)/1 is clearly a necessary condition because an LCS is necessarily a WLCS. Next note that for an LCS, beyond the stationarity condition (38), we must necessarily have the nondegenerate local maximum condition

$$\frac{\partial^2}{\partial \varepsilon^2} \rho_{t_0}^{\varepsilon, t_0+T}(\mathbf{x}_\varepsilon(\mathbf{s}, t_0), \mathbf{n}_\varepsilon(\mathbf{s}, t_0))|_{\varepsilon=0} < 0 \quad (50)$$

by Definition 6.

To evaluate condition (50), we differentiate (39) twice with respect to  $\varepsilon$  to obtain

$$\begin{aligned} \rho''|_{\varepsilon=0} &= \left[ \frac{3}{\rho} (\rho')^2 \right]_{\varepsilon=0} \\ &\quad - \left( \frac{\rho^3}{2} \left[ C_{ij,k}^{-1} n_\varepsilon^i n_\varepsilon^j (x_\varepsilon^k)' + 2C_{ij}^{-1} (n_\varepsilon^i)' n_\varepsilon^j \right]' \right)_{\varepsilon=0} \\ &= -\frac{\sqrt{\lambda_n}^3}{2} [C_{ij,k}^{-1} n_\varepsilon^i n_\varepsilon^j (x_\varepsilon^k)' + 2C_{ij}^{-1} (n_\varepsilon^i)' n_\varepsilon^j]_{\varepsilon=0}, \end{aligned} \quad (51)$$

where we have used the fact that  $\rho'|_{\varepsilon=0} = 0$  holds at the extremum location by (38).

Evaluating (51) further, we note that

$$\begin{aligned} &[C_{ij,k}^{-1} n_\varepsilon^i n_\varepsilon^j (x_\varepsilon^k)' + 2C_{ij}^{-1} (n_\varepsilon^i)' n_\varepsilon^j]_{\varepsilon=0} \\ &= [C_{ij,kl}^{-1} n_\varepsilon^i n_\varepsilon^j (x_\varepsilon^k)' (x_\varepsilon^l)' + 4C_{ij,k}^{-1} (n_\varepsilon^i)' n_\varepsilon^j (x_\varepsilon^k)' \\ &\quad + 2C_{ij}^{-1} (n_\varepsilon^i)'' n_\varepsilon^j + 2C_{ij}^{-1} (n_\varepsilon^i)' (n_\varepsilon^j)']_{\varepsilon=0} \\ &= \alpha^2 C_{ij,kl}^{-1} \xi_n^i \xi_n^j \xi_n^k \xi_n^l - 4\alpha \alpha_p C_{ij,k}^{-1} e_p^i e_p^j \xi_n^k \\ &\quad + 2C_{ij}^{-1} \left( -\frac{1}{2} \alpha_p \alpha_p \xi_n^i - \alpha \xi_p^k \beta^k e_p^i \right) \xi_n^j \\ &\quad + 2\alpha_p \alpha_p C_{ij}^{-1} e_p^i e_p^j \\ &= \alpha^2 C_{ij,kl}^{-1} \xi_n^i \xi_n^j \xi_n^k \xi_n^l - 4\alpha \alpha_p C_{ij,k}^{-1} \xi_p^i \xi_p^j \xi_n^k \\ &\quad - \frac{\alpha_p \alpha_p}{\lambda_n} - \frac{2\alpha}{\lambda_n} \xi_p^k \beta^k \xi_p^i \xi_n^i + 2 \frac{\alpha_p \alpha_p}{\lambda_p} \\ &= \alpha^2 C_{ij,kl}^{-1} \xi_n^i \xi_n^j \xi_n^k \xi_n^l - 4\alpha \alpha_p C_{ij,k}^{-1} \xi_p^i \xi_p^j \xi_n^k \\ &\quad + \alpha_p \alpha_p \left[ \frac{2}{\lambda_p} - \frac{1}{\lambda_n} \right], \end{aligned} \quad (52)$$

where we have used (49).

Eqs. (51)–(52) show that (50) holds for all choices of  $\alpha(\mathbf{s})$  if and only if the matrix (Eq. (53)) given in Box II is positive definite.

To compute  $\mathbf{L}(\mathbf{x}_0, t_0, T)$  in a coordinate-free form, we differentiate the identity  $\xi_q^i \xi_n^i = \delta_{qn}$  with respect to  $x^k$  to obtain

$$\xi_{q,k}^i \xi_n^i + \xi_q^i \xi_{n,k}^i = 0, \quad q = 1, \dots, n-1. \quad (54)$$

Next, for any  $q = 1, \dots, n-1$ , we differentiate the identity  $C_{ij}^{-1} \xi_q^i \xi_n^j = 0$  with respect to  $x^k$  to obtain

$$C_{ij,k}^{-1} \xi_q^i \xi_n^j + C_{ij}^{-1} \xi_{q,k}^i \xi_n^j + C_{ij}^{-1} \xi_q^i \xi_{n,k}^j = 0, \quad q = 1, \dots, n-1.$$

Multiplying this last equation by  $\xi_n^k$  and using the definition of  $\boldsymbol{\xi}_n$  and  $\boldsymbol{\xi}_q$  gives

$$C_{ij,k}^{-1} \xi_q^i \xi_n^j \xi_n^k + \frac{1}{\lambda_n} \xi_{q,k}^i \xi_n^i \xi_n^k + \frac{1}{\lambda_q} \xi_q^i \xi_n^i \xi_n^k = 0, \quad q = 1, \dots, n-1, \quad (55)$$

$$\mathbf{L} = \begin{pmatrix} C_{ij,kl}^{-1} \xi_n^i \xi_n^j \xi_n^k \xi_n^l & -2C_{ij,k}^{-1} \xi_n^i \xi_n^j \xi_n^k & -2C_{ij,k}^{-1} \xi_n^i \xi_n^j \xi_n^k & \cdots & -2C_{ij,k}^{-1} \xi_n^i \xi_n^j \xi_n^k \\ -2C_{ij,k}^{-1} \xi_n^i \xi_n^j \xi_n^k & \frac{2}{\lambda_1} - \frac{1}{\lambda_n} & 0 & \cdots & 0 \\ -2C_{ij,k}^{-1} \xi_n^i \xi_n^j \xi_n^k & 0 & \frac{2}{\lambda_2} - \frac{1}{\lambda_n} & \cdots & 0 \\ \vdots & \vdots & \vdots & \ddots & \vdots \\ -2C_{ij,k}^{-1} \xi_n^i \xi_n^j \xi_n^k & 0 & 0 & 0 & \frac{2}{\lambda_{n-1}} - \frac{1}{\lambda_n} \end{pmatrix} \quad (53)$$

### Box II.

where  $q$  indicates that there is no summation implied over  $q$ . Substituting (54) into (55), we obtain

$$C_{ij,k}^{-1} \xi_n^i \xi_n^j \xi_n^k = -\frac{\lambda_n - \lambda_q}{\lambda_n \lambda_q} \xi_n^i \xi_n^j \xi_n^k, \quad q = 1, \dots, n-1. \quad (56)$$

Next, we differentiate Eq. (46) with respect to  $x^l$  to obtain

$$\lambda_{n,kl} = -2\lambda_n \lambda_{n,l} C_{ij,k}^{-1} \xi_n^i \xi_n^j - \lambda_n^2 C_{ij,k}^{-1} \xi_n^i \xi_n^j - 2\lambda_n^2 C_{ij,k}^{-1} \xi_n^i \xi_n^j. \quad (57)$$

Multiplying (57) by  $\xi_n^k \xi_n^l$  and using the fact that  $\lambda_{n,l} \xi_n^l = 0$  by condition (i)/3, we obtain

$$\lambda_{n,kl} \xi_n^k \xi_n^l = -\lambda_n^2 C_{ij,k}^{-1} \xi_n^i \xi_n^j \xi_n^k \xi_n^l - 2\lambda_n^2 C_{ij,k}^{-1} \xi_n^i \xi_n^j \xi_n^k \xi_n^l,$$

or, equivalently,

$$C_{ij,kl}^{-1} \xi_n^i \xi_n^j \xi_n^k \xi_n^l = -\frac{1}{\lambda_n^2} \lambda_{n,kl} \xi_n^k \xi_n^l - 2C_{ij,k}^{-1} \xi_n^i \xi_n^j \xi_n^k \xi_n^l. \quad (58)$$

To evaluate the second term on the right-hand side of (58), we left-multiply the identity  $(\nabla \xi_n)^* \xi_n = \mathbf{0}$  by  $\xi_n^*$  to conclude that

$$\nabla \xi_n \xi_n \perp \xi_n, \quad (59)$$

and hence

$$\nabla \xi_n \xi_n = \sum_{q=1}^{n-1} \langle \xi_q, \nabla \xi_n \xi_n \rangle \xi_q.$$

Using this identity and (56), we can write

$$\begin{aligned} C_{ij,kl}^{-1} \xi_n^i \xi_n^j \xi_n^k \xi_n^l &= C_{ij,k}^{-1} \langle \xi_q, \nabla \xi_n \xi_n \rangle \xi_n^i \xi_n^j \xi_n^k \\ &= \langle \xi_q, \nabla \xi_n \xi_n \rangle C_{ij,k}^{-1} \xi_n^i \xi_n^j \xi_n^k \\ &= -\frac{\lambda_n - \lambda_q}{\lambda_n \lambda_q} \langle \xi_q, \nabla \xi_n \xi_n \rangle \xi_n^i \xi_n^j \xi_n^k \\ &= -\sum_{q=1}^{n-1} \frac{\lambda_n - \lambda_q}{\lambda_n \lambda_q} \langle \xi_q, \nabla \xi_n \xi_n \rangle^2, \end{aligned}$$

thus (58) can be re-written as

$$\begin{aligned} C_{ij,kl}^{-1} \xi_n^i \xi_n^j \xi_n^k \xi_n^l &= -\frac{1}{\lambda_n^2} \langle \xi_n, \nabla^2 \lambda_n \xi_n \rangle \\ &\quad + 2 \sum_{q=1}^{n-1} \frac{\lambda_n - \lambda_q}{\lambda_n \lambda_q} \langle \xi_q, \nabla \xi_n \xi_n \rangle^2, \end{aligned} \quad (60)$$

as we claimed in (32).

Substituting the expressions (56) and (60) into the expression (53) for  $\mathbf{L}(\mathbf{x}_0, t_0, T)$ , we obtain the coordinate-free form (31) for  $\mathbf{L}(\mathbf{x}_0, t_0, T)$ . This completes the proof that condition (ii) is necessary for  $\mathcal{M}(t_0)$  to be an LCS.

B. Conditions (i)–(ii) are also sufficient

We first note that applying Proposition 2 and using assumptions (i)/1 and (i)/2 for any point  $\mathbf{x}_0 \in \mathcal{M}(t_0)$  and unit normal  $\mathbf{n}_0 \equiv \xi_n(\mathbf{x}_0, t_0, T) \in N_{\mathbf{x}_0} \mathcal{M}(t_0)$ , we obtain

$$\begin{aligned} \rho_{t_0}^{t_0+T}(\mathbf{x}_0, \mathbf{n}_0) &= \frac{1}{\sqrt{\langle \xi_n, [\mathbf{C}_{t_0}^{t_0+T}(\mathbf{x}_0)]^{-1} \xi_n \rangle}} \\ &= \sqrt{\lambda_n(\mathbf{x}_0, t_0, T)} > 1, \\ \nu_{t_0}^{t_0+T}(\mathbf{x}_0, \mathbf{n}_0) &= \min_{\substack{|\mathbf{e}_0|=1 \\ \mathbf{e}_0 \in T_{\mathbf{x}_0} \mathcal{M}(t_0)}} \frac{\rho_{t_0}^t(\mathbf{x}_0)}{\sqrt{\langle \mathbf{e}_0, \mathbf{C}_{t_0}^t(\mathbf{x}_0) \mathbf{e}_0 \rangle}} \\ &= \frac{\sqrt{\lambda_n(\mathbf{x}_0, t_0, T)}}{\sqrt{\lambda_{n-1}(\mathbf{x}_0, t_0, T)}} > 1. \end{aligned} \quad (61)$$

Since  $\mathcal{M}(t_0)$  is assumed compact, (61) implies the existence of constants  $a, b > 0$  such that Definition 3 holds for  $\mathcal{M}(t_0)$ , and hence  $\mathcal{M}(t_0)$  is a repelling material surface over  $[t_0, t_0 + T]$ .

Given this, condition (38) ensures that  $\mathcal{M}(t_0)$  is a stationary surface for the repulsion rate  $\rho_{t_0}^{t_0+T}(\mathbf{x}_0, \mathbf{n}_0)$ . We have seen that if conditions (43) hold,  $\mathcal{M}(t_0)$  is indeed a stationary surface which proves the sufficiency of conditions (ii)/1–(ii)/3 for  $\mathcal{M}(t_0)$  to be a WLCS. We have also seen that the positive definiteness of  $\mathbf{L}(\mathbf{x}_0, t_0, T)$  guarantees that the strict extremum condition (50) holds, and hence  $\mathcal{M}(t_0)$  is an LCS under conditions (ii)/1 and (ii)/2 of the theorem. This completes the proof that conditions (i) and (ii) of Theorem 7 are also sufficient.  $\square$

A consequence of Theorem 7 is the following set of necessary conditions for hyperbolic LCS:

**Proposition 8** (Necessary Conditions for Hyperbolic LCS). Consider a compact material surface  $\mathcal{M}(t) \subset U$  which is a repelling LCS over the interval  $[t_0, t_0 + T]$ . Then the following must hold for all  $\mathbf{x}_0 \in \mathcal{M}(t_0)$ , the corresponding inverse Cauchy–Green strain tensor  $\mathbf{C}^{-1}(\mathbf{x}_0) \stackrel{\text{def}}{=} [\mathbf{C}_{t_0}^{t_0+T}(\mathbf{x}_0)]^{-1}$ , and its largest strain eigenvector  $\xi_n(\mathbf{x}_0) \stackrel{\text{def}}{=} \xi_n(\mathbf{x}_0, t_0, T)$ :

- (1)  $\lambda_{n-1}(\mathbf{x}_0, t_0, T) \neq \lambda_n(\mathbf{x}_0, t_0, T) > 1$ ,
- (2)  $\xi_n(\mathbf{x}_0, t_0, T) \perp T_{\mathbf{x}_0} \mathcal{M}(t_0)$ ,
- (3)

$$\nabla \mathbf{C}^{-1}(\mathbf{x}_0)[\xi_n(\mathbf{x}_0), \xi_n(\mathbf{x}_0), \xi_n(\mathbf{x}_0)] = 0,$$

or, equivalently,

$$\langle \nabla \lambda_n(\mathbf{x}_0, t_0, T), \xi_n(\mathbf{x}_0) \rangle = 0.$$

- (4)  $\nabla^2 \mathbf{C}^{-1}(\mathbf{x}_0)[\xi_n(\mathbf{x}_0), \xi_n(\mathbf{x}_0), \xi_n(\mathbf{x}_0), \xi_n(\mathbf{x}_0)] > 0$ .

**Proof.** Conditions (1) and (2) are just re-statements of the corresponding conditions in Theorem 7. Condition (3) is equivalent to condition (i)/3 of Theorem 7 by formula (47). Finally, condition (4) of the proposition as a necessary condition follows from the application of Sylvester's theorem to the matrix  $\mathbf{L}(\mathbf{x}_0, t_0, T)$  defined

in (31). Specifically, the positivity of the first diagonal entry of  $\mathbf{L}(\mathbf{x}_0, t_0, T)$  is a necessary condition for the positive definiteness of  $\mathbf{L}(\mathbf{x}_0, t_0, T)$ .  $\square$

Another consequence of note arises from an inspection of the proof of Theorem 7.

**Proposition 9** (Nonexistence of a Least Repelling Material Surface). *There exists no normally repelling material surface along which the repulsion rate  $\rho_{t_0}^{t_0+T}$  admits a pointwise nondegenerate local minimum among all  $C^1$ -close material surfaces.*

**Proof.** Assume the contrary, i.e., assume that  $\mathcal{M}(t)$  is such that at some  $\mathbf{x}_0 \in \mathcal{M}(t_0)$ , we have

$$\begin{aligned} \frac{\partial}{\partial \varepsilon} \rho_{t_0}^{t_0+T}(\mathbf{x}_\varepsilon(\mathbf{s}, t_0), \mathbf{n}_\varepsilon(\mathbf{s}, t_0))|_{\varepsilon=0} &= 0, \\ \frac{\partial^2}{\partial \varepsilon^2} \rho_{t_0}^{t_0+T}(\mathbf{x}_\varepsilon(\mathbf{s}, t_0), \mathbf{n}_\varepsilon(\mathbf{s}, t_0))|_{\varepsilon=0} &> 0, \end{aligned} \quad (62)$$

where we used the framework and formula (38) of the proof of Theorem 7.

Again, the first extremum condition in (62) is equivalent to

$$\lambda_{n-1} \neq \lambda_n > 1, \quad \hat{\xi}_n = \mathbf{n}_0, \quad \langle \nabla \lambda_n, \hat{\xi}_n \rangle = 0,$$

and the second condition in (62) would require the matrix  $\mathbf{L}(\mathbf{x}_0, t_0, T)$  defined in (31) to be negative definite. For  $\mathbf{L}(\mathbf{x}_0, t_0, T)$  to be negative definite, all its diagonal elements would need to be strictly negative. This is, however, not possible, because  $\lambda_q < \lambda_n$  holds for all  $q = 1, \dots, n-1$  on a repelling material surface by the requirement  $v_{t_0}^{t_0+T} > 1$ .  $\square$

## 5. Robustness of hyperbolic LCS

A major question about any coherent structure identification scheme is its robustness. If small data imperfections, numerical errors, or other sources of noise can significantly alter the identified structures, then the structures are of little practical use.

The only non-robust feature of an LCS turns out to be the exact alignment of its normals with the  $\hat{\xi}_n$  field. For material surfaces that are normally repelling for long enough  $T$ , however, the alignment error becomes numerically undetectable by Theorem 4. This motivates the following relaxed definition of a quasi-LCS (QLCS) for the purposes of establishing robustness.

**Definition 10** (Hyperbolic Quasi-LCS). Assume that  $\mathcal{M}(t) \subset U$  is a normally repelling material surface over  $[t_0, t_0 + T]$ . We call  $\mathcal{M}(t)$  a repelling quasi-LCS (QLCS) over  $[t_0, t_0 + T]$  if for all points  $\mathbf{x}_0 \in \mathcal{M}(t_0)$ :

1.  $\lambda_{n-1}(\mathbf{x}_0, t_0, T) \neq \lambda_n(\mathbf{x}_0, t_0, T) > 1$ .
2.  $\langle \nabla \lambda_n(\mathbf{x}_0, t_0, T), \hat{\xi}_n(\mathbf{x}_0, t_0, T) \rangle = 0$ .
3.  $\mathbf{L}(\mathbf{x}_0, t_0, T)$  is positive definite.

We call  $\mathcal{M}(t)$  an attracting QLCS over  $[t_0, t_0+T]$  if it is a repelling QLCS over  $[t_0, t_0 + T]$  in backward time. Finally, we call  $\mathcal{M}(t)$  a hyperbolic QLCS over  $[t_0, t_0 + T]$  if it is a repelling or an attracting QLCS over  $[t_0, t_0 + T]$ .

Note that a hyperbolic QLCS is only a candidate for a hyperbolic LCS: one has to verify that the time interval  $T$  is long enough so that  $\hat{\xi}_n(\mathbf{x}_0, t_0, T)$  is practically aligned with the normal of the QLCS modulo exponentially small errors in  $T$ . We have the following robustness result for QLCS.

**Theorem 11** (Sufficient Condition for Robustness of Hyperbolic LCS). Assume that  $\mathcal{M}(t_0) \subset U$  is a compact repelling LCS over  $[t_0, t_0 + T]$  such that

$$\langle \hat{\xi}_n, \nabla^2 \lambda_n \hat{\xi}_n \rangle + \langle \nabla \lambda_n, \nabla \hat{\xi}_n \hat{\xi}_n \rangle \neq 0 \quad (63)$$

holds at each point  $\mathbf{x}_0 \in \mathcal{M}(t_0)$ . Then, for any small enough smooth perturbation of the flow map  $\mathbf{F}_{t_0}^{t_0+T}$ , there exists a unique repelling QLCS that perturbs smoothly from  $\mathcal{M}(t_0)$ .

**Proof.** We first note that properties (1) and (3) in Definition 10 are defined by open conditions that are smooth with respect to small changes in  $\mathbf{F}_{t_0}^{t_0+T}$ . It remains to show that for small perturbations to  $\mathbf{F}_{t_0}^{t_0+T}$ , the zero set defined by condition (2) of Definition 10 smoothly persists.

For a small parameter  $\delta \geq 0$ , let

$$\hat{\mathbf{F}}_{t_0}^{t_0+T} = \mathbf{F}_{t_0}^{t_0+T} + \delta \Phi_{t_0}^{t_0+T}$$

denote a smooth perturbation of  $\mathbf{F}_{t_0}^{t_0+T}$ . We seek to solve the equation

$$\langle \nabla \hat{\lambda}_n(\mathbf{x}_0, t_0, T; \delta), \hat{\xi}_n(\mathbf{x}_0, t_0, T; \delta) \rangle = 0, \quad (64)$$

for the perturbed flow map. By assumption, any  $\mathbf{x}_0 \in \mathcal{M}(t_0)$  is a solution to this equation for  $\delta = 0$ . Eq. (64) has a unique solution that is  $\mathcal{O}(\delta)C^1$ -close to  $\mathcal{M}(t_0)$  for  $\delta > 0$  small enough, if from Eq. (64) we can locally express one coordinate  $x_0^i$  in the form

$$x_0^i = f(x_0^1, \dots, x_0^{i-1}, x_0^{i+1}, \dots, x_0^n, \delta),$$

for some smooth function  $f$ . By the implicit function theorem, this is possible if (i) the left-hand side of (64) is differentiable in  $\mathbf{x}_0$  and  $\delta$ , which is the case, and (ii) at least one coordinate of the gradient of the left-hand side of (64) is nonzero at  $\delta = 0$ , i.e.,

$$\nabla^2 \lambda_n \hat{\xi}_n + (\nabla \hat{\xi}_n)^* \nabla \lambda_n \neq \mathbf{0}.$$

Since  $\mathcal{M}(t_0)$  is assumed to be an LCS, the above gradient is parallel to the unit vector  $\hat{\xi}_n$ , and hence the gradient is nonzero precisely when its inner product with  $\hat{\xi}_n$  is nonzero, as assumed in (63).  $\square$

We close by noting that LCSs are also expected to be robust with respect to stochastic perturbations of the flow map, as long as individual realizations of the perturbation are smooth, and the mean of the perturbed flow satisfies the robustness condition (63). We will explore stochastic persistence of LCSs in more detail in another publication.

## 6. When does an FTLE ridge indicate a hyperbolic LCS?

First, we give a definition of an FTLE ridge that is somewhat weaker than the second-derivative ridge definition we used in analyzing the examples of Section 2.3 (cf. Appendix B).

**Definition 12** (FTLE Ridge). For a fixed time interval  $[t_0, t_0 + T]$ , we call a compact hypersurface  $\mathcal{M}(t_0) \subset U$  an FTLE ridge if for all  $\mathbf{x}_0 \in \mathcal{M}(t_0)$ , we have

$$\begin{aligned} \nabla \lambda_n(\mathbf{x}_0, t_0, T) &\in T_{\mathbf{x}_0} \mathcal{M}(t_0), \\ \langle \hat{\xi}_n(\mathbf{x}_0, t_0, T), \nabla^2 \lambda_n(\mathbf{x}_0, t_0, T) \hat{\xi}_n(\mathbf{x}_0, t_0, T) \rangle &< 0. \end{aligned} \quad (65)$$

This definition formulates the ridge conditions in terms of the  $\lambda_n$  field, which is equivalent to similar conditions on the FTLE field  $\Lambda_{t_0}^{t_0+T}$  by formula (9).

**Theorem 13** (Sufficient and Necessary Condition for a Hyperbolic LCS Based on an FTLE Ridge). Assume that  $\mathcal{M}(t_0) \subset U$  is a

compact FTLE ridge. Then  $\mathcal{M}(t) = F_t^t[\mathcal{M}(t_0)]$  is a repelling LCS over  $[t_0, t_0 + T]$  if and only if its points  $\mathbf{x}_0 \in \mathcal{M}(t_0)$  satisfy the following conditions:

1.  $\lambda_{n-1}(\mathbf{x}_0, t_0, T) \neq \lambda_n(\mathbf{x}_0, t_0, T) > 1$ ,
2.  $\xi_n(\mathbf{x}_0, t_0, T) \perp T_{\mathbf{x}_0}\mathcal{M}(t_0)$ ,
3. The matrix  $\mathbf{L}(\mathbf{x}_0, t_0, T)$  is positive definite.

**Proof.** Applying Theorem 7, we first note that assumptions (1) and (2) above are just re-statements of conditions (i)/1 and (i)/2 of that theorem. Next note that the first condition in (65) along with assumption (2) of this proposition implies that assumption (i)/3 of Theorem 7 is also satisfied, and hence  $\mathcal{M}(t_0)$  is a repelling WLCS. It remains to note that assumption (3) is identical to assumption (ii)/2 of Theorem 7, and hence the statement of Theorem 13 follows.  $\square$

The following sufficient condition for an FTLE-ridge-based LCS gives more geometric insight into the types of FTLE ridges on which condition (3) of Theorem 13 is known to hold. (At the same time, preliminary calculations show that this sufficient condition may reveal significantly fewer LCS than a direct application of Proposition 14.)

**Proposition 14** (Sufficient Condition for a Hyperbolic LCS Based on an FTLE Ridge). Assume that  $\mathcal{M}(t_0) \subset U$  is a compact FTLE ridge whose points  $\mathbf{x}_0 \in \mathcal{M}(t_0)$  satisfy all the following conditions:

- (1)  $\lambda_{n-1}(\mathbf{x}_0, t_0, T) \neq \lambda_n(\mathbf{x}_0, t_0, T) > 1$ ,
- (2)  $\xi_n(\mathbf{x}_0, t_0, T) \perp T_{\mathbf{x}_0}\mathcal{M}(t_0)$ ,
- (3)  $|\nabla \xi_n \xi_n| \leq 1$ ,
- (4)  $\langle \xi_n, \nabla^2 \lambda_n \xi_n \rangle < -2\lambda_n |\nabla \xi_n \xi_n| \sum_{q=1}^{n-1} [\lambda_n/\lambda_q - 1]$ .

Then  $\mathcal{M}(t) = F_t^t[\mathcal{M}(t_0)]$  is a repelling LCS over  $[t_0, t_0 + T]$ .

**Proof.** We only need to show that under assumptions (3)–(4) of the present proposition, assumption (3) of Theorem 13 is satisfied, i.e.,  $\mathbf{L}(\mathbf{x}_0, t_0, T)$  is positive definite. To see this, recall the classic criterion from linear algebra that a symmetric matrix with positive diagonal elements and with row-diagonal dominance is positive definite. Applying this criterion to  $\mathbf{L}(\mathbf{x}_0, t_0, T)$  translates to the sufficient conditions

$$\begin{aligned}
 & -\langle \xi_n, \nabla^2 \lambda_n \xi_n \rangle + 2\lambda_n^2 \sum_{q=1}^{n-1} \frac{\lambda_n - \lambda_q}{\lambda_n \lambda_q} \langle \xi_q, \nabla \xi_n \xi_n \rangle^2 > 0, \\
 & 2\lambda_n^2 \sum_{q=1}^{n-1} \frac{\lambda_n - \lambda_q}{\lambda_q \lambda_n} [|\langle \xi_q, \nabla \xi_n \xi_n \rangle| - \langle \xi_q, \nabla \xi_n \xi_n \rangle^2] \\
 & < -\langle \xi_n, \nabla^2 \lambda_n \xi_n \rangle, \\
 & |\langle \xi_q, \nabla \xi_n \xi_n \rangle| < 1 + \frac{\lambda_q}{2(\lambda_n - \lambda_q)}, \quad q = 1, \dots, n-1. \tag{66}
 \end{aligned}$$

Since for all  $q < n$ , we have  $\lambda_n > \lambda_q$  by assumption (1) of the proposition, the first condition in (66) is always satisfied on an FTLE ridge (cf. the second inequality in (65)).

Under assumption (3) of the proposition, we have

$$|\langle \xi_q, \nabla \xi_n \xi_n \rangle| < 1, \quad q = 1, \dots, n-1, \tag{67}$$

which ensures that the last condition in (66) is satisfied.

Finally, note that

$$\begin{aligned}
 & 2\lambda_n^2 \sum_{i=1}^{n-1} \frac{\lambda_n - \lambda_q}{\lambda_q \lambda_n} [|\langle \xi_q, \nabla \xi_n \xi_n \rangle| - \langle \xi_q, \nabla \xi_n \xi_n \rangle^2] \\
 & \leq 2\lambda_n \sum_{i=1}^{n-1} \left[ \frac{\lambda_n}{\lambda_q} - 1 \right] |\langle \xi_q, \nabla \xi_n \xi_n \rangle| \\
 & \leq 2\lambda_n |\nabla \xi_n \xi_n| \sum_{i=1}^{n-1} \left[ \frac{\lambda_n}{\lambda_q} - 1 \right],
 \end{aligned}$$

where we have used (67). Therefore, the second condition in (66) is also satisfied if assumption (4) of the proposition is satisfied.  $\square$

Assumptions (3)–(4) of Proposition 14 hold, for example, if the Cauchy–Green strain tensor is globally diagonal, and hence the derivative  $\nabla \xi_n$  vanishes identically (see Examples 1, 2, and 4).

We close this section by pointing out that the robustness condition (63) can be made more specific for FTLE ridges.

**Proposition 15** (Sufficient Condition for Robustness of an LCS Marked by an FTLE Ridge). Assume that  $\mathcal{M}(t_0) \subset U$  is a compact FTLE ridge whose points  $\mathbf{x}_0 \in \mathcal{M}(t_0)$  satisfy all the assumptions of Proposition 14. Assume further that

$$\langle \xi_n, \nabla^2 \lambda_n \xi_n \rangle + \langle \nabla \lambda_n, \nabla \xi_n \xi_n \rangle < 0 \tag{68}$$

holds at each point  $\mathbf{x}_0 \in \mathcal{M}(t_0)$ . Then, for any small enough smooth perturbation of the flow map  $F_{t_0}^{t_0+T}$ , there exists a unique nearby repelling QLCS that perturbs smoothly from  $\mathcal{M}(t_0)$ .

**Proof.** By Definition 12, we have  $\langle \xi_n, \nabla^2 \lambda_n \xi_n \rangle < 0$  along an FTLE ridge, and hence if that ridge is guaranteed to be an LCS by Proposition 14, then (63) follows from (68), as claimed.  $\square$

## 7. On the numerical detection of LCS

### 7.1. Alignment of the LCS normal with the largest strain eigenvector

As we remarked earlier, requiring the zero set of  $\langle \nabla \lambda_n, \xi_n \rangle$  to be orthogonal to the vector field  $\xi_n(\mathbf{x}_0, t_0, T)$  appears to be a restrictive condition, yet it emerges as a necessary requirement for the existence of an LCS by Theorem 7.

In view of the alignment result in Theorem 4, this orthogonality requirement is no longer surprising. Specifically, for a material surface that is normally repelling over a long enough time interval, the strain eigenvectors  $\xi_n(\mathbf{x}_0, t_0, T)$  align with the normals of the surface up to errors that are exponentially small in the time interval length  $T$  (cf. Fig. 11). If, for a given  $T$ , the normals to the zero set of  $\langle \nabla \lambda_n, \xi_n \rangle$  are not yet fully aligned with the  $\xi_n$  field, then there is not yet a locally strongest repelling material surface emerging over the time interval  $[t_0, t_0 + T]$ . This means that there exist small deformations of the zero set that produces slightly stronger repelling surfaces.

### 7.2. Algorithmic steps in LCS extraction

Theorem 7 suggests the following procedure for locating hyperbolic LCSs:

For the total time interval  $[t_0, t_0 + T]$  of interest,

- Step 1 Compute the two largest strain eigenvalue fields,  $\lambda_n(\mathbf{x}_0, t_0, T)$  and  $\lambda_{n-1}(\mathbf{x}_0, t_0, T)$ , as well as the largest strain eigenvector field  $\xi_n(\mathbf{x}_0, t_0, T)$ .
- Step 2 Locate the solution set  $Z$  of the nonlinear equation  $\langle \nabla \lambda_n(\mathbf{x}_0, t_0, T), \xi_n(\mathbf{x}_0, t_0, T) \rangle = 0$ .
- Step 3 Identify repelling WLCSs at time  $t_0$  as the subset  $Z_{\text{WLCS}} \subset Z$  on which (i)  $\lambda_{n-1} \neq \lambda_n > 1$  and (ii)  $\xi_n(\mathbf{x}_0, t_0, T) \perp T_{\mathbf{x}_0} Z_{\text{WLCS}}$ .
- Step 4 Identify repelling LCSs as the  $n - 1$ -dimensional surface  $Z_{\text{LCS}} \subset Z_{\text{WLCS}}$  on which  $\mathbf{L}(\mathbf{x}_0, t_0, T)$  (cf. (31)) is positive definite.
- Step 5 Repeat the above steps starting from  $t_0 + T$  back to  $t_0$  in backward time to obtain attracting WLCSs and LCSs at time  $t_0 + T$ .
- Step 6 Verify that the quantity  $\langle \xi_n, (\nabla^2 \lambda_n) \xi_n \rangle + \langle \nabla \lambda_n, (\nabla \xi_n) \xi_n \rangle$  is bounded away from zero to ensure the robustness of the LCSs.

As we have discussed, the angle between  $\xi_n$  and a local normal to a repelling LCS becomes exponentially small for large enough  $T$ . As a result, an approximate alignment between  $\xi_n$  and the normals of  $Z$  in Step 3 above is sufficient for computational purposes.

### 7.3. Numerical errors

The computation of the invariants of the Cauchy–Green strain tensor  $\mathbf{C}_{t_0}^t$  is numerically sensitive along LCSs. This is due to the (locally strongest) exponential separation of trajectories near repelling LCSs, which makes the accurate calculation of derivatives with respect to initial conditions challenging. In addition, Steps 2, 4, and 6 involve the calculation of second derivatives, further increasing the demand for a high-end numerical platform for the reliable extraction of LCSs. As a payoff, this computational investment leads to a sufficient and necessary mathematical criterion that eliminates false positives and missed structures.

### 7.4. Tracking LCS in time

By the approach taken in this paper, LCSs are truly Lagrangian structures: they are material surfaces across which no phase space transport occurs. By Definition 6, the existence of such an LCS is tied to a finite time-interval  $[t_0, t_0 + T]$  over which it satisfies an extremum problem.

The same material surface is not guaranteed to satisfy a similar extremum problem over another time interval  $[t_1, t_1 + T]$  in dynamical systems with general time dependence. It is natural to try and estimate the degree of non-invariance for LCS computed over a rolling time interval  $[t, t + T]$ , but the resulting flux estimate, in general, is more complicated than previously thought (see Appendix C) and requires the computation of higher-order terms. Overall, therefore, the benefit of deriving a general flux formula over calculating the flux through an FTLE ridge numerically is unclear.

Applying the following steps will ensure that the extracted LCSs are fully Lagrangian, i.e., invariant, not just almost invariant:

**Step A** Find  $\mathcal{M}(t_0)$  by computing the conditions of Theorem 7 (or one of the related propositions) over the maximum time interval  $[t_0, t_0 + T]$  available.

**Step B** Locate later positions of the LCS  $\mathcal{M}(t_0)$  as

$$\mathcal{M}(t) = \mathbf{F}_{t_0}^t[\mathcal{M}(t_0)]. \quad (69)$$

Step B requires accurate numerical advection schemes, as the implementation of (69) involves the propagation of an unstable surface under the flow map. Still, we gain conceptual clarity and invariance using the above construction. Employing (69) also eliminates the emergence of ill-defined LCS (manifested by a fade-out of FTLE plots for larger  $t$ ) as we approach the end of a finite-time data set.

## 8. Examples of hyperbolic LCS

### 8.0.1. Example 5: linear saddle flow

Consider again the linear strain flow

$$\begin{aligned} \dot{x} &= x, \\ \dot{y} &= -y, \end{aligned} \quad (70)$$

analyzed in Example 1. The Cauchy–Green strain tensor for this example is simply

$$\mathbf{C}_{t_0}^{t_0+T}(\mathbf{x}_0) = \begin{pmatrix} e^{2T} & 0 \\ 0 & e^{-2T} \end{pmatrix},$$

with eigenvalues and eigenvectors

$$\begin{aligned} \lambda_1 &= e^{-2T}, & \lambda_2 &= e^{2T}, \\ \xi_1 &= \begin{pmatrix} 0 \\ 1 \end{pmatrix}, & \xi_2 &= \begin{pmatrix} 1 \\ 0 \end{pmatrix}. \end{aligned} \quad (71)$$

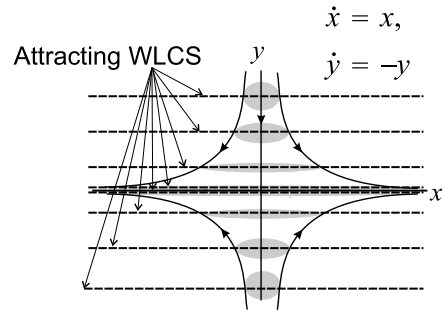


**Fig. 13.** Each advected horizontal line of this linear strain flow forms a material surface that is an attracting WLCS. Indeed, all blobs of initial conditions are visibly attracted at the same normal rate to these material surfaces while all WLCSs converge to each other.

Since  $\lambda_2$  is a constant field, condition (ii)/2 of Theorem 7 is violated, and hence system (70) admits *no repelling LCS* in the sense Definition 6.

As for WLCS, note that conditions (i)/1 and (i)/3 of Theorem 7 hold at any point  $\mathbf{x}_0$  in the phase space. Then condition (i)/2 and (71) imply that *all vertical material lines are repelling WLCSs*. Similarly, we obtain that *all horizontal material lines are attracting WLCSs* by applying Theorem 7 to system (70) in backward time. Indeed, each horizontal line is advected by this linear flow into a moving material line that acts as a core Lagrangian structure on which trajectories accumulate, as shown in Fig. 13.

### 8.0.2. Example 6: linear–cubic saddle flow

Consider again the linear–cubic saddle point flow

$$\begin{aligned} \dot{x} &= x, \\ \dot{y} &= -y - y^3, \end{aligned} \quad (72)$$

already analyzed in Example 1. We have concluded that this system has a trough in backward time along the  $x$  axis; therefore the  $x$  axis is not an attracting LCS by Theorem 7 (applied in backward time).

The Cauchy–Green strain tensor for this example is explicitly computable as

$$\mathbf{C}_{t_0}^t(\mathbf{x}_0) = \begin{pmatrix} e^{2(t-t_0)} & 0 \\ 0 & \frac{e^{4(t-t_0)}}{[(1+y_0^2)e^{2(t-t_0)} - y_0^2]^3} \end{pmatrix},$$

as we show in Appendix B. In backward time (i.e., for  $t_0 - \log \sqrt{5} < t < t_0$ ; cf. Appendix B) we find for the above tensor that

$$\lambda_2(y_0, t_0, t - t_0) = \frac{e^{4(t-t_0)}}{[(1+y_0^2)e^{2(t-t_0)} - y_0^2]^3} > 0,$$

$$\lambda_1 = e^{2(t-t_0)} < \lambda_2, \quad \xi_2 = \begin{pmatrix} 0 \\ 1 \end{pmatrix},$$

$$\langle \nabla \lambda_2(0, t_0, t - t_0), \xi_2(0, t_0, t - t_0) \rangle \equiv 0.$$

Therefore, applying Theorem 7 in backward time, we conclude that the  $y = 0$  axis is an *attracting WLCS*, as originally expected from Fig. 4.

Since the strain eigenvector field is constant in  $\mathbf{x}_0$ , we have  $\nabla \xi_n \equiv \mathbf{0}$ . Therefore, Theorem 7 requires  $\langle \xi_2, \nabla^2 \lambda_2 \xi_2 \rangle < 0$  as a necessary condition for a repelling LCS for system (72) in backward time. As we have seen in Appendix A, the  $x$  axis is a trough for the backward FTLE field, and hence  $\langle \xi_2, \nabla^2 \lambda_2 \xi_2 \rangle > 0$ . We therefore conclude that the  $x$  axis is *not* an attracting LCS.

8.0.3. Example 7: parallel shear flow

Consider again the parallel shear flow

$$\begin{aligned} \dot{x} &= 2 + \tanh y, \\ \dot{y} &= 0, \end{aligned}$$

analyzed in Example 2, with its phase portrait sketched in Fig. 6. Recall that this system has a second-derivative forward FTLE ridge along the  $y = 0$  axis, yet that axis is not a repelling LCS.

From the explicit solutions (112), we obtain that along the  $y_0 = 0$  axis, the Cauchy–Green strain tensor takes the form

$$\mathbf{C}_{t_0}^{t_0+T}((x_0, 0)) = \begin{pmatrix} 1 & 1+T \\ 1+T & 1+T^2 \end{pmatrix}.$$

For any  $t > t_0$ , the eigenvalues and unit eigenvectors of this tensor can be written as

$$\begin{aligned} \lambda_2 &= 1 + \frac{1}{2}T^2a^2 + \frac{1}{2}Ta\sqrt{T^2a^2 + 4}, \\ \xi_2 &= \begin{pmatrix} \frac{-\frac{1}{2}\sqrt{T^2a^2 + 4} - \frac{1}{2}Ta}{\sqrt{1 + \frac{1}{2}T^2a^2 + \frac{1}{2}Ta\sqrt{T^2a^2 + 4}}} \\ 1 \end{pmatrix}, \\ \lambda_1 &= 1 + \frac{1}{2}T^2a^2 - \frac{1}{2}Ta\sqrt{T^2a^2 + 4}, \\ \xi_1 &= \begin{pmatrix} \frac{\frac{1}{2}\sqrt{T^2a^2 + 4} - \frac{1}{2}Ta}{\sqrt{1 + \frac{1}{2}T^2a^2 - \frac{1}{2}Ta\sqrt{T^2a^2 + 4}}} \\ 1 \end{pmatrix}. \end{aligned}$$

Observe that for any  $T \in \mathbb{R}$ , we have

$$\xi_2 \neq \mathbf{n}_0^\pm = \begin{pmatrix} 0 \\ \pm 1 \end{pmatrix},$$

with  $\mathbf{n}_0^\pm$  denoting the two possible choices of a unit normal along the  $y_0 = 0$  axis. As a result, condition (i)2 of Theorem 7 fails, and the  $y_0 = 0$  axis is therefore neither a WLCS nor an LCS.

8.0.4. Example 8: LCS in Example 4

Recall the dynamical system

$$\begin{aligned} \dot{x} &= 1 + \tanh^2 x \\ \dot{y} &= -y, \end{aligned} \tag{73}$$

from Example 4, with its phase portrait shown in Fig. 7. We have shown that defining LCSs as FTLE ridges would yield a repelling LCS of the form

$$\hat{\mathcal{M}}(t) \equiv \left\{ \begin{pmatrix} 0 \\ y_0 \end{pmatrix} \in \mathbb{R}^2 : y_0 \in \mathbb{R} \right\}. \tag{74}$$

We have pointed out, however, that  $\hat{\mathcal{M}}(t)$  is not even approximately Lagrangian: the area flux per unit length through this axis is equal to one.

We now show how Definition 6 and Proposition 14 resolve the above contradiction. First, recall from Appendix A that the Cauchy–Green strain tensor for this example is of the form

$$\mathbf{C}_{t_0}^t(\mathbf{x}_0) = \begin{pmatrix} \left[ \frac{1 + \frac{e^{2x_0}}{e^{4x_0} + 1}}{1 + \frac{e^{2x(t-t_0;x_0)}}{e^{4x(t-t_0;x_0)} + 1}} \right]^2 & 0 \\ 0 & e^{-2(t-t_0)} \end{pmatrix}, \tag{75}$$

with eigenvalues and unit eigenvectors satisfying

$$\begin{aligned} \lambda_2((0, y_0), t_0) &= \left[ \frac{1 + \frac{e^{2x_0}}{e^{4x_0} + 1}}{1 + \frac{e^{2x(t-t_0;x_0)}}{e^{4x(t-t_0;x_0)} + 1}} \right]^2, \\ \xi_2((0, y_0), t_0) &= \begin{pmatrix} 1 \\ 0 \end{pmatrix}, \\ \lambda_1((0, y_0), t_0) &= e^{-2(t-t_0)}, \quad \xi_1((0, y_0), t_0) = \begin{pmatrix} 0 \\ 1 \end{pmatrix}. \end{aligned}$$

Observe that

$$\xi_2((0, y_0), t_0) = \mathbf{n}_0((0, y_0), t_0),$$

and by our analysis in Appendix A, for large enough  $t = t_0 + T$ , we have

$$\begin{aligned} \lambda_1((0, y_0), t_0) &\neq \lambda_2((0, y_0), t_0) > 1, \\ \langle \nabla \lambda_2((0, y_0), t_0), \xi_2((0, y_0), t_0) \rangle &= 0. \end{aligned} \tag{76}$$

Also observe from Eq. (75) that the that strain eigenvector field,  $\xi_2 = (1, 0)^*$ , is constant at all points in the phase space. As a result, we have  $\nabla \xi_n \xi_n \equiv \mathbf{0}$  and hence assumptions (3)–(4) of Proposition 14 are satisfied if the  $y_0$  axis is an FTLE ridge.

To apply Proposition 14, it remains to show that the  $y_0$  axis is an FTLE ridge in the sense of Definition 12. The first condition in (65) is satisfied, and the second condition in (65) takes the specific form

$$\langle \xi_2((0, y_0), t_0), \nabla^2 \lambda_2((0, y_0), t_0) \xi_2((0, y_0), t_0) \rangle < 0, \tag{77}$$

which we have already verified for system (73) in Appendix A. We conclude that by (76) and (77), assumptions (1)–(3) of Proposition 14 hold.

Therefore, by Proposition 14, for any choice of the initial time  $t_0$  and for large enough  $T$ , the material surface

$$\mathcal{M}(t) = \left\{ \begin{pmatrix} 0 \\ y \end{pmatrix} \in \mathbb{R}^2 : \begin{pmatrix} 0 \\ y \end{pmatrix} = \mathbf{F}_{t_0}^t \left( \begin{pmatrix} 0 \\ y_0 \end{pmatrix} \right) \right\} \tag{78}$$

is a repelling LCS over the time interval  $[t_0, t_0 + T]$ . Here the flow map  $\mathbf{F}_{t_0}^t$  is defined implicitly by the formula (113) for the solutions of system (16).

The LCS defined in (78) is guaranteed to be locally the strongest repelling material line, and should therefore be observable as the core of an expanding Lagrangian trajectory pattern. To verify this, we slightly modify (16) to the form

$$\begin{aligned} \dot{x} &= 1 + 40 \tanh^2 \frac{x}{2}, \\ \dot{y} &= -0.1y, \end{aligned} \tag{79}$$

to enhance the extremum property of  $\mathcal{M}(t)$  on shorter time scales for the purposes of illustration.

In Fig. 14, we show three snapshots of an array of trajectories starting at time  $t_0 = 0$ , then evolving into their later positions at time  $T = 1.05$ . Note that the FTLE field develops a ridge which gradually moves towards the  $x = 0$  axis, becoming indistinguishable from that axis by time  $T$ . Accordingly, the material surface  $\mathcal{M}(t)$  defined in (78) emerges as the strongest normally repelling material surface over the time interval  $[0, T]$ , as confirmed by the subplot (c). On shorter times scales, the FTLE ridge is still further away from the  $x = 0$  axis; accordingly, the strongest normally repelling LCS is a vertical material line that is different from the  $x = 0$  axis, as shown in subplot (b).

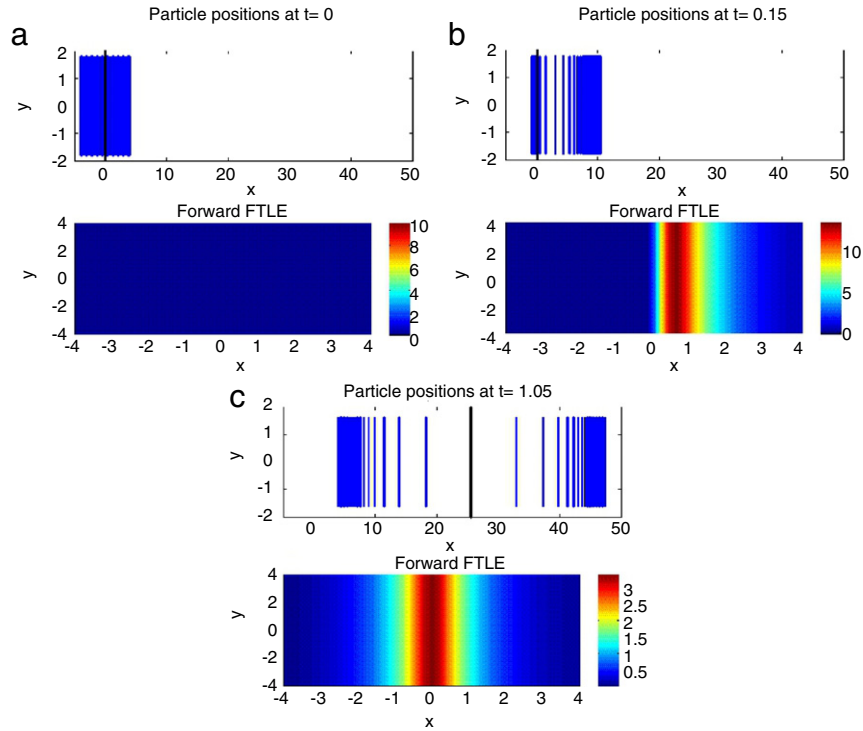


**Fig. 14.** Three snapshots of the evolution of an array of trajectories for system (79). (a) Initial positions, with the  $x = 0$  line highlighted, which approximates a repelling SLCS over  $[0, 1.06]$ . (b) Intermediate positions, with the FTLE plot revealing a strong repelling LCS over  $[0, 0.15]$ , which is initially located along the vertical line  $x \approx 0.6$  at time  $t = 0$ . (c) Final particle positions at  $T = 1.05$ , confirming that the surface defined in Eq. (78) is indeed the strongest repelling material surface over the time interval  $[0, 1.05]$ .

### 9. Constrained LCS

So far, we have identified hyperbolic LCSs as solutions of an extremum problem. Here we restrict this general extremum problem to a constrained extremum problem: we seek to find the most attracting or repelling material surface out of a prescribed family of codimension-one surfaces.

An example where this approach is conceptually useful is the linear saddle flow  $\dot{x} = x, \dot{y} = -y$ . Out of all the attracting WLCS we have identified for this system in Example 5 (i.e., all horizontal material lines), the  $x$  axis is the only one that is also an invariant manifold in the phase space of (70). Seeking the most normally repelling or attracting *invariant manifold* (as opposed to a general material line) in this flow is therefore a constrained LCS problem.

Another example of interest is finding an LCS in a Hamiltonian system. Again, instead of seeking general material surfaces that pointwise extremize the normal repulsion rate, one may restrict the extremum search to material surfaces that are codimension-one level sets of the Hamiltonian.

In both of the above examples, the LCS constraint can be implemented by expressing the unit normal  $\mathbf{n}_0$  in the definition of the repulsion rate  $\rho_{i_0}^{t_0+T}$  (cf. (19)) as a function of  $\mathbf{x}_0$  and  $t_0$ . Below we discuss this approach for two classes of dynamical systems: planar autonomous systems and  $n$ -dimensional non-autonomous dynamical systems with a first integral.

#### 9.1. Constrained LCS in two-dimensional autonomous systems

Consider the two-dimensional autonomous system

$$\dot{\mathbf{x}} = \mathbf{v}(\mathbf{x}), \quad \mathbf{x} \in U \subset \mathbb{R}^2, \quad (80)$$

with the one-parameter flow map

$$\mathbf{F}^T: U \rightarrow U,$$

$$\mathbf{x}_0 \mapsto \mathbf{x}(T, 0, \mathbf{x}_0).$$

The corresponding Cauchy–Green strain tensor field is defined as

$$\mathbf{C}^T(\mathbf{x}_0) = (\nabla \mathbf{F}^T(\mathbf{x}_0))^* \nabla \mathbf{F}^T(\mathbf{x}_0),$$

with eigenvalues and eigenvectors

$$0 \leq \lambda_1(\mathbf{x}_0, T) \leq \lambda_2(\mathbf{x}_0, T),$$

$$\mathbf{C}^T(\mathbf{x}_0) \xi_i(\mathbf{x}_0, T) = \lambda_i(\mathbf{x}_0, T) \xi_i(\mathbf{x}_0, T), \quad i = 1, 2.$$

For any  $\mathbf{x}$  with  $\mathbf{v}(\mathbf{x}) \neq \mathbf{0}$ , we define the unit vector fields

$$\mathbf{n}(\mathbf{x}) = \frac{\Omega \mathbf{v}(\mathbf{x})}{|\mathbf{v}(\mathbf{x})|}, \quad \Omega = \begin{pmatrix} 0 & 1 \\ -1 & 0 \end{pmatrix}, \quad (81)$$

$$\mathbf{e}(\mathbf{x}) = \frac{\mathbf{v}(\mathbf{x})}{|\mathbf{v}(\mathbf{x})|},$$

which are pointwise normal and tangential, respectively, to all non-equilibrium trajectories of (80).

For any trajectory crossing a point  $\mathbf{x}_0 \in U$  with  $\mathbf{v}(\mathbf{x}_0) \neq \mathbf{0}$ , we define locally the *trajectory-normal repulsion rate*  $\rho_T(\mathbf{x}_0)$  over the time interval  $[0, T]$  as

$$\rho_T(\mathbf{x}_0) = \langle \mathbf{n}(\mathbf{F}^T(\mathbf{x}_0)), \nabla \mathbf{F}^T(\mathbf{x}_0) \mathbf{n}(\mathbf{x}_0) \rangle, \quad (82)$$

where  $\mathbf{n}(\mathbf{x}_0)$  is a smooth unit normal vector field to the trajectories of (80). We also define the *trajectory-normal repulsion ratio*

$$v_T(\mathbf{x}_0) = \frac{\langle \mathbf{n}(\mathbf{F}^T(\mathbf{x}_0)), \nabla \mathbf{F}^T(\mathbf{x}_0) \mathbf{n}(\mathbf{x}_0) \rangle}{|\nabla \mathbf{F}^T(\mathbf{x}_0) \mathbf{e}(\mathbf{x}_0)|}. \quad (83)$$

As before,  $\rho_T(\mathbf{x}_0) > 1$  indicates strict normal growth of infinitesimal normal perturbations to the trajectory through  $\mathbf{x}_0$  over the time interval  $[0, T]$ . Similarly,  $v_T(\mathbf{x}_0) > 1$  implies that this normal growth dominates any potential infinitesimal growth in the tangent direction along the trajectory.

In analogy with Proposition 2, the above finite-time normal repulsion measures can be computed as follows:

**Proposition 16.** The quantities  $\rho_T(\mathbf{x}_0)$  and  $v_T(\mathbf{x}_0)$  satisfy the expressions

$$\begin{aligned}\rho_T(\mathbf{x}_0) &= \sqrt{\frac{|\mathbf{v}(\mathbf{x}_0)|^2 \det \mathbf{C}^T(\mathbf{x}_0)}{\langle \mathbf{v}(\mathbf{x}_0), \mathbf{C}^T(\mathbf{x}_0) \mathbf{v}(\mathbf{x}_0) \rangle}}, \\ v_T(\mathbf{x}_0) &= \frac{|\mathbf{v}(\mathbf{x}_0)|^2 \sqrt{\det \mathbf{C}^T(\mathbf{x}_0)}}{\langle \mathbf{v}(\mathbf{x}_0), \mathbf{C}^T(\mathbf{x}_0) \mathbf{v}(\mathbf{x}_0) \rangle}.\end{aligned}\quad (84)$$

**Proof.** We obtain this result by following the proof of Proposition 2, and noting that

$$\mathbf{\Omega}^* [\mathbf{C}^T(\mathbf{x}_0)]^{-1} \mathbf{\Omega} = \frac{1}{\det \mathbf{C}^T(\mathbf{x}_0)} \mathbf{C}^T(\mathbf{x}_0),$$

which can be verified by direct calculation, using the symmetry of  $\mathbf{C}^T$  and the definition of  $\mathbf{\Omega}$ .  $\square$

We now reformulate our earlier general definitions of finite-time normal repulsion and attraction for a trajectory segment of the two-dimensional autonomous system (80).

**Definition 17 (Hyperbolic Trajectory Segment).** A trajectory segment  $\mathcal{M} \subset U$  is normally repelling over  $[0, T]$  if there exist constants  $a, b > 0$  such that for all points  $\mathbf{x}_0 \in \mathcal{M}$  we have

$$\begin{aligned}\rho_T(\mathbf{x}_0) &\geq e^{aT}, \\ v_T(\mathbf{x}_0) &\geq e^{bT}.\end{aligned}$$

Similarly, we call  $\mathcal{M}$  normally attracting over  $[0, T]$  if it is repelling over  $[0, T]$  in backward time. Finally, we call  $\mathcal{M}$  hyperbolic over  $[0, T]$  if it is normally repelling or normally attracting over  $[0, T]$ .

The following two definitions are analogues of our earlier definitions for weak LCS and LCS:

**Definition 18 (Hyperbolic Weak Constrained LCS).** Assume that a trajectory segment  $\mathcal{M} \subset U$  is normally repelling over  $[0, T] \subset \mathcal{I}$ . We call  $\mathcal{M}$  a repelling Weak Constrained LCS (WCLCS) over  $[0, T]$  if its normal repulsion rate admits a pointwise stationary value along  $\mathcal{M}$  among all locally  $C^1$ -close trajectories. Similarly, we call  $\mathcal{M}$  an attracting WCLCS over  $[0, T]$  if it is a repelling WCLCS over  $[0, T]$  in backward time. Finally, we call  $\mathcal{M}$  a hyperbolic WCLCS over  $[0, T]$  if it is a repelling or attracting WCLCS over  $[0, T]$ .

**Definition 19 (Hyperbolic Constrained LCS).** Assume that a trajectory segment  $\mathcal{M} \subset U$  normally repelling over  $[0, T]$ . We call  $\mathcal{M}$  a repelling Constrained LCS (CLCS) over  $[0, T]$  if its normal repulsion rate admits a nondegenerate maximum along  $\mathcal{M}$  among all locally  $C^1$ -close trajectories. Similarly, we call  $\mathcal{M}$  an attracting CLCS over  $[0, T]$  if it is a repelling CLCS over  $[0, T]$  in backward time. Finally, we call  $\mathcal{M}$  a hyperbolic CLCS over  $[0, T]$  if it is a repelling or attracting CLCS over  $[0, T]$ .

The following theorem is a reformulation of Theorem 7 for the present two-dimensional, constrained LCS context.

**Theorem 20 (Sufficient and Necessary Condition for Hyperbolic Weak CLCS and CLCS).** Consider a compact trajectory segment  $\mathcal{M} \subset U$ . Then

- (i)  $\mathcal{M}$  is a repelling WCLCS over  $[0, T]$  if and only if all the following hold for all  $\mathbf{x}_0 \in \mathcal{M}$ :
  1.  $\rho_T(\mathbf{x}_0) > 1$ ,  $v_T(\mathbf{x}_0) > 1$ ,
  2.  $\langle \nabla \rho_T(\mathbf{x}_0), \mathbf{n}(\mathbf{x}_0) \rangle = 0$ .
- (ii)  $\mathcal{M}$  is a repelling CLCS over  $[0, T]$  if and only if
  1.  $\mathcal{M}$  is a repelling WCLCS over  $[0, T]$ ,
  2.  $\langle \mathbf{n}(\mathbf{x}_0), \nabla^2 \rho_T(\mathbf{x}_0) \mathbf{n}(\mathbf{x}_0) \rangle < 0$  for all  $\mathbf{x}_0 \in \mathcal{M}$ .

**Proof.** The proof of the theorem follows closely the proof of Theorem 7. The only difference is that in our search for WCLCS and CLCS, we restrict the class of  $C^1$ -close material surfaces to  $C^1$ -close trajectory segments. As a result, we have constraints on the normal  $\mathbf{n}_\varepsilon(s, t_0)$  and the perturbed trajectory point  $\mathbf{x}_\varepsilon(s, t_0)$  in the form

$$\begin{aligned}\mathbf{n}_\varepsilon(s, t_0) &= \mathbf{n}(\mathbf{x}_\varepsilon(s, t_0)) = \frac{\mathbf{\Omega} \mathbf{v}(\mathbf{x}_\varepsilon(s, t_0))}{|\mathbf{v}(\mathbf{x}_\varepsilon(s, t_0))|}, \\ \mathbf{x}_\varepsilon(s, t_0) &= \mathbf{x}_0(s) + \varepsilon \alpha(s, t_0) \mathbf{n}(\mathbf{x}_\varepsilon(s, t_0)) \\ &= \mathbf{x}_0(s) + \varepsilon \alpha(s, t_0) \mathbf{n}(\mathbf{x}_0(s)) + \varepsilon^2 \alpha(s, t_0) \frac{\partial \mathbf{n}(\mathbf{x}_0(s))}{\partial \mathbf{x}_0}.\end{aligned}$$

The two extremum conditions, (38) and (50), used in the proof of Theorem 7 now simplify to

$$\begin{aligned}\frac{\partial}{\partial \varepsilon} \rho_{t_0}^{t_0+T}(\mathbf{x}_\varepsilon(s, t_0), \mathbf{n}(\mathbf{x}_\varepsilon(s, t_0)))|_{\varepsilon=0} &= \frac{\partial}{\partial \varepsilon} \rho_T(\mathbf{x}_\varepsilon(s, t_0))|_{\varepsilon=0} \\ &= 0, \\ \frac{\partial^2}{\partial \varepsilon^2} \rho_{t_0}^{t_0+T}(\mathbf{x}_\varepsilon(s, t_0), \mathbf{n}(\mathbf{x}_\varepsilon(s, t_0)))|_{\varepsilon=0} &= \frac{\partial^2}{\partial \varepsilon^2} \rho_T(\mathbf{x}_\varepsilon(s, t_0))|_{\varepsilon=0} \\ &< 0,\end{aligned}\quad (85)$$

or, equivalently,

$$\alpha \left\langle \frac{\partial \rho_T(\mathbf{x}_0)}{\partial \mathbf{x}_0}, \mathbf{n}(\mathbf{x}_0) \right\rangle = 0,$$

and

$$\begin{aligned}\frac{\partial^2}{\partial \varepsilon^2} \rho_T(\mathbf{x}_\varepsilon(s, t_0))|_{\varepsilon=0} &= \alpha(s, t_0) \frac{\partial}{\partial \varepsilon} \left\langle \frac{\partial}{\partial \mathbf{x}_0} \rho_T(\mathbf{x}_\varepsilon(s, t_0)), \mathbf{n}(\mathbf{x}_\varepsilon(s, t_0)) \right\rangle \Big|_{\varepsilon=0} \\ &= \alpha^2(s, t_0) \left\langle \mathbf{n}(\mathbf{x}_0), \frac{\partial^2 \rho_T(\mathbf{x}_0)}{\partial \mathbf{x}_0^2} \mathbf{n}(\mathbf{x}_0) \right\rangle \\ &\quad + \alpha^2(s, t_0) \left\langle \frac{\partial \rho_T(\mathbf{x}_0)}{\partial \mathbf{x}_0}, [\nabla \mathbf{n}(\mathbf{x}_0)]^* \mathbf{n}(\mathbf{x}_0) \right\rangle \\ &= \alpha^2(s, t_0) \left\langle \mathbf{n}(\mathbf{x}_0), \frac{\partial^2 \rho_T(\mathbf{x}_0)}{\partial \mathbf{x}_0^2} \mathbf{n}(\mathbf{x}_0) \right\rangle < 0,\end{aligned}$$

where we have used the relation  $[\nabla \mathbf{n}(\mathbf{x}_0)]^* \mathbf{n}(\mathbf{x}_0) = \mathbf{0}$ , obtained by differentiating  $\langle \mathbf{n}(\mathbf{x}_0), \mathbf{n}(\mathbf{x}_0) \rangle = 1$  with respect to  $\mathbf{x}_0$ .

We conclude that the extremum conditions (85) are equivalent to

$$\begin{aligned}\alpha \left\langle \frac{\partial \rho_T(\mathbf{x}_0)}{\partial \mathbf{x}_0}, \mathbf{n}(\mathbf{x}_0) \right\rangle &= 0, \\ \alpha^2 \left\langle \mathbf{n}(\mathbf{x}_0), \frac{\partial^2 \rho_T(\mathbf{x}_0)}{\partial \mathbf{x}_0^2} \mathbf{n}(\mathbf{x}_0) \right\rangle &< 0.\end{aligned}\quad (86)$$

The first of these conditions in (86) (to be satisfied for any choice of the smooth function  $\alpha$ ) is sufficient and necessary for  $\rho_T$  to admit stationary values along the trajectory segment  $\mathcal{M}$  with respect to  $C^1$ -close trajectories. The first and second conditions in (86) together are sufficient and necessary for  $\rho_T$  to admit nondegenerate local maxima along  $\mathcal{M}$  with respect to  $C^1$ -close trajectories. Based on these considerations, the proof of the theorem is complete.  $\square$

### 9.1.1. Example 9: attracting CLCS in a linear saddle flow

We again consider the linear flow

$$\begin{aligned}\dot{x} &= x, \\ \dot{y} &= -y,\end{aligned}\quad (87)$$

analyzed in Examples 1 and 5. Recall from Example 5 that any horizontal line

$$\mathcal{M}(t_0) = \{(x, y) \in \mathbb{R}^2 : y = y_0\}$$

gives rise to an attracting WLCS,  $\mathcal{M}(t) = \mathbf{F}_t^1[\mathcal{M}(t_0)]$ , over any finite time-interval  $[0, T]$ . So far, we have not found a way to distinguish the  $\{y_0 = 0\}$  axis from all other WLCSs even though this axis is the fundamental attracting structure to which all WLCSs converge.

Intuitively, however, we expect  $\{y_0 = 0\}$  to be the locally strongest normally attracting trajectory (as opposed to material line) away from the origin. This is because the direction of strongest attraction is parallel to the  $y$  axis, and hence during any finite time-interval, the  $\{y_0 = 0\}$  experiences the largest attraction in its normal direction. All other trajectories only experience a projection of that normal growth rate to their pointwise varying normal directions. Below we use Theorem 20 to verify this assertion.

In our simplified notation for autonomous systems, the Cauchy–Green strain tensor of Example 5 can be re-written as

$$\mathbf{C}^T(\mathbf{x}_0) = \begin{pmatrix} e^{2T} & 0 \\ 0 & e^{-2T} \end{pmatrix}.$$

For any  $T < 0$ , the corresponding eigenvalues and eigenvectors are

$$\lambda_1(\mathbf{x}_0, T) = e^{2T} < \lambda_2(\mathbf{x}_0, T) = e^{-2T} \neq 1, \quad T < 0, \quad (88)$$

$$\xi_1(\mathbf{x}_0, T) = \begin{pmatrix} 1 \\ 0 \end{pmatrix}, \quad \xi_2(\mathbf{x}_0, T) = \begin{pmatrix} 0 \\ 1 \end{pmatrix}.$$

Using Proposition 16, we obtain

$$\begin{aligned} \rho_T(\mathbf{x}_0) &= \sqrt{\frac{x^2 + y^2}{e^{-2|T|x^2} + e^{2|T|y^2}}}, \\ \nu_T(\mathbf{x}_0) &= \frac{x^2 + y^2}{e^{-2|T|x^2} + e^{2|T|y^2}} \end{aligned} \quad (89)$$

for all  $T < 0$ .

Substituting  $\xi_2$  from (88) into condition (i)/3 of Theorem 20, we obtain that along any attracting weak CLCS of system (87), we must have  $\partial_y \rho_T(\mathbf{x}_0) = 0$ , i.e., by (89), we must have

$$\frac{2y_0 x_0^2 (e^{-2|T|} - 2y_0 e^{2|T|})}{(e^{-2|T|x_0^2} + e^{2|T|y_0^2})^2} = 0. \quad (90)$$

This leaves us with the  $\{x_0 = 0\}$  and  $\{y_0 = 0\}$  axes as potential attracting WLCS candidates, with the origin excluded from both for technical reasons to avoid the blow-up in the definition (81). Note that condition (i)/2 Theorem 20 only holds for the  $\{y = 0\}$  axis, which is therefore an attracting WLCS by (88), (90) and (i) of Theorem 20. This is nothing new yet compared with our earlier results on this example, which established that the  $\{y = 0\}$  axis is one of the infinitely many attracting WLCS in the flow.

However, as opposed to  $\lambda_2(\mathbf{x}_0, T)$  defined in (88), the normal repulsion rate  $\rho_T(\mathbf{x}_0)$  is not a constant function, and hence  $\{y_0 = 0\}$  may satisfy (ii)/2 of Theorem 20 and qualify as an attracting CLCS. Indeed,

$$\begin{aligned} &\langle \xi_2((x_0, 0), T), \nabla^2 \rho_T((x_0, 0)) \xi_2((x_0, 0), T) \rangle \\ &= \partial_y^2 \rho_T((x_0, 0)) = \frac{e^{|T|} - e^{5|T|}}{x_0^2} < 0, \quad x_0 \neq 0. \end{aligned}$$

Therefore, with the exception of the origin  $\mathbf{x}_0 = \mathbf{0}$ , we have established that (ii)/1–(ii)/4 of Theorem 20 hold, and hence any compact trajectory segment of the  $\{y = 0\}$  axis away from the origin is an attracting CLCS over any finite time-interval  $[0, T]$ . We show the graph of  $\rho_T$  for  $T = -1$  in Fig. 15, confirming that the  $\{y = 0\}$  axis is indeed a ridge of the  $\rho_{-1}$  field away from the origin.

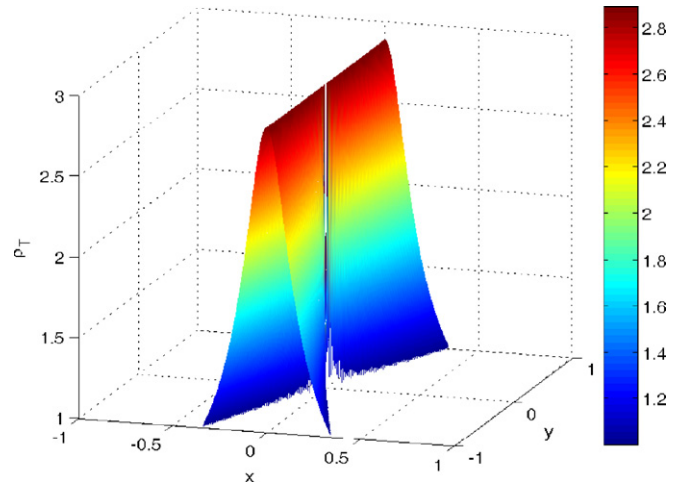


Fig. 15. The graph of the normal repulsion rate  $\rho_T$  for the linear saddle flow  $\dot{x} = x, \dot{y} = -y$ . (The function  $\rho_T$  is only plotted over the domain where  $\rho_T > 1$  holds.) Note that away from the origin, any segment of the  $\{y = 0\}$  axis is a ridge for  $\rho_T$ , and hence any such segment in a strong attracting CLCS.

Note that the  $\rho_T$  surface in Fig. 15 loses its smoothness at the origin. This is consistent with the fact that in any neighborhood of  $\mathbf{x}_0 = \mathbf{0}$ , there are no other trajectories of system (70) that are locally  $C^1$  close to the  $\{y = 0\}$  axis. As a result, the construction in the proof of Theorem 20 does not apply.

Recall, however, that on an empty set, all statements are true by definition, and hence  $\{y = 0\}$  is the locally strongest attracting trajectory segment among all  $C^1$  close trajectories in any small neighborhood of  $\mathbf{x}_0 = \mathbf{0}$ . As a result, Definition 19 deems the full  $\{y_0 = 0\}$  axis an attracting CLCS globally, including the neighborhood of  $\mathbf{x}_0 = \mathbf{0}$ .

### 9.1.2. Example 10: nonexistence of CLCS in Example 4

Consider again the dynamical system

$$\begin{aligned} \dot{x} &= 1 + \tanh^2 x, \\ \dot{y} &= -y, \end{aligned} \quad (91)$$

analyzed earlier in Examples 4 and 8. Note that for any  $\mathbf{x}_0 \in \mathbb{R}^2$ , we have

$$\begin{aligned} \mathbf{e}(\mathbf{x}_0) &= \begin{pmatrix} 1 \\ 0 \end{pmatrix}, \quad \mathbf{n}(\mathbf{x}_0) = \begin{pmatrix} 0 \\ -1 \end{pmatrix}, \\ \nabla \mathbf{F}^T(\mathbf{x}_0) &= \begin{pmatrix} \partial x(t; \mathbf{x}_0) & 0 \\ \partial x_0 & e^{-T} \end{pmatrix}, \end{aligned}$$

and hence from the original definition of  $\rho_T$  in (82), we have, for any  $T > 0$ ,

$$\begin{aligned} \rho_T(\mathbf{x}_0) &= \langle \mathbf{n}(\mathbf{F}^T(\mathbf{x}_0)), \nabla \mathbf{F}^T(\mathbf{x}_0) \mathbf{n}(\mathbf{x}_0) \rangle, \\ &= e^{-T} < 1. \end{aligned} \quad (92)$$

We conclude that system (91) has no normally repelling trajectory segments, and hence no repelling WLCS or CLCS. Recall that the same system has a repelling LCS, which is a material line starting from the  $y$  axis at time zero.

### 9.1.3. Example 11: unique weak unstable manifold as repelling CLCS

Consider the autonomous system

$$\begin{aligned} \dot{x} &= x + \tanh \frac{x^2}{4}, \\ \dot{y} &= x + 2y, \end{aligned} \quad (93)$$

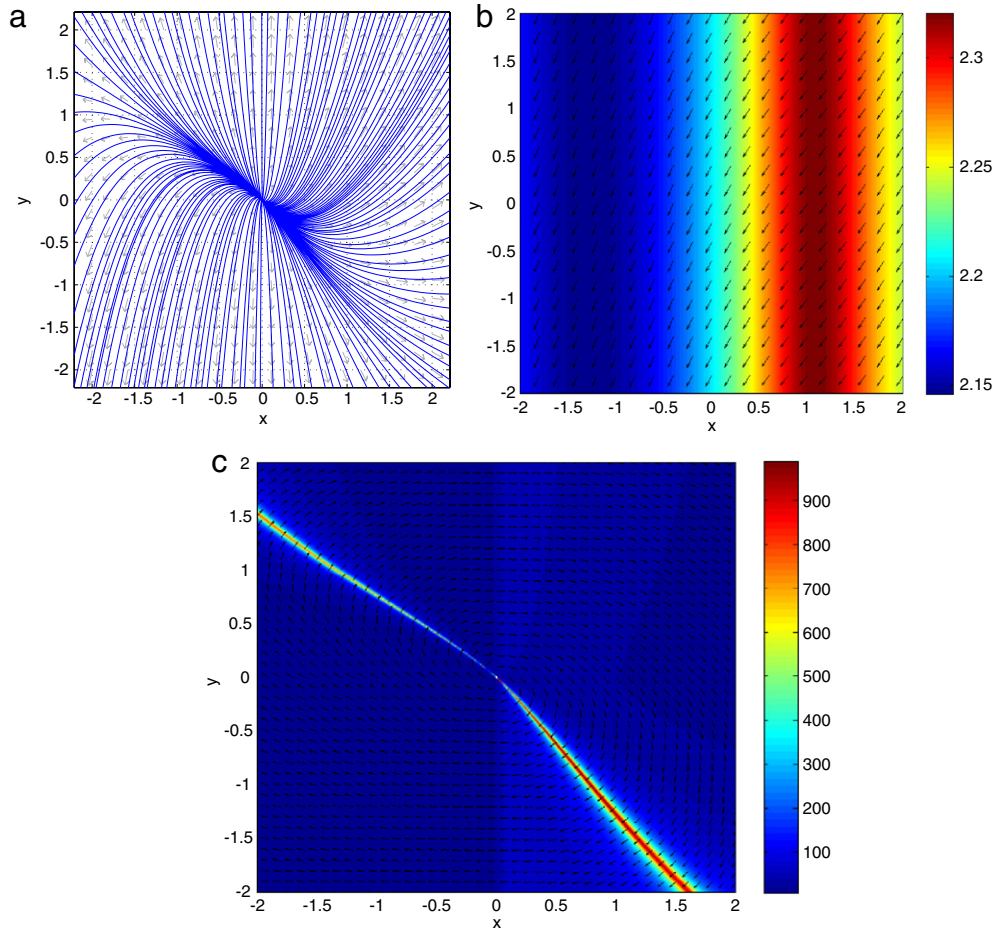


**Fig. 16.** LCS and CLCS analysis of (93): (a) Trajectories of the system. (b) FTLE field and directions of maximum strain computed over the interval  $[0, 3.19]$ . (c) Trajectory-normal repulsion rate  $\rho_T$  and trajectory-normal vectors at  $T = 3.19$ .

whose origin is an unstable node with a weaker and a stronger instability (cf. Fig. 16a).

The  $\tanh(x^2/4)$  term in the first equation of (93) introduces strong but highly localized stretching into the system on the two sides of the  $y$  axis. On the right-hand side of the  $y$  axis, the nonlinearity causes large trajectory separation and creates an FTLE ridge (cf. Fig. 16b). This ridge, however, is not a hyperbolic LCS or WLCS by Theorem 7, since it is not normal to the directions  $\xi_2$  of maximal stretching. We also deduce from Fig. 16a that the flux through the FTLE ridge is  $\mathcal{O}(1)$  as  $T \rightarrow \infty$ . Note that the flux formula (107) incorrectly predicts an  $\mathcal{O}(1/T)$  flux through the present FTLE ridge.

By contrast, the trajectory-normal growth rate field,  $\rho_T$  admits a ridge along one of the weak unstable manifolds of the origin. As seen in Fig. 16c, the ridge is pointwise normal to trajectory normals, and hence is a repelling CLCS by Theorem 20.

On a more general note, we recall that the classic theory of invariant manifolds is unable to identify a unique weak unstable manifold in system (93). Indeed, all we have guaranteed by the classic theory is the existence of infinitely many weak unstable manifolds, all of which are tangent to the weak unstable eigenvector of the origin. By contrast, the  $\rho_T(\mathbf{x}_0)$  field marks precisely one of these manifolds as the most influential one, i.e., the one that normally repels other such manifolds at the largest rate. Although not pursued here, a unique most attracting or repelling center manifold could also be extracted in two-dimensional flows using our CLCS approach.

## 9.2. Constrained LCS in systems with first integrals

The results of the above section carry over with minor modifications to  $n$ -dimensional systems with a conserved quantity, such as Hamiltonian systems. We consider an  $n$ -dimensional smooth dynamical system

$$\dot{\mathbf{x}} = \mathbf{v}(\mathbf{x}, t), \quad \mathbf{x} \in U \subset \mathbb{R}^n, \quad n \geq 2, \quad t \in [\alpha, \beta], \quad (94)$$

with a conserved quantity  $H(\mathbf{x}, t)$ . Specifically, for the smooth function  $H: U \times [\alpha, \beta] \rightarrow \mathbb{R}$ , we assume

$$\frac{DH}{Dt} = \frac{\partial H}{\partial t} + \langle \nabla H, \mathbf{v} \rangle = 0. \quad (95)$$

The level surfaces of  $H$  in the extended phase space  $U \times [\alpha, \beta]$ , defined as

$$\mathcal{M}_C = \{(\mathbf{x}, t) \in U \times [\alpha, \beta]: H(\mathbf{x}, t) = C\},$$

are therefore invariant sets in  $U \times [\alpha, \beta]$ . By the implicit function theorem,  $\mathcal{M}_C$  is a codimension-one manifold in  $U$  if  $\nabla H(\mathbf{x}, t) \neq \mathbf{0}$  holds at each point  $(\mathbf{x}, t) \in \mathcal{M}_C$ . In that case, the time  $t$  slice of  $\mathcal{M}_C$  is a material surface, denoted as

$$\mathcal{M}_C(t) = \{\mathbf{x} \in U: H(\mathbf{x}, t) = C\}. \quad (96)$$

We will refer to  $\mathcal{M}_C(t)$  as an *integral material surface* to distinguish it from other material surfaces that do not lie in a single level set of the first integral  $H$ .

Some of the invariant level sets of  $H$  are dynamically distinguished in that they repel or attract nearby trajectories

at locally the highest rate in the flow. A simple example of such distinguished level sets are open subsets of the stable and unstable manifolds of the classic pendulum equation containing the origin. In this example, the system is Hamiltonian, and hence the conserved quantity is the Hamiltonian, i.e., the energy of the pendulum.

The main elements of our theory developed for material surfaces carry over to integral material surfaces. The fundamental difference is that we now seek the locally most repelling or attracting material surface among  $C^1$ -close integral material surfaces of the form (96), as opposed to all  $C^1$ -close material surfaces.

The normal repulsion rate  $\rho_{t_0}^{t_0+T}(\mathbf{x}_0)$  for integral material surfaces takes the form

$$\rho_{t_0}^{t_0+T}(\mathbf{x}_0) = \langle \mathbf{n}_{t_0+T}(\mathbf{F}_{t_0}^{t_0+T}(\mathbf{x}_0)), \nabla \mathbf{F}_{t_0}^{t_0+T}(\mathbf{x}_0) \mathbf{n}_{t_0}(\mathbf{x}_0) \rangle, \tag{97}$$

and the normal repulsion ratio is defined as

$$v_{t_0}^{t_0+T}(\mathbf{x}_0) = \min_{\substack{|\mathbf{e}_0|=1 \\ \mathbf{e}_0 \in T_{\mathbf{x}_0} \mathcal{M}(t_0)}} \frac{\rho_{t_0}^{t_0+T}(\mathbf{x}_0)}{|\nabla \mathbf{F}_{t_0}^{t_0+T}(\mathbf{x}_0) \mathbf{e}_0|}. \tag{98}$$

Again,  $\rho_{t_0}^{t_0+T}(\mathbf{x}_0) > 1$  indicates a strict normal growth of infinitesimal normal perturbations to the integral surface through  $\mathbf{x}_0$  over the time interval  $[t_0, t_0 + T]$ . Similarly,  $v_{t_0}^{t_0+T}(\mathbf{x}_0) > 1$  implies that this normal growth dominates any growth in directions tangent to the integral surface.

As in Proposition 16, the above finite-time normal repulsion measures can be computed as follows:

**Proposition 21.** *The quantities  $\rho_{t_0}^{t_0+T}(\mathbf{x}_0)$  and  $v_{t_0}^{t_0+T}(\mathbf{x}_0)$  satisfy the expressions*

$$\rho_{t_0}^{t_0+T}(\mathbf{x}_0) = \frac{|\nabla H(\mathbf{x}_0, t_0)|}{\sqrt{\langle \nabla H(\mathbf{x}_0, t_0), [\mathbf{C}_{t_0}^{t_0+T}(\mathbf{x}_0)]^{-1} \nabla H(\mathbf{x}_0, t_0) \rangle}}, \tag{99}$$

$$v_{t_0}^{t_0+T}(\mathbf{x}_0) = \min_{\substack{|\mathbf{e}_0|=1 \\ \mathbf{e}_0 \in T_{\mathbf{x}_0} \mathcal{M}(t_0)}} \frac{\rho_{t_0}^{t_0+T}(\mathbf{x}_0)}{\sqrt{\langle \mathbf{e}, \mathbf{C}_{t_0}^{t_0+T}(\mathbf{x}_0) \mathbf{e} \rangle}}.$$

**Proof.** The proof of this proposition is identical to that of Proposition 2, once one observes that

$$\mathbf{n}_{t_0}(\mathbf{x}_0) = \nabla H(\mathbf{x}_0, t_0) / |\nabla H(\mathbf{x}_0, t_0)| \tag{100}$$

is a unit normal to  $\mathcal{M}_C(t_0)$  at the point  $\mathbf{x}_0 \in \mathcal{M}_C(t_0)$ .  $\square$

Finite-time normal repulsion, attraction and hyperbolicity for the material surface  $\mathcal{M}_C(t)$  are defined in Definition 3. The following two definitions are generalizations of our CLCS definitions given in the two-dimensional context.

**Definition 22 (Hyperbolic Weak Constrained LCS).** Assume that the integral material surface  $\mathcal{M}_C(t) \subset U$  is normally repelling over  $[t_0, t_0 + T]$ . We call  $\mathcal{M}_C(t)$  a *repelling Weak CLCS (WCLCS)* over  $[t_0, t_0 + T]$  if its normal repulsion rate admits pointwise stationary values along  $\mathcal{M}_C(t_0)$  among all locally  $C^1$ -close integral surfaces of  $H$ . Similarly, we call  $\mathcal{M}_C(t)$  an *attracting WCLCS* over  $[t_0, t_0 + T]$  if it is a repelling WCLCS over  $[t_0, t_0 + T]$  in backward time. Finally, we call  $\mathcal{M}_C(t)$  a *hyperbolic WCLCS* over  $[t_0, t_0 + T]$  if it is a repelling or attracting WCLCS over  $[t_0, t_0 + T]$ .

**Definition 23 (Hyperbolic Constrained LCS).** Assume that the integral material surface  $\mathcal{M}_C(t) \subset U$  is normally repelling over  $[t_0, t_0 + T]$ . We call  $\mathcal{M}_C(t)$  a *repelling Constrained LCS (CLCS)* over  $[0, T] \subset \mathcal{I}$  if its normal repulsion rate admits strict pointwise

maxima along  $\mathcal{M}_C(t_0)$  among all locally  $C^1$ -close integral surfaces of  $H$ . Similarly, we call  $\mathcal{M}_C(t)$  an *attracting CLCS* over  $[0, T]$  if it is a repelling CLCS over  $[t_0, t_0 + T]$  in backward time. Finally, we call  $\mathcal{M}_C(t)$  a *hyperbolic CLCS* over  $[t_0, t_0 + T]$  if it is a repelling or attracting CLCS over  $[t_0, t_0 + T]$ .

The following theorem is a direct extension of our two-dimensional result on constrained LCSs to  $n$ -dimensional systems.

**Theorem 24 (Sufficient and Necessary Conditions for Hyperbolic WCLCS and CLCS).** *Consider a compact integral material surface  $\mathcal{M}_C(t) \subset U$  on which  $\nabla H(\mathbf{x}, t)$  is nonvanishing. Then*

- (i)  $\mathcal{M}_C(t)$  is a repelling WCLCS over  $[t_0, t_0 + T]$  if and only if all the following hold for all  $\mathbf{x}_0 \in \mathcal{M}_C(t_0)$ :
  1.  $\rho_{t_0}^{t_0+T}(\mathbf{x}_0) > 1, v_{t_0}^{t_0+T}(\mathbf{x}_0) > 1,$
  2.  $\langle \nabla \rho_{t_0}^{t_0+T}(\mathbf{x}_0), \nabla H(\mathbf{x}_0, t_0) \rangle = 0.$
- (ii)  $\mathcal{M}_C(t)$  is a repelling CLCS over  $[t_0, t_0 + T]$  if and only if
  1.  $\mathcal{M}_C(t)$  is a repelling WCLCS over  $[t_0, t_0 + T],$
  2.  $\langle \nabla H(\mathbf{x}_0, t_0), \nabla^2 \rho_{t_0}^{t_0+T}(\mathbf{x}_0) \nabla H(\mathbf{x}_0, t_0) \rangle < 0$  for all  $\mathbf{x}_0 \in \mathcal{M}_C(t_0).$

**Proof.** The proof of this theorem is identical to that of Theorem 7, with the class of  $C^1$ -close material surfaces restricted to the class of  $C^1$ -close integral surfaces, whose normals satisfy formula (100).  $\square$

9.2.1. Example 12: CLCS in a rotating saddle flow

Consider the two-dimensional rotating saddle flow

$$\dot{\mathbf{x}} = \begin{pmatrix} \sin 4t & 2 + \cos 4t \\ -2 + \cos 4t & -\sin 4t \end{pmatrix} \mathbf{x} \tag{101}$$

from [14]. This is an example of a non-autonomous dynamical system whose instantaneous phase portraits taken at constant  $t$  all suggest center-type behavior around the origin. Indeed, for any fixed  $t$ , the eigenvalues of the coefficient matrix of (101) are equal to  $\pm 3i$ .

The origin, however, turns out to be a saddle point with Lyapunov exponents  $\pm 1$ . Since the largest FTLE is constant in this linear example, the stable and unstable manifolds of (101) cannot be detected as ridges of the Lyapunov exponent field. Along with infinitely many parallel lines, the stable and unstable manifolds are found to be repelling and attracting WCLCSs, respectively, from an application of Theorem 7.

System (101) admits a first integral given by

$$H(x, y, t) = \frac{1}{2}(y^2 - x^2) \cos 4t - xy \sin 4t,$$

which can be constructed in a rotating frame where the system becomes autonomous (cf. [14]). To illustrate Theorem 24, we note that

$$\nabla H(x, y, 0) = \begin{pmatrix} -x \\ y \end{pmatrix}, \tag{102}$$

which we use in formula (99) to locate the unstable manifold of the origin as an attracting CLCS. Fig. 17 shows the results obtained from computing  $\rho_0^{0+T}$  with  $T = -0.1$ .

The gradient field (102) is seen to be normal to the emerging ridge of  $\rho_0^{0+T}$  and hence (i)/2 of Theorem 24 also holds. As a result, the computation correctly identifies a repelling CLCS whose  $t = 0$  slice,

$$\mathcal{M}(0) = \{(x, y) \in \mathbb{R}^2 : x = y\},$$

is the  $t = 0$  slice of the unstable manifold of the origin.

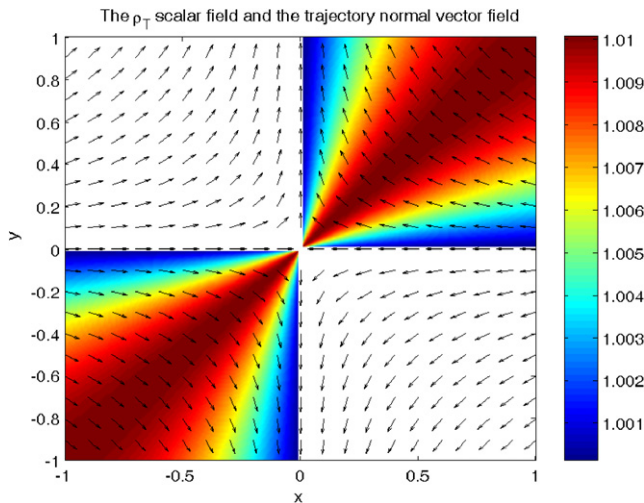


**Fig. 17.** The graph of  $\rho_0^{-0.1}$  is plotted over the subset of the plane where condition (i)1 of Theorem 24 is satisfied. Note the emergence of a ridge along the  $x = y$  line. Also shown is the gradient field (102).

## 10. Conclusions

We have developed a variational theory of hyperbolic Lagrangian Coherent Structures (LCSs) in finite-time dynamical systems of arbitrary dimension. Our objective was to identify observed cores of Lagrangian patterns rigorously without *a priori* favoring any particular Lagrangian diagnostic tool. Our analysis has yielded an exact relationship between observable LCSs and invariants of the Cauchy–Green strain tensor.

We have defined hyperbolic LCSs as locally the strongest normally repelling or attracting material surfaces (codimension-one invariant manifolds in the extended phase space). We then employed a variational approach to derive sufficient and necessary criteria for the existence of LCSs. We have also introduced the notion of a Weak LCS (WLCS) that is a stationary surface (but not necessarily an extremum) for the above variational principle.

WLCSs turn out to be zero sets for a three-tensor, the inverse Cauchy–Green strain tensor, evaluated along directions of maximal strain. Out of all WLCSs, the material surfaces on which an appropriate tensor field (defined in (31)) is positive definite turn out to be LCSs. A necessary condition for this to happen is the positivity of the second derivative of the Cauchy–Green strain tensor (a four-tensor) along directions of maximal strain.

Efficient implementation of our theory will require further development in the computational tools used in LCS detection. Specifically, both WLCS and LCS are now understood to be solutions of a nonlinear equation (cf. (1), or equivalently, (2)), which needs to be solved automatically with high accuracy, even though its left-hand side is typically only known on a numerical or experimental grid. Once the solution set is found, its subsets satisfying the conditions for WLCS and LCS need to be identified. While this involves the evaluation of higher derivatives, the robustness criteria for LCS (cf. Section 5) also imply robustness with respect to numerical errors.

The variational approach used in this paper extremizes the pointwise normal repulsion rate of material surfaces, as opposed to an integral of the repulsion rate. We have favored this formulation because (1) it ensures that the LCSs act as observed cores of Lagrangian patterns at all of their points; (2) it enables us to solve the variational problem without posing any boundary conditions for the LCS. Applications of the present ideas in controlling LCS will, however, likely lead to a variational problem for the integral of the repulsion rate along the LCS. In that case, the boundary conditions will be obtained from the desired spatial location of the LCS.

The present work has focused on hyperbolic LCS. Similar variational formulations for the locally most shearing material surfaces are possible and will appear elsewhere. By contrast, defining and extracting an elliptic LCS (i.e., finite-time generalizations of KAM tori) appears more challenging. An initial numerical study of such surfaces appears in [21].

Finally, lower-dimensional LCS can be defined and analyzed in a manner similar to what we pursued for codimension-one LCS in this paper. Normal perturbations to a lower-dimensional material surface, however, span higher-dimensional normal spaces. As a result, several normal repulsion rates and ratios will need to be defined and extremized simultaneously.

## Acknowledgements

I am grateful to Harry Dankowitz, Mohammad Farazmand, Jim Meiss, Ronny Peikert, Gilead Tadmor, and Lai-Sang Young for their insightful questions and comments that have led to improvements in this manuscript. I am also thankful to Wenbo Tang for reviewing some of the proofs in detail. Finally, I would like to express my gratitude to Shawn Shadden for reading this work in detail, catching a number of misprints, and providing a number of thoughtful suggestions.

## Appendix A. An Eulerian upper estimate for FTLE

We derive here a simple upper bound for the FTLE based on global properties of the vector field  $\mathbf{v}$ .

**Proposition 25 (Upper Bound of FTLE).** *The maximum of the largest singular value of  $\nabla \mathbf{v}$  over the domain  $\bar{U} \times [\alpha, \beta]$  is always an upper bound for all forward and backward FTLE computed on the same domain. Specifically, we have*

$$\Lambda_{t_0}^t(\mathbf{x}_0) \leq \max_{\mathbf{x} \in \bar{U}, t \in [\alpha, \beta]} \sqrt{\lambda_{\max}[\nabla \mathbf{v}(\mathbf{x}, t) \nabla \mathbf{v}(\mathbf{x}, t)]},$$

$$\mathbf{x}_0 \in \bar{U}, t, t_0 \in [\alpha, \beta], \quad (103)$$

with  $\bar{U}$  denoting the closure of  $U$ .

**Proof.** The deformation gradient  $\nabla \mathbf{F}_{t_0}^t(\mathbf{x}_0)$  is the fundamental matrix solution of the equation of variations along  $\mathbf{x}(t, t_0, \mathbf{x}_0)$ , i.e., it satisfies the initial value problem

$$\frac{d}{dt} \nabla \mathbf{F}_{t_0}^t(\mathbf{x}_0) = \nabla \mathbf{v}(\mathbf{x}(t, t_0, \mathbf{x}_0), t) \nabla \mathbf{F}_{t_0}^t(\mathbf{x}_0), \quad (104)$$

$$\nabla \mathbf{F}_{t_0}^{t_0}(\mathbf{x}_0) = \mathbf{I}.$$

Integrating both sides of the first line of (104) from  $t_0$  to  $t \geq t_0$ , and using the initial condition from the second line of (104) gives

$$\nabla \mathbf{F}_{t_0}^t(\mathbf{x}_0) = \mathbf{I} + \int_{t_0}^t \nabla \mathbf{v}(\mathbf{x}(s, t_0, \mathbf{x}_0), s) \nabla \mathbf{F}_{t_0}^s(\mathbf{x}_0) ds.$$

Taking the operator norm of both sides and applying Gronwall's inequality gives

$$\|\nabla \mathbf{F}_{t_0}^t(\mathbf{x}_0)\| \leq \exp \int_{t_0}^t \|\nabla \mathbf{v}(\mathbf{x}(s, t_0, \mathbf{x}_0), s)\| ds.$$

Taking the logarithm of both sides and dividing by  $t - t_0$ , we obtain

$$\Lambda_{t_0}^t(\mathbf{x}_0) \leq \frac{1}{t - t_0} \int_{t_0}^t \|\nabla \mathbf{v}(\mathbf{x}(s, t_0, \mathbf{x}_0), s)\| ds, \quad t > t_0. \quad (105)$$

Reversing the direction of time in the above derivation yields the similar result

$$\Lambda_{t_0}^t(\mathbf{x}_0) \leq \frac{1}{t_0 - t} \int_t^{t_0} \|\nabla \mathbf{v}(\mathbf{x}(s, t_0, \mathbf{x}_0), s)\| ds, \quad t < t_0. \quad (106)$$

Using the relationship between the singular value of a matrix and its operator norm (cf. (9)), we obtain from (105)–(106) the estimate (103). The max on the right-hand side is finite due to the assumption that  $U$  is bounded, and hence its closure,  $\bar{U}$ , is compact.  $\square$

## Appendix B. Details for Examples 1–4

In this appendix, we provide detailed calculations for Examples 1–4 that illustrate inconsistencies with defining repelling LCSs as ridges of the FTLE field. The first and most precise idea of such a definition appears in [4] for two-dimensional flows, and in [5] for  $n$ -dimensional flows, which we recall below for reference.

### B.1. The definition of an LCS as an FTLE ridge

Since all three examples we discuss here are two-dimensional, we list below the main regularity and nondegeneracy assumptions of Shadden et al. [4] under which they define LCSs as FTLE ridges in two dimensions.

The assumptions in [4] are as follows:

(A1) The vector field  $\mathbf{v}(\mathbf{x}, t)$  is at least class  $C^0$  in  $t$  and class  $C^2$  in  $\mathbf{x}$ .

(A2) There exists a constant  $K$  such that

$$\|\nabla \mathbf{F}_{t_0}^t\| \leq e^{K(t-t_0)}$$

holds for all  $t \in [\alpha, \beta]$ .

(A3) For all  $t_0, t_0 + T \in [\alpha, \beta]$  and for all  $\mathbf{x}_0 \in U$ , we have

$$\log \lambda_{\min}[\mathbf{C}_{t_0}^{t_0+T}(\mathbf{x}_0)] < 0 < \log \lambda_{\max}[\mathbf{C}_{t_0}^{t_0+T}(\mathbf{x}_0)].$$

Under these assumptions, Shadden et al. [4] use the following definition for an FTLE ridge:

**Definition 26** (Second-Derivative FTLE Ridge). A second-derivative ridge of  $\Lambda_{t_0}^t$  is an injective curve  $\mathbf{c}: [a, b] \rightarrow U$  satisfying the following conditions for all  $s \in (a, b)$ :

SR1 The vectors  $\mathbf{c}'(s)$  and  $\nabla \Lambda_{t_0}^t(\mathbf{c}(s))$  are parallel

SR2 For the Hessian  $\Sigma_{t_0}^t(\mathbf{x}_0) = \nabla^2 \Lambda_{t_0}^t(\mathbf{x}_0)$  and for a unit normal  $\mathbf{n}(s)$  to the curve  $\mathbf{c}(s)$ , we have

$$\langle \mathbf{n}(s), \Sigma_{t_0}^t(\mathbf{c}(s))\mathbf{n}(s) \rangle = \min_{|\mathbf{u}|=1} \langle \mathbf{u}, \Sigma_{t_0}^t(\mathbf{c}(s))\mathbf{u} \rangle < 0.$$

With the above definition at hand, the definition of a repelling LCS as an FTLE ridge can be stated as follows:

**Definition 27** (Shadden et al. [4] and Lekien et al. [5]). At each time  $t_0$ , a repelling Lagrangian Coherent Structure (LCS) is a second-derivative ridge of the field  $\Lambda_{t_0}^{t_0+T}(\mathbf{x}_0)$ .

We note that the repelling nature of the LCS in the above definition appears first in the more general setting of Lekien et al. [5], which, however, also covers the two-dimensional context relevant for the examples below. We also note that Lekien et al. [5] replaces assumption (A2) of [4] with the assumption that the domain  $\bar{U}$  is compact, and point out that the existence of a  $K > 0$  satisfying (A2) then follows (see our Proposition 25 for details).

### B.2. Flux through an FTLE ridge

Shadden et al. [4] propose that at time  $t_0$ , the area flux per unit length at a point  $\mathbf{p}$  of a ridge of a two-dimensional FTLE field  $\Lambda_{t_0}^{t_0+T}$

is given by

$$\varphi(\mathbf{p}, t) = \frac{\langle \mathbf{t}, \nabla \Lambda_{t_0}^t \rangle}{\langle \mathbf{n}, \Sigma_{t_0}^t \mathbf{n} \rangle} \left\langle \mathbf{t}, \frac{\partial \mathbf{n}}{\partial t_0} - \nabla \mathbf{v}(\mathbf{p}, t_0)\mathbf{n} \right\rangle + \mathcal{O}\left(\frac{1}{|T|}\right), \quad (107)$$

where  $\mathbf{n}(\mathbf{p}, t_0)$  and  $\mathbf{t}(\mathbf{p}, t_0)$  are the unit normal and unit tangent to the FTLE at the point  $\mathbf{p}$  at time  $t_0$ , respectively;  $\nabla \mathbf{v}(\mathbf{p}, t_0)$  is the Jacobian of the vector field at the same location and time; and  $T$  is the length of time over which the FTLE field is computed starting from time  $t_0$ . A version of the flux formula (107) appears for  $n$ -dimensional dynamical systems in [5].

As we show in Appendix C, however, formula (107) is not generally applicable without further assumptions, some of which turn out to be restrictive. Without such assumptions, the higher-order terms denoted as  $\mathcal{O}\left(\frac{1}{|T|}\right)$  in (107) may be of equal magnitude or larger than the leading-order terms, even as  $T \rightarrow \infty$ .

### B.3. Details for Example 1

The  $x$  and  $y$  components of system (10) decouple, and hence the Cauchy–Green strain tensor can be written in the general form

$$\mathbf{C}_{t_0}^t(\mathbf{x}_0) = \begin{pmatrix} \left[ \frac{\partial x(t, t_0, x_0)}{\partial x_0} \right]^2 & 0 \\ 0 & \left[ \frac{\partial y(t, t_0, y_0)}{\partial y_0} \right]^2 \end{pmatrix} = \begin{pmatrix} e^{2(t-t_0)} & 0 \\ 0 & \left[ \frac{\partial y(t, t_0, y_0)}{\partial y_0} \right]^2 \end{pmatrix}. \quad (108)$$

Differentiation of the second equation in (10) with respect to  $y_0$  gives

$$\frac{d}{dt} \frac{\partial y(t)}{\partial y_0} = -[1 + 3y^2(t)] \frac{\partial y(t)}{\partial y_0},$$

which, after integration, leads to the estimate

$$\left| \frac{\partial y(t)}{\partial y_0} \right| = e^{-\int_{t_0}^t [1+3y^2(s)] ds} \leq e^{-(t-t_0)} \quad (109)$$

for all  $t > t_0$ . From (108), (109), and definition (9), we obtain the result (11) for the forward FTLE field. As a result, according to Definition 27, there would be no repelling LCS in (10).

### B.4. Details for Example 2

For  $t \leq t_0$ , system (10) admits the explicit solution

$$\begin{aligned} x(t) &= x_0 e^{(t-t_0)}, \\ y(t) &= \frac{y_0}{\sqrt{(y_0^2 + 1)e^{2(t-t_0)} - y_0^2}}. \end{aligned} \quad (110)$$

Note that for nonzero  $y_0$ , the  $y$  component of the above solution blows up in finite time. Restricting initial conditions to the set

$$U = \left\{ (x, y) \in \mathbb{R}^2 : |y| < \frac{1}{2} \right\},$$

however, we obtain that the solution (110) will exist at least on the backward-time interval  $\mathcal{I} = [t_0, t_0 - \log \sqrt{5}]$ .

For all  $(x_0, y_0) \in U$  and for all  $t \in \mathcal{I}$ , the Cauchy–Green strain tensor in (108) can be explicitly computed as

$$\mathbf{C}_{t_0}^t(\mathbf{x}_0) = \begin{pmatrix} e^{2(t-t_0)} & 0 \\ 0 & \frac{e^{4(t-t_0)}}{[(1+y_0^2)e^{2(t-t_0)} - y_0^2]^3} \end{pmatrix}, \quad (111)$$

with the two eigenvalues

$$\lambda_2(y_0, t_0) = \frac{e^{4(t-t_0)}}{[(1 + y_0^2)e^{2(t-t_0)} - y_0^2]^3} > 0,$$

$$\lambda_1 = e^{2(t-t_0)} < \lambda_2.$$

Hence

$$\frac{\partial}{\partial y_0} \lambda_2(y_0, t_0) = -6(e^{2(t-t_0)} - 1)e^{4(t-t_0)} \frac{y_0}{(e^{2(t-t_0)} + y_0^2 e^{2(t-t_0)} - y_0^2)^4},$$

$$\frac{\partial^2}{\partial y_0^2} \lambda_2(y_0, t_0) = -6(e^{2(t-t_0)} - 1)e^{4(t-t_0)} \frac{e^{2(t-t_0)} - 7y_0^2 e^{2(t-t_0)} + 7y_0^2}{(e^{2(t-t_0)} + y_0^2 e^{2(t-t_0)} - y_0^2)^5}.$$

Consequently, we have

$$\frac{d}{dy_0} \lambda_2(0, t_0) = 0,$$

$$\frac{d^2}{dy_0^2} \lambda_2(0, t_0) = 6(1 - e^{2(t-t_0)})e^{4(t-t_0)} > 0, \quad t < t_0.$$

Therefore,  $\lambda_2(y_0, t_0)$  has a *minimum ridge (trough)* at  $y_0 = 0$ .

### B.5. Details for Example 3

System (15) is arbitrary many times differentiable, and hence assumption (A1) holds. By (103), the FTLE obeys the global bound  $\Lambda_{t_0}^t(\mathbf{x}_0) \leq 1$ , thus

$$\|\nabla \mathbf{F}_{t_0}^t(\mathbf{x}_0)\| \leq e^{|t-t_0|}$$

for all  $t, t_0 \in \mathbb{R}$  and all  $\mathbf{x}_0 \in \mathbb{R}^2$ . Consequently, assumption (A2) also holds.

The trajectories of (15) are given by

$$x(t; t_0, \mathbf{x}_0) = x_0 + (t - t_0)(\tanh y_0 + 2), \tag{112}$$

$$y(t; t_0, \mathbf{x}_0) = y_0.$$

With the notation  $a(y) = \tanh'(y_0)$  and  $T = t - t_0$ , we obtain from (112) the eigenvalues

$$\lambda_{\max}[\mathbf{C}_{t_0}^{t_0+T}(\mathbf{x}_0)] = \frac{1}{2}T^2 a^2 + \frac{1}{2}\sqrt{T^4 a^4 + 4} + 1,$$

$$\lambda_{\min}[\mathbf{C}_{t_0}^{t_0+T}(\mathbf{x}_0)] = \frac{1}{2}T^2 a^2 - \frac{1}{2}\sqrt{T^4 a^4 + 4} + 1,$$

which satisfy, for any  $\mathbf{x}_0$ , the relation

$$\log \lambda_{\min}[\mathbf{C}_{t_0}^{t_0+T}(\mathbf{x}_0)] < 0 < \log \lambda_{\max}[\mathbf{C}_{t_0}^{t_0+T}(\mathbf{x}_0)].$$

This means that the nondegeneracy condition (A3) holds.

Next note that  $\Lambda_{t_0}^{t_0+T} = \frac{1}{2T} \log \lambda_{\max}[\mathbf{C}_{t_0}^{t_0+T}(\mathbf{x}_0)]$  has a nondegenerate ridge along the  $y = 0$  axis for any choice of  $t_0$  and  $T$ . To see this, it is enough to observe that  $\lambda_{\max}[\mathbf{C}_{t_0}^{t_0+T}(\mathbf{x}_0)]$  has a nondegenerate ridge along the same axis, because it reaches a strict maximum wherever  $a^2 = [\tanh'(y_0)]^2$  reaches a strict maximum, i.e., at  $y_0 = 0$ . The corresponding ridge of  $\Lambda_{t_0}^{t_0+T}$  has constant height, as  $\Lambda_{t_0}^{t_0+T}$  does not depend on  $y_0$ .

Based on the above, Definition 27 pronounces the  $x$  axis of system to be a repelling LCS for system (15).

### B.6. Details for Example 4

Solutions of system (16) are given by the system of equations

$$\frac{1}{2}x - \frac{1}{2}x_0 + \frac{1}{2} \arctan(e^{2x}) - \frac{1}{2} \arctan(e^{2x_0}) = t - t_0,$$

$$y(t) = y_0 e^{-(t-t_0)}. \tag{113}$$

Implicit differentiation of the first equation with respect to  $x_0$  yields

$$\frac{1}{2} \frac{\partial x}{\partial x_0} - \frac{1}{2} + \frac{1}{2} \frac{e^{2x}}{e^{4x} + 1} \frac{\partial x}{\partial x_0} - \frac{1}{2} \frac{e^{2x_0}}{e^{4x_0} + 1} = 0,$$

or, equivalently,

$$\frac{\partial x}{\partial x_0}(t; x_0) = \frac{1 + \frac{e^{2x_0}}{e^{4x_0} + 1}}{1 + \frac{e^{2x(t; x_0)}}{e^{4x(t; x_0)} + 1}}. \tag{114}$$

By inspection of the right-hand side of (16), we find that on any fixed trajectory, we have  $\dot{x} > 0$  uniformly bounded away from zero for all forward times. Therefore, we have  $\lim_{t \rightarrow \infty} x(t) = \infty$  on all trajectories, and hence taking the  $t \rightarrow \infty$  limit in (114), we obtain the function

$$\lim_{t \rightarrow \infty} \frac{\partial x}{\partial x_0}(t; x_0) = 1 + \frac{e^{2x_0}}{e^{4x_0} + 1}, \tag{115}$$

which has a unique global maximum at  $x_0 = 0$ .

From system (16) and expression (114), the Cauchy–Green strain tensor can be written as

$$\mathbf{C}_{t_0}^t(\mathbf{x}_0) = \begin{pmatrix} \left[ \frac{1 + \frac{e^{2x_0}}{e^{4x_0} + 1}}{1 + \frac{e^{2x(t; t_0, x_0)}}{e^{4x(t; t_0, x_0)} + 1}} \right]^2 & 0 \\ 0 & e^{-2(t-t_0)} \end{pmatrix},$$

with eigenvalues satisfying

$$\lambda_{\max}[\mathbf{C}_{t_0}^t(\mathbf{x}_0)] = \left[ \frac{1 + \frac{e^{2x_0}}{e^{4x_0} + 1}}{1 + \frac{e^{2x(t; t_0, x_0)}}{e^{4x(t; t_0, x_0)} + 1}} \right]^2,$$

$$\lambda_{\min}[\mathbf{C}_{t_0}^t(\mathbf{x}_0)] = e^{-2(t-t_0)}.$$

Note that the larger eigenvalue of  $\mathbf{C}_{t_0}^t(\mathbf{x}_0)$  also satisfies

$$\lim_{t \rightarrow \infty} \lambda_{\max}[\mathbf{C}_{t_0}^t(\mathbf{x}_0)] = \left( 1 + \frac{e^{2x_0}}{e^{4x_0} + 1} \right)^2,$$

$$\frac{\partial}{\partial x_0} \lim_{t \rightarrow \infty} \lambda_{\max}[\mathbf{C}_{t_0}^t(\mathbf{x}_0)] = 4 \frac{-e^{10x_0} - e^{8x_0} + e^{4x_0} + e^{2x_0}}{(e^{4x_0} + 1)^3},$$

$$\frac{\partial^2}{\partial x_0^2} \lim_{t \rightarrow \infty} \lambda_{\max}[\mathbf{C}_{t_0}^t(\mathbf{x}_0)]$$

$$= \frac{4}{(e^{4x_0} + 1)^3} (2e^{2x_0} + 4e^{4x_0} - 8e^{8x_0} - 10e^{10x_0})$$

$$- 48 \frac{e^{4x_0}}{(e^{4x_0} + 1)^4} (e^{2x_0} + e^{4x_0} - e^{8x_0} - e^{10x_0}), \tag{116}$$

$$\frac{\partial}{\partial y_0} \lim_{t \rightarrow \infty} \lambda_{\max}[\mathbf{C}_{t_0}^t(\mathbf{x}_0)] \equiv 0.$$

Therefore, at any  $\mathbf{x}_0 = (0, y_0)$ , we have

$$\lim_{t \rightarrow \infty} \lambda_{\max}[\mathbf{C}_{t_0}^t((0, y_0))] = \frac{9}{4}, \tag{117}$$

$$\frac{\partial}{\partial x_0} \lim_{t \rightarrow \infty} \lambda_{\max}[\mathbf{C}_{t_0}^t((0, y_0))] = 0,$$

$$\frac{\partial^2}{\partial x_0^2} \lim_{t \rightarrow \infty} \lambda_{\max}[\mathbf{C}_{t_0}^t((0, y_0))] = -6,$$

$$\frac{\partial}{\partial y_0} \lim_{t \rightarrow \infty} \lambda_{\max}[\mathbf{C}_{t_0}^t(\mathbf{x}_0)] = \frac{\partial}{\partial x_0} \lim_{t \rightarrow \infty} \lambda_{\max}[\mathbf{C}_{t_0}^t((0, y_0))] = 0,$$

$$\frac{\partial^2}{\partial x_0 \partial y_0} \lim_{t \rightarrow \infty} \lambda_{\max}[\mathbf{C}_{t_0}^t(\mathbf{x}_0)] = \frac{\partial^2}{\partial y_0^2} \lim_{t \rightarrow \infty} \lambda_{\max}[\mathbf{C}_{t_0}^t((0, y_0))] = 0.$$

From (116) and (117), we conclude that for large enough times  $t > t_0$ :

(1) The scalar field  $\lambda_{\max}[\mathbf{C}_{t_0}^t(\mathbf{x}_0)]$  develops a ridge approaching the unique global maximum of (115) as  $t$  increases. This ridge persists for all later times while both Lyapunov exponents tend to zero.

(2) At any  $t > 0$ , the above ridge has constant height because  $\Lambda_{t_0}^t = \frac{1}{2(t-t_0)} \log \lambda_{\max}[\mathbf{C}_{t_0}^t((0, y_0))]$  does not depend on  $y_0$ . As a result,  $\nabla \Lambda_{t_0}^t$  vanishes along the ridge.

(3) It follows from (114) that for any  $t > t_0$ ,

$$\begin{aligned} \log \lambda_{\max}[\mathbf{C}_{t_0}^t((0, y_0))] &= \log \left( \frac{1 + \frac{e^{2x_0}}{e^{4x_0} + 1}}{1 + \frac{e^{2x(t)}}{e^{4x(t)} + 1}} \right)^2 \geq \mu_{\max} \\ &= \log \left( \frac{1 + \frac{e^{2x_0}}{e^{4x_0} + 1}}{1 + \frac{1}{2}} \right)^2 > 0. \end{aligned}$$

Also, for any  $t \geq t_0 + 1$ , we have

$$\log \lambda_{\min}[\mathbf{C}_{t_0}^t((0, y_0))] = -2(t - t_0) \leq \mu_{\min} \stackrel{\text{def.}}{=} -2 < 0.$$

We conclude that assumption (A3) is satisfied.

(4) The vector field on the right-hand side of Eq. (16) is arbitrary many times differentiable, and hence assumption (A1) is satisfied.

(5) The linearized flow map obeys the bound

$$\|\mathbf{V}\mathbf{F}_{t_0}^t(\mathbf{x}_0)\| = e^{\Lambda_{t_0}^t(\mathbf{x}_0)|t-t_0|} \leq e^{K|t-t_0|},$$

where  $K = 3.5$  can be selected based on Proposition 25 and on the observation

$$\begin{aligned} \max_{\mathbf{x} \in \mathbb{R}^2} \sqrt{\lambda_{\max}[\mathbf{V}\mathbf{v}(\mathbf{x})^* \mathbf{V}\mathbf{v}(\mathbf{x})]} \\ = \max \left( \left( 1 + \frac{d}{dx} \tanh^2 x \right)^2 \right) < 3.5, \end{aligned} \quad (118)$$

which can be deduced by calculating the global maximum of  $(1 + \frac{d}{dx} \tanh^2 x)^2$ . We conclude that assumption (A2) is satisfied.

(6) The limit of the Hessian of the FTLE field computed on the ridge is given by (cf. (117))

$$\begin{aligned} \lim_{t \rightarrow \infty} \Sigma_{t_0}^t(\mathbf{x}_0) \\ = \lim_{t \rightarrow \infty} \begin{pmatrix} \frac{1}{2(t-t_0)} \frac{\partial^2}{\partial x_0^2} \log \lambda_{\max}[\mathbf{C}_{t_0}^t(\mathbf{x}_0)] & 0 \\ 0 & 0 \end{pmatrix}_{\mathbf{x}_0=(0, y_0)} \\ = \lim_{t \rightarrow \infty} \begin{pmatrix} \frac{\frac{\partial^2}{\partial x_0^2} \lambda_{\max}[\mathbf{C}_{t_0}^t(\mathbf{x}_0)]}{\lambda_{\max}[\mathbf{C}_{t_0}^t((0, y_0))]} & 0 \\ 0 & 0 \end{pmatrix}_{\mathbf{x}_0=(0, y_0)} \\ = \lim_{t \rightarrow \infty} \frac{1}{2(t-t_0)} \begin{pmatrix} -6 \\ \left(\frac{3}{2}\right)^2 & 0 \\ 0 & 0 \end{pmatrix}. \end{aligned} \quad (119)$$

Therefore, for the unit normal  $\mathbf{n} = (1, 0)$  to the  $\{x = 0\}$  FTLE ridge, and for large enough times  $t > t_0$ , we have

$$\langle \mathbf{n}, \Sigma_{t_0}^t(\mathbf{x}_0) \mathbf{n} \rangle \approx \frac{-4}{3(t-t_0)} < 0.$$

We conclude that for any  $t_0$  and large enough times  $t > t_0$ , the  $y$  axis is a nondegenerate ridge of the FTLE field, and hence would be defined a repelling Lagrangian coherent structure at all times  $t_0$  by Definition 27. Note, however, that the  $y$  axis is far from being Lagrangian, as all trajectories cross it perpendicularly with velocity  $\dot{x} = 1$ .

To evaluate the flux formula (107), recall that the above ridge has constant height. As a result,  $\nabla \Lambda_{t_0}^t$  vanishes along the ridge, and the flux formula (107) gives the flux per unit length for this ridge as

$$\varphi(\mathbf{x}_0, t_0) = \mathcal{O} \left( \frac{1}{|t-t_0|} \right)$$

as  $|t-t_0| \rightarrow \infty$ . This implies  $\lim_{|t-t_0| \rightarrow \infty} \varphi(\mathbf{x}_0, t_0)|_{\text{ridge}} = 0$ , as opposed to the correct value  $\varphi(\mathbf{x}_0, t_0)|_{\text{ridge}} \equiv 1$ .

### Appendix C. More on the flux through FTLE ridges

Here we provide a simplified derivation of the phase space flux formula (107) through an FTLE ridge, originally obtained by Shadden et al. [4]. We also identify three additional assumptions that are not made explicitly in [4], but are necessary for formula (107) to be correct.

First, the derivation of (107) implicitly assumes that the underlying dynamical system is known for all times, otherwise the term  $\mathcal{O}(1/|T|)$  in (107) cannot be defined. Accordingly, we have to assume that

(H1) System (5) is defined for all times, i.e.,

$$[\alpha, \beta] = [-\infty, \infty].$$

Under this assumption, we fix a time  $T > 0$  and let  $\mathcal{R}(t_0)$  denote an  $n-1$ -dimensional second-derivative ridge of the FTLE field  $\Lambda_{t_0}^{t_0+T}(\mathbf{x}_0)$ . We select a local parametrization of  $\mathcal{R}(t_0)$  in the form

$$\mathcal{R}(t_0) = \{\mathbf{x} \in U: \mathbf{x} = \mathbf{r}(\mathbf{s}, t_0), \mathbf{s} \in V \subset \mathbb{R}^{n-1}\},$$

with  $V$  denoting an open subset of  $\mathbb{R}^{n-1}$ , and  $\mathbf{r}: V \times [\alpha, \beta] \mapsto U$  denoting a smooth function. In the domain of this local parametrization,  $\mathbf{n}(\mathbf{s}, t_0)$  will denote a smoothly varying unit normal vector field to  $\mathcal{R}(t_0)$ .

Denoting the  $n$  eigenvalues of the Hessian  $\nabla^2 \Lambda_{t_0}^{t_0+T}(\mathbf{x}_0)$  by

$$\mu_{\min}(\mathbf{x}_0, t_0) \leq \dots \leq \mu_{\max}(\mathbf{x}_0, t_0),$$

we recall that the following conditions must hold for  $\mathcal{R}(t_0)$  to be a second-derivative ridge:

$$\langle \nabla \Lambda_{t_0}^{t_0+T}(\mathbf{r}(\mathbf{s}, t_0)), \mathbf{n}(\mathbf{s}, t_0) \rangle = 0, \quad (120)$$

$$\nabla^2 \Lambda_{t_0}^{t_0+T}(\mathbf{x}_0) \mathbf{n}(\mathbf{s}, t_0) = \mu_{\min}(\mathbf{x}_0, t_0) \mathbf{n}(\mathbf{s}, t_0), \quad (121)$$

$$\mu_{\min}(\mathbf{x}_0, t_0) < 0. \quad (122)$$

For small enough  $\varepsilon > 0$ , there exists a nearby ridge  $\mathcal{R}(t_0 + \varepsilon)$  that is a smooth deformation of  $\mathcal{R}(t_0)$ . (This can be concluded from the smoothness of the underlying flow map, as well as from the implicit function theorem using (120)–(122).) Specifically, we can locally represent the points and unit normals of the ridge  $\mathcal{R}(t_0 + \varepsilon)$  as

$$\begin{aligned} \mathbf{r}(\mathbf{s}, t_0 + \varepsilon) &= \mathbf{r}(\mathbf{s}, t_0) + \alpha(\mathbf{s}, t_0; \varepsilon) \mathbf{n}(\mathbf{s}, t_0) \\ &= \mathbf{r}(\mathbf{s}, t_0) + \varepsilon \alpha_1(\mathbf{s}, t_0) \mathbf{n}(\mathbf{s}, t_0) + \mathcal{O}(\varepsilon^2), \end{aligned}$$

$$\mathbf{n}(\mathbf{s}, t_0 + \varepsilon) = \mathbf{n}(\mathbf{s}, t_0) + \partial_{t_0} \mathbf{n}(\mathbf{s}, t_0) \varepsilon + \mathcal{O}(\varepsilon^2). \quad (123)$$

Since  $\mathcal{R}(t_0 + \varepsilon)$  is a second-derivative ridge, it should also satisfy the conditions (120)–(122). Specifically, substitution of the expressions (123) into (120) gives

$$\langle \nabla \Lambda_{t_0}^{t_0+T}(\mathbf{r}(\mathbf{s}, t_0 + \varepsilon)), \mathbf{n}(\mathbf{s}, t_0 + \varepsilon) \rangle = 0.$$

Taylor expanding this expression in  $\varepsilon$ , comparing  $\mathcal{O}(\varepsilon)$  terms in the expansion, and using (120)–(121) gives

$$\alpha_1(\mathbf{s}, t_0) = -\frac{\partial_{t_0} \langle \nabla \Lambda_{t_0}^{t_0+T}(\mathbf{r}(\mathbf{s}, t_0)), \mathbf{n}(\mathbf{s}, t_0) \rangle}{\mu_{\min}(\mathbf{r}(\mathbf{s}, t_0), t_0)}. \quad (124)$$

Here  $\partial_{t_0}$  refers to partial differentiation with respect to the explicit dependence of  $\Lambda_{t_0}^{t_0+T}$  and  $\mathbf{n}$  on  $t_0$ . This is to be contrasted with the vanishing total derivative

$$\frac{d}{dt_0} \langle \nabla \Lambda_{t_0}^{t_0+T}(\mathbf{r}(\mathbf{s}, t_0)), \mathbf{n}(\mathbf{s}, t_0) \rangle \equiv 0$$

obtained by differentiating (120) with respect to  $t_0$ .

By definition, the local instantaneous volume flux per unit area through a point  $\mathbf{r}(\mathbf{s}, t_0) \in \mathcal{R}(t_0)$  is given by

$$\varphi(\mathbf{r}(\mathbf{s}, t_0), t_0) = \left\langle \left[ \mathbf{v}(\mathbf{r}(\mathbf{s}, t_0), t_0) - \frac{d\mathbf{r}(\mathbf{s}, t_0)}{dt_0} \right], \mathbf{n}(\mathbf{s}, t_0) \right\rangle,$$

i.e., by the ridge-normal projection of the velocity of a trajectory relative to the moving ridge. From the first equation in (123) and from (124), we obtain

$$\begin{aligned} \frac{d\mathbf{r}(\mathbf{s}, t_0)}{dt_0} &= \alpha_1(\mathbf{s}, t_0) \mathbf{n}(\mathbf{s}, t_0) \\ &= -\frac{\partial_{t_0} \langle \nabla \Lambda_{t_0}^{t_0+T}(\mathbf{r}(\mathbf{s}, t_0)), \mathbf{n}(\mathbf{s}, t_0) \rangle}{\mu_{\min}(\mathbf{r}(\mathbf{s}, t_0), t_0)} \mathbf{n}(\mathbf{s}, t_0), \end{aligned}$$

therefore we have

$$\begin{aligned} \varphi(\mathbf{r}(\mathbf{s}, t_0), t_0) &= \langle \mathbf{v}(\mathbf{r}(\mathbf{s}, t_0), t_0), \mathbf{n}(\mathbf{s}, t_0) \rangle \\ &\quad + \frac{\partial_{t_0} \langle \nabla \Lambda_{t_0}^{t_0+T}(\mathbf{r}(\mathbf{s}, t_0)), \mathbf{n}(\mathbf{s}, t_0) \rangle}{\mu_{\min}(\mathbf{r}(\mathbf{s}, t_0), t_0)}. \end{aligned} \quad (125)$$

We note that the second term on the right-hand side of (125) is identically zero for any autonomous dynamical system. Also note that this term will remain small for slowly varying dynamical systems.

Shadden et al. [4] prove that along a trajectory  $\mathbf{x}(t)$  with a well-defined Lyapunov exponent, we have

$$\frac{d}{dt_0} \Lambda_{t_0}^{t_0+T}(\mathbf{x}(t_0)) = \mathcal{O}\left(\frac{1}{|T|}\right),$$

which implies

$$\partial_{t_0} \Lambda_{t_0}^{t_0+T}(\mathbf{x}_0) = -\langle \nabla \Lambda_{t_0}^{t_0+T}(\mathbf{x}_0), \mathbf{v}(\mathbf{x}_0, t_0) \rangle + w(\mathbf{x}_0, t_0, T), \quad (126)$$

$$w(\mathbf{x}_0, t_0, T) = \mathcal{O}\left(\frac{1}{|T|}\right). \quad (127)$$

Next, Shadden et al. [4] differentiate (126) with respect to  $\mathbf{x}_0$  and conclude

$$\partial_{t_0} \nabla \Lambda_{t_0}^{t_0+T} = -[\nabla^2 \Lambda_{t_0}^{t_0+T} \mathbf{v} + [\nabla \mathbf{v}]^* \nabla \Lambda_{t_0}^{t_0+T}] + \mathcal{O}\left(\frac{1}{|T|}\right). \quad (128)$$

This equation, however, is not correct without further assumptions, because the spatial derivative of an  $\mathcal{O}\left(\frac{1}{|T|}\right)$  term is not necessarily of order  $\mathcal{O}\left(\frac{1}{|T|}\right)$ . (An example is the function  $\frac{1}{T} \sin(T \langle \mathbf{x}_0, \mathbf{x}_0 \rangle)$ .) To deduce (128), we therefore have to assume

$$(H2) \limsup_{|T| \rightarrow \infty} T |\partial_{\mathbf{x}_0} w(\mathbf{x}_0, t_0, T)| < \infty \text{ for all points } \mathbf{x}_0 \text{ in a neighborhood of the ridge } \mathcal{R}(t_0).$$

If assumption (H2) holds, (125) and (128) imply

$$\begin{aligned} \varphi &= \langle \mathbf{v}, \mathbf{n} \rangle + \frac{1}{\mu_{\min}} \langle \partial_{t_0} \nabla \Lambda_{t_0}^{t_0+T}, \mathbf{n} \rangle + \frac{1}{\mu_{\min}} \langle \nabla \Lambda_{t_0}^{t_0+T}, \partial_{t_0} \mathbf{n} \rangle \\ &= \langle \mathbf{v}, \mathbf{n} \rangle - \frac{1}{\mu_{\min}} \left\langle \left[ \nabla^2 \Lambda_{t_0}^{t_0+T} \mathbf{v} + [\nabla \mathbf{v}]^* \nabla \Lambda_{t_0}^{t_0+T} \right. \right. \\ &\quad \left. \left. + \mathcal{O}\left(\frac{1}{|T|}\right) \right], \mathbf{n} \right\rangle + \frac{1}{\mu_{\min}} \langle \nabla \Lambda_{t_0}^{t_0+T}, \partial_{t_0} \mathbf{n} \rangle + \mathcal{O}\left(\frac{1}{|\mu_{\min} T|}\right) \\ &= \frac{1}{\mu_{\min}} \langle \nabla \Lambda_{t_0}^{t_0+T}, \partial_{t_0} \mathbf{n} - [\nabla \mathbf{v}] \mathbf{n} \rangle + \mathcal{O}\left(\frac{1}{|\mu_{\min} T|}\right), \end{aligned}$$

which is only equivalent to the flux formula (107) given in Shadden et al. [4] if we assume

$$(H3) \limsup_{|T| \rightarrow \infty} \frac{1}{|\mu_{\min}(\mathbf{x}_0, t_0, T)|} < \infty \text{ for all } \mathbf{x}_0 \in \mathcal{R}(t_0).$$

For instance, in Example 4, formula (119) implies

$$\limsup_{|T| \rightarrow \infty} \frac{1}{|\mu_{\min}(\mathbf{x}_0, t_0, T)|} = \lim_{|T| \rightarrow \infty} \frac{1}{|\mu_{\min}(\mathbf{x}_0, t_0, T)|} = \infty,$$

and hence assumption (H3) is *not* satisfied for Example 4. Accordingly, as we have seen, the flux formula (107) gives an incorrect value.

In general, unless assumptions (H1)–(H3) hold, the terms denoted as  $\mathcal{O}\left(\frac{1}{|T|}\right)$  by Shadden et al. [4] in formula (107) may be as large or larger than the leading-order terms, even as  $T \rightarrow \infty$ .

## References

- [1] G. Haller, G. Yuan, Lagrangian coherent structures and mixing in two-dimensional turbulence, *Physica D* 147 (2000) 352–370.
- [2] G. Haller, Distinguished material surfaces and coherent structures in three-dimensional fluid flows, *Physica D* 149 (2001) 248–277.
- [3] G. Haller, Lagrangian coherent structures from approximate velocity data, *Phys. Fluids A* 14 (2002) 1851–1861.
- [4] S.C. Shadden, F. Lekien, J.E. Marsden, Definition and properties of Lagrangian coherent structures from finite-time Lyapunov exponents in two-dimensional aperiodic flows, *Physica D* 212 (2005) 271–304.
- [5] F. Lekien, S.C. Shadden, J.E. Marsden, Lagrangian coherent structures in  $n$ -dimensional systems, *J. Math. Phys.* 48 (2007) 065404. 1–19.
- [6] T. Peacock, J. Dabiri, Introduction to focus issue: Lagrangian coherent structures, *Chaos* 20 (2010) 01750.
- [7] F. Lekien, A. Coulliette, A.J. Mariano, E.H. Ryan, L.K. Shay, G. Haller, J. Marsden, Pollution release tied to invariant manifolds: a case study for the coast of Florida, *Physica D* 210 (2005) 1–20.
- [8] W. Tang, M. Mathur, G. Haller, D.C. Hahn, F.H. Ruggiero, Lagrangian coherent structures near a subtropical jet stream, *J. Atmospheric Sci.* 67 (2010) 2307–2319.
- [9] N. Fenichel, Persistence and smoothness of invariant manifolds for flows, *Indiana Univ. Math. J.* 21 (1971) 193–225.
- [10] G. Froyland, S. Lloyd, N. Santitissadeekorn, Coherent sets for nonautonomous dynamical systems, *Physica D* 239 (2010) 1527–1541.
- [11] V.I. Arnold, *Ordinary Differential Equations*, MIT Press, Cambridge, 1978.
- [12] G. Haller, A. Poje, Finite-time transport in aperiodic flows, *Physica D* 119 (1998) 352–380.
- [13] G. Haller, Finding finite-time invariant manifolds in two-dimensional velocity fields, *Chaos* 10 (2000) 99–108.
- [14] G. Haller, An objective definition of a vortex, *J. Fluid Mech.* 525 (2005) 1–26.
- [15] L.H. Duc, S. Siegmund, Hyperbolicity and invariant manifolds for planar nonautonomous systems on finite time intervals, *Internat. J. Bifur. Chaos Appl. Sci. Engrg.* 18 (2008) 641–674.
- [16] A. Berger, T.S. Doan, S. Siegmund, Non-autonomous finite-time dynamics, *Discrete Contin. Dyn. Syst. Ser. B* 9 (2008) 463–492.
- [17] A. Berger, T.S. Doan, S. Siegmund, A remark on finite-time hyperbolicity, *PAMM Proc. Appl. Math. Mech.* 8 (2008) 10917–10918.
- [18] A. Berger, On finite-time hyperbolicity, *Discrete Contin. Dyn. Syst. Ser. S* (2010) (in press).
- [19] M. Mathur, G. Haller, T. Peacock, J.E. Ruppert-Felsot, H.L. Swinney, Uncovering the Lagrangian skeleton of turbulence, *Phys. Rev. Lett.* 98 (2007) 144502.
- [20] K. Lin, L.-S. Young, Shear-induced chaos, *Nonlinearity* 21 (2008) 899–915.
- [21] F.J. Beron-Vera, M.J. Olascoaga, M.G. Brown, H. Koçak, I.I. Rypina, Invariant-tori-like Lagrangian coherent structures in geophysical flows, *Chaos* 20 (2010) 017514/1–13.
- [22] G. Haller, Lagrangian structures and the rate of strain in a partition of two-dimensional turbulence, *Phys. Fluids* 13 (2001) 3365–3385.